สารออกฤทธิ์ทางชีวภาพจากเครือเขาแกลบ *Ventilago denticulata* Willd.

นางสาววรรณภา โมฬี

วิทยานิพนธ์นี้เป็นส่วนหนึ่งของการศึกษาตามหลักสูตรปริญญาวิทยาศาสตรมหาบัณฑิต
สาขาวิชาเทคโนโลยีชีวภาพ
คณะวิทยาศาสตร์ จุฬาลงกรณ์มหาวิทยาลัย
ปีการศึกษา 2560

BIOACTIVE COMPOUNDS FROM *Ventilago denticulata* Willd.

Miss Wannapha Molee

A Thesis Submitted in Partial Fulfillment of the Requirements
for the Degree of Master of Science Program in Biotechnology
Faculty of Science
Chulalongkorn University
Academic Year 2017

Thesis Title	BIOACTIVE COMPOUNDS FROM *Ventilago denticulata* Willd.
By	Miss Wannapha Molee
Field of Study	Biotechnology
Thesis Advisor	Associate Professor Nattaya Ngamrojanavanich, Ph.D.
Thesis Co-Advisor	Prasat Kittakoop, Ph.D.

Accepted by the Faculty of Science, Chulalongkorn University in Partial Fulfillment of the Requirements for the Master's Degree

.....Dean of the Faculty of Science
(Associate Professor Polkit Sangvanich, Ph.D.)

THESIS COMMITTEE

.....Chairman
(Associate Professor Vudhichai Parasuk, Ph.D.)

.....Thesis Advisor
(Associate Professor Nattaya Ngamrojanavanich, Ph.D.)

.....Thesis Co-Advisor
(Prasat Kittakoop, Ph.D.)

.....Examiner
(Associate Professor Preecha Phuwapraisirisan, Ph.D.)

.....External Examiner
(Supaporn Pitiporn, Ph.D.)

วรรณภา โมพี : สารออกฤทธิ์ทางชีวภาพจากเครือเขาแกลบ *Ventilago denticulata* Willd. (BIOACTIVE COMPOUNDS FROM *Ventilago denticulata* Willd.) อ.ที่ปรึกษาวิทยานิพนธ์หลัก: รศ. ดร.นาตยา งามโรจนวณิชย์, อ.ที่ปรึกษาวิทยานิพนธ์ร่วม: ดร. ประสาท กิตตะคุปต์, 90 หน้า.

สารอนุพันธ์ naphthalene ชนิดใหม่ (1 และ 2) และ ไอโซเมอร์ใหม่ของ ventilagolin (3) พร้อมกับสาร anthraquinone ที่มีรายงานแล้วประกอบด้วย chrysophanol (4), physcion หรือ emodin 3-methyl ether (5), และ emodin (6) ถูกแยกจากสารสกัดของเถาเครือเขาแกลบ (*Ventilago denticulata*) สารประกอบที่แยกได้แสดงความเป็นพิษต่อเซลล์มะเร็งด้วยค่า IC_{50} 1.15-40.54 µg/mL สารประกอบ 1-3 แสดงการต้านการเจริญของเชื้อแบคทีเรียที่อ่อน (MIC 200.0-400.0 µg/mL) ในขณะที่ emodin (6) แสดงการต้านเชื้อแบคทีเรียปานกลาง (MIC 25.0 µg/mL) สารประกอบ1-3, 5 และ 6 สามารถกำจัดอนุมูลอิสระของ nitric oxide radical สารประกอบ 1 และ 2 สามารถกำจัดอนุมูลอิสระด้วยวิธี DPPH radical scavenging activity มีค่า IC_{50} 44.1 µM และ 85.7 µM ตามลำดับ สารประกอบที่ 1-3 และ 6 มีฤทธิ์ยับยั้ง xanthine oxidase ที่อ่อนขณะที่ emodin (6) ทำหน้าที่เป็นตัวยับยั้ง aromatase ที่มีค่า IC_{50} 10.1 µM สารประกอบที่ 1 และ 2 แสดงการยับยั้งฟอสโฟไดเอสเทอเรส ด้วยค่า IC_{50} 8.28 µM และ 6.48 µM ตามลำดับ

สาขาวิชา เทคโนโลยีชีวภาพ ลายมือชื่อนิสิต .....

ปีการศึกษา 2560 ลายมือชื่อ อ.ที่ปรึกษาหลัก .....

ลายมือชื่อ อ.ที่ปรึกษาร่วม .....

5772134323 : MAJOR BIOTECHNOLOGY

KEYWORDS: VENTILAGO / QUINONE / BIOATIVE COMPOUND

WANNAPHA MOLEE: BIOACTIVE COMPOUNDS FROM *Ventilago denticulata* Willd.. ADVISOR: ASSOC. PROF. NATTAYA NGAMROJANAVANICH, Ph.D., CO-ADVISOR: PRASAT KITTAKOOP, Ph.D., 90 pp.

New naphthalene derivatives (1 and 2) and a new isomer of ventilagolin (3), together with three known anthraquinones, including chrysophanol (4), physcin or emodin 3-methyl ether (5), and emodin (6), were isolated from vines of *Ventilago denticulata*. The isolated compounds exhibited cytotoxic activity against cancer cell lines (HuCCA-1, A549, HepG-2, MOLT-3) with IC_{50} values of 1.15-40.54 µg/mL. Compounds 1-3 exhibited weak antibacterial activity (MIC 200.0-400.0 µg/mL), while emodin (6) displayed moderate antibacterial activity with MIC 25.0 µg/mL. Compounds 1-3, 5, and 6 exhibited nitric oxide radical scavenging activities with IC_{50} 232.0-604.3 µM and compounds 1 and 2 exhibited DPPH radical scavenging activities with IC_{50} values of 44.1 µM and 85.7 µM, respectively. Compounds 1-3 and 6 exhibited weak xanthine oxidase inhibitory activity, while emodin (6) acted as an aromatase inhibitor with the IC_{50} value of 10.1 µM. Compounds 1 and 2 exhibited phosphodiesterase 5 inhibitory activity with IC_{50} values of 8.28 µM and 6.48 µM, respectively.

Field of Study: Biotechnology
Academic Year: 2017

Student's Signature .....
Advisor's Signature .....
Co-Advisor's Signature .....

ACKNOWLEDGEMENTS

I would like to express my earnest respect and gratitude to my advisor Assoc. Prof. Dr. Nattaya ngamrojanavanich and my co-advisor Dr. Prasat Kittakoop for invaluable guidance, kind supervision, and encouragement throughout this research.

I would like to thank the Chulabhorn Research Institute (CRI) for providing all facilities and also all the staffs of Natural Products. Special thanks are given to the cri staffe, especially, Mr. Sanya Sureram, Mr. Surasuk Prachya and the members in my laboratory for valuable suggestion and help.

I take this opportunity to special thanks to Mrs. Sangchan Puthong at The Institute of Biotechnology and Genetic Engineering (IBGE), Chulalongkorn University. I am grateful for kind supports, teaching the research methodologies about biological tests.

I would like to special thank Abhaiphubet Chaopraya Hospital Foundation for scholarship support, valuable suggestion and encouragement throughout this research.

I would like to thanks Assoc. Prof. Dr. Kornkanok Ingkaninan for Phosphodiesterase5 inhibitory activity.

Finally, I am deeply grateful my family for encouragement, care and understanding.

CONTENTS

Page

Page

LIST OF TABLES

LIST OF FIGURES

LIST OF SCHEMES

LIST OF ABBBREVIATIONS

acetone-d6	deuterated acetone
Br	broad
ºC	degree Celsius
$CDCl_3$	deuterated chloroform
CH_2Cl_2	dichloromethane
COSY	correlation spectroscopy
calcd.	calculated
DEPT	distortionless enhancement by polarization transfer
DMSO	Dimethyl sulfoxide
d	doublet
g	gram
h	hour
HMBC	heteronuclear multiple bond correlation
HMQC	heteronuclear multiple quantum coherence
IR	Fourier-Transform Infrared Spectroscopy
J	coupling constant
L	liter
MTT	3-(4, 5-dimethylthiazol-2-yl)-2,5-diphenyltetrazolium bromide
mg	milligram
mL	milliliter
nm	nanometer
NMR	nuclear magnetic resonance
NOESY	nuclear overhauser effect spectroscopy
PED 5	phosphodiesterase 5
ppm	part per million
UV	ultraviolet radiation
µL	microliter
µM	micro molar

μg	microgram
ν_{max}	maximum wave number
λ_{max}	maximum absorption wavelength
δ	chemical shift (ppm)
ε	the reciprocating wavelength
$[\alpha]_D$	specific rotation

CHAPTER I

INTRODUCTION

Natural products are organic compounds produced or extracted from living organisms such as plants, animals and microorganisms. Most of them possess biological activities and have been widely used in traditional food and medicines. It is well known that Thai medical plants are one of the important sources for bioactive compounds that are applicable in various fields, especially, pharmaceutical purpose. Thailand is located in the tropical areas which have a great biodiversity of plant species, and they are rich sources of bioactive compounds.

Natural products have gained widely interests from pharmaceutical, food, and cosmetic industries since people nowadays are more conscious of their health, and leaning towards healthy products rather than artificial ones. Medicinal plants are one of the most popular products due to their medical effectiveness in terms of preventing and relieving diseases.

The genus *Ventilago* belongs to the family of Rhamnaceae. In general, *Ventilago* species are widely spreaded along tropical and subtropical areas of Southeast and South Asia, Australia and Africa. The genus *Ventilago* comprising twelve species including *V. denticulata* Willd., *V. ecorollata* F. Muell., *V. elegans* Hemsl., *V. harmandiana* Pierre, *V. kurzii* Ridl., *V. leiocarpa* Benth., *V. maderaspatana* Gaertn., *V. maingayi* M. A. Lawson, *V. neocaledonica* Schltr., *V. pseudocalyculata* Guillaumin, *V. pubiflora* C. T. White, and *V. viminalis* Hook.

Preliminary evaluation for biological activities of the genus *Ventilago* showed anticancer, anti-inflammatory and antioxidant activities.

1.1 The genus *Ventilago* in Thailand

The genus *Ventilago* (Rhamnaceae) found in Thailand reported by the Royal Forest Department (2001) are as follows.

Ventilago denticulata Willd. Rang daeng (รางแดง), Kreua khao klaep (เครือเขาแกลบ), Thao wan lek (เถาวัลย์เหล็ก)

Ventilago harmandiana Pierre. Kreua plok (เครือปลอก)

1.2 Taxonomical and botanical characteristics of *Ventilago denticulata* Willd.

Taxonomy of *Ventilago denticulata* Willd. is categorized as

Kingdom : Plantae

Division : Magnoliophyta

Class : Magnoliopsida

Order : Rosales

Family : Rhamnaceae

Genus : *Ventilago*

Species : *denticulata*

V. denticulata Willd. [synonyms, *V. calyculata* Tul. *V. macrantha* Tul.] can be found in Southeast Asia region and India. In Thailand, *V. denticulata* is an indigenous plant known in Thai as “Rang Daeng” or “Kreua Khao klaep”. The plant is generally found in sparse forest areas. Lianas; stem 10-25 cm across; branches pubescent; bark fissured, grey or dark brown, usually red in fissures. Leaves alternate, 3-15 x 2-6 cm, ovate-lanceolate, oblique at base, crenate-serrate at margin, obtuse or subacute at apex, subcoriaceous, pubescent; lateral nerves 5-8 pairs; petioles 3-10 mm long, furrowed, pubescent. Flowers have greenish-yellow; pedicels 1-4 mm long. Calyx lobes deltoid, 2-2.5 mm long, hairy.

1.3 Objectives of this research

1.3.1 To extract, isolate and purify chemical constituents from the stems of *Ventilago denticulata* Willd.

1.3.2 To elucidate chemical structures of the isolated compounds by spectroscopic techniques.

1.3.3 To evaluate biological activities of pure compounds including anticancer, anti-inflammatory, antibacterial, and antioxidant activities.

A

B

C D

Figure 1.1 Parts of *Ventilago denticulata* Willd. A) Leaves, B) Stems, C) Flowers, and D) Fruits.

CHAPTER II

LITERATURE REVIEW

2.1 Phytochemical and pharmacological aspects of some species in the genus *Ventilago.*

Several types of compounds have been isolated from the genus *Ventilago*. They can be classified as anthraquinones, naphthalenes, naphthoquinones, benzisochromanquinones, naphthoquinone-lactones, and emodin glycosides.

2.1.1 *Ventilago maderaspatana*

In 1985, Hanumaiah and coworkers isolated compounds from root bark of *V. maderaspatana* (Rhamnaceae) and five isofuranonaphthoquinones (ventilones A–E) were obtained, structures of ventilones A–E were determined by spectroscopic methods, and X-ray crystallographic analysis of ventilone C was performed [1].

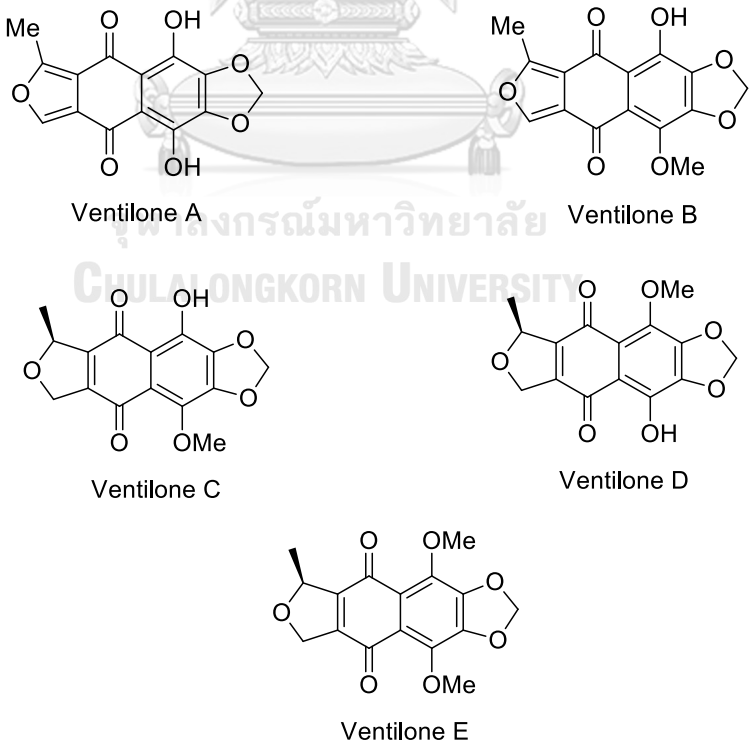

Figure 2.1 Ventilones A-E isolated from *V. maderaspatapa*

In 1985, Hanumaiah and coworkers isolated compounds from root bark of *V. maderaspatana* (Rhamnaceae), and eight benzisochromanquinones including ventiloquinones A-H were isolated from an acetone extract of the root bark [2]

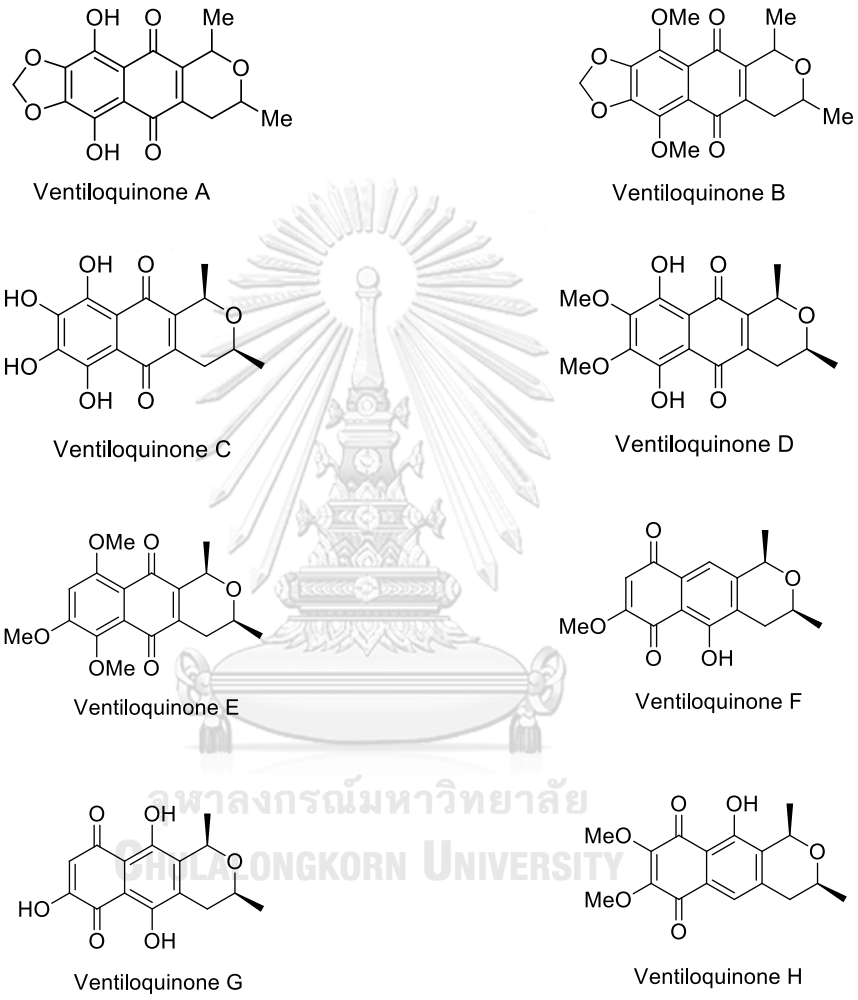

Figure 2.2 Ventiloquinones A-H isolated from *V. maderaspatapa*

In 1985, Rao and coworkers reported the isolation of two naphthalenes and three naphthoquinone derivatives including ventilaginone, ventilagol, maderone, cordeauxione, and isocordeauxione from the root bark of *V. maderaspatana* [3].

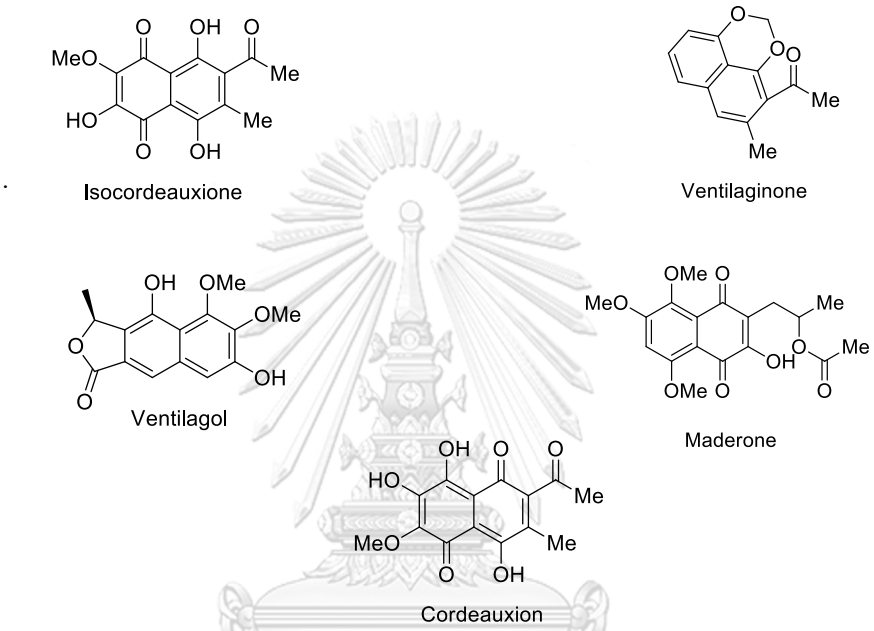

Figure 2.3 Compounds isolated from *V. maderaspatapa*

In 2016, Periyasamy and coworkers reported that the ethanolic and hydroethanolic root extracts of *V. maderaspatana* exhibited a significant antioxidant effect eliciting and increasing catalase levels and decreasing levels of LPO and glutathione. Alcoholic extract at the dose of 500 mg/kg elicited slightly greater antioxidant activity than that of hydroalcoholic extract at the dose of 500 mg/kg. Methanolic extract of root bank has potential to inhibit the DPPA activity and has IC_{50} volue of 60.15 kg/ml. Ethanolic extract whole plant of *V. maderaspatana* possessed the antioxidant and antidenaturation activities[4].

2.1.2 *Ventilago goughii*

In 1991, Jammula and coworkers isolated acetonaphthone and isofuranonaphthoquinone derivatives from the root bark of *V. goughii.* Their structures are 2-acetyl-4-hydroxy-5,6-dimethoxy-3-methyl-1,8-methylenedioxy-naphthalene (goughione) and 4,6 or (7),9-trihydroxy-7(or 6)-methoxy-1-methyl-naphtho-[2,3-c]furan-4,9-quinone (ventilone F) [5].

Figure 2.4 Compounds isolated from *V. goughii*

2.1.3 *Ventilago bombaiensis*

In 1992, Pepalla and coworkers isolated seventeen compounds including chrysophanol, 10-(chrysophanol-7'-yl)-10-hydroxychrysophanol-9-anthrone, chrysophanol, 8-methyl ether, citreorosein, emodin, emodin 1-*O*-**α**-L-rhamnopyranoside, islandicin, physcion, physcion 8-methyl ether, xanthorin, calyxanthone, lupeol, sitosterol 3-*O*-**β**-*D*-glucoside, ventiloquinone C, ventiloquinone O, **β**-sitosterol, and tetracosanolide from an acetone extract of stem bark of *V. bombaiensis* [6].

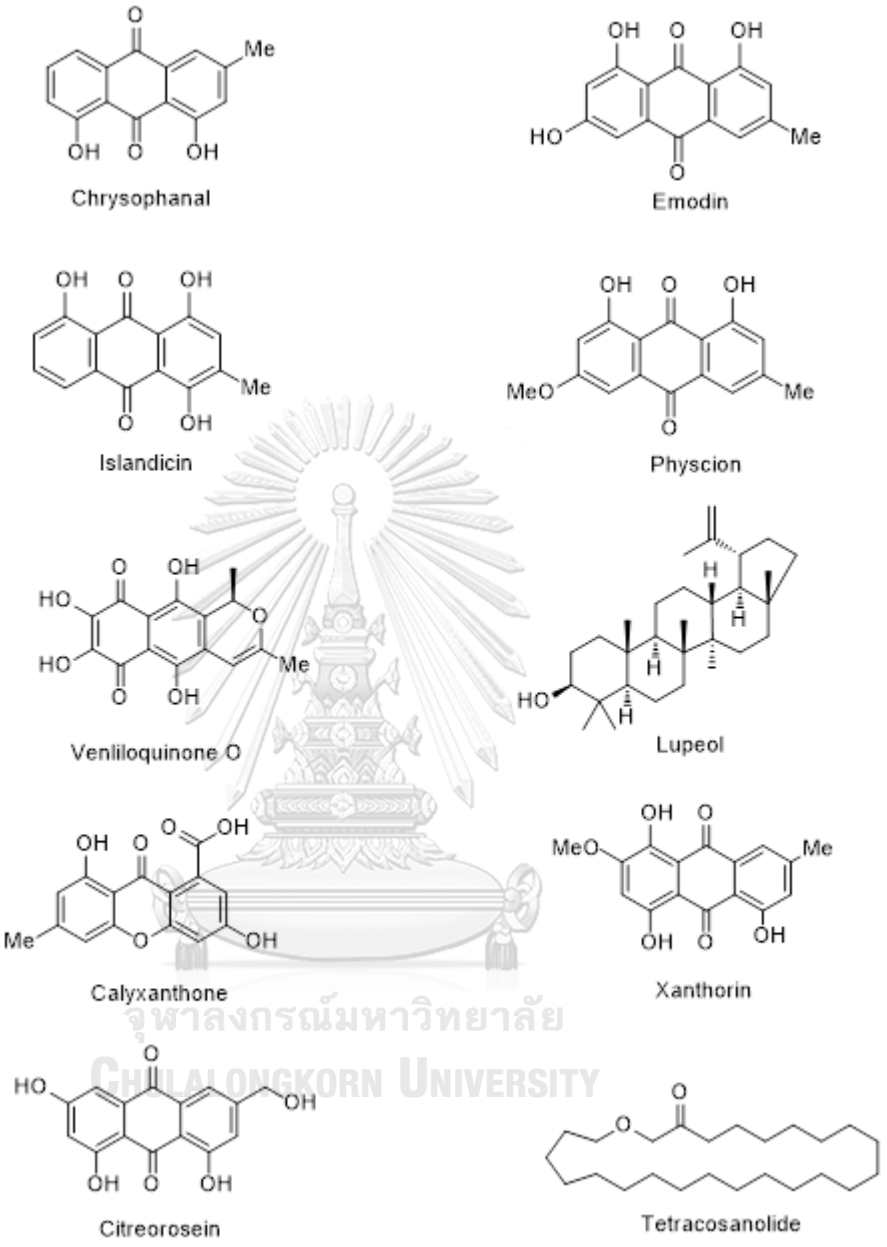

Figure 2.5 Compounds isolated from *V. bombaiensis*

2.1.4 *Ventilago leiocarpa*

In 1996, Lin and coworkers isolated three anthraquinones (islandicin 4-methyl ether, 1,2,6-trihydroxy-7,8-dimethoxy-3-methylanthraquinone, and 2-hydroxyemodin 1-methyl ether), two triterpenoids (taraxerol, lupeol), six anthraquinones (chrysophanol, islandicin, parietin, emodin, catenarin, and skyrin), two benzisochromanquinones (ventiloquinone I and ventiloquinone K), and stigmasterol from *V. leiocarpa*. The cytotoxicities of these compounds toward various tumor cell lines were evaluated, and the result shown that skyrin significantly suppressed growth of HeLa, Vero, K562, Raji, Wish, and Calu-1 tumor cell lines. With the exception of K562 celline, the proliferation of other tumor cell lines was inhibited by emodin and 2-hydroxyemodin 1-methyl ether [7].

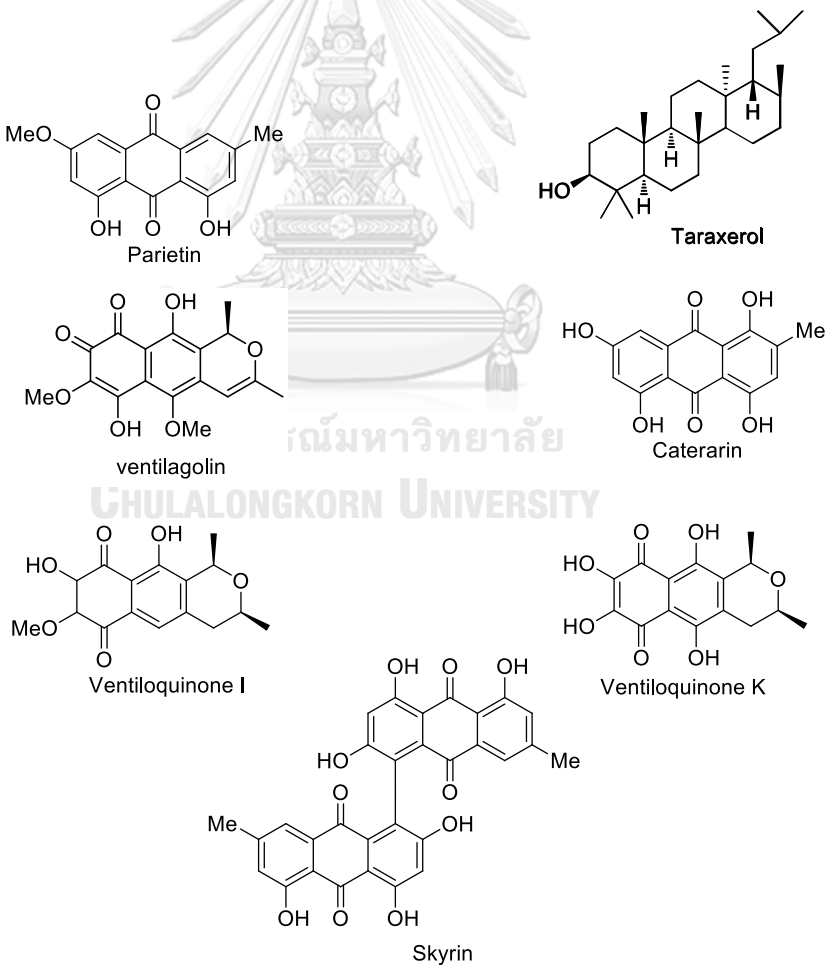

Figure 2.6 Compounds isolated from *V. leiocarpa*

In 1995 Lin and coworkers demanstrated two animal experimental models including carrageenin-induced oedema and CCl_4-induced liver injury. A comparison studies of anti-inflammatory and hepatoprotective effects of four crude extracts ($CHCl_3$, EtOAc, n-BuOH, and H_2O) obtained from the stem bark of *V. leiocarpa* were carried out. The results showed that each of a crude extract displayed both anti-inflammatory and hepatoprotective activities. The H_2O extract (50, 100 mg/kg) exhibited better activity than that of a standard drug indomethacin (10 mg/kg) in reducing carrageenin-induced oedema, and also had the greatest protecting against CCl_4 induced liver injury; it significantly lowered the acute increasing in SCOT and sGPT levels caused by CCl_4. Histopathological alterlation such as necrosis, fatty change, ballooning degeneration, and inflammatory infiltration of lymphocytes and Kupffer cells around the central veins were concurrently improved by the treatment with $CHCl_3$, EtOAc, n-BuOH and H_2O crude extracts. In addition the H_2O extract (50, 100 mg/kg) exhibited a comparable effects to those of indomethacin (10 mg/kg) [8].

2.2 Chemical constituents of *V. calyculata* Tul. (*V. denticulata* Willd.)

V. calyculata Tul. is a synonym of *V. denticulata* Willd. *(family Rhamnaceae).* The phytochemical studies of this plant were published with the name of *V. calyculata;* a few classes of compound have been isolated from this plant including anthraquinone, benzoquinone, naphthalenes, and naphthoquinone.

Table 2.1 Compounds isolated from the root bark of *V. calyculata* Tul. (*V. dentilago* Willd.)

Compound and structure	Type	Reference
2-Methoxystypandrone 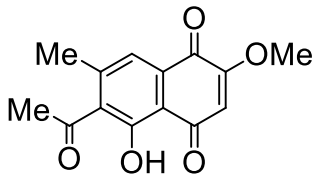	Naphthoquinone	[3]
Calyxanthone 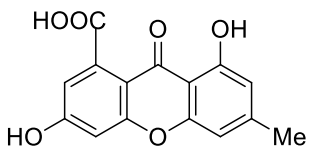	Naphthoquinone	[3]

Table2.1 Compounds isolated from the root bark of *V. calyculata* Tul. (*V. dentilago* Willd.) (continued)

Compound and structure	Type	Reference
Ventilatone A 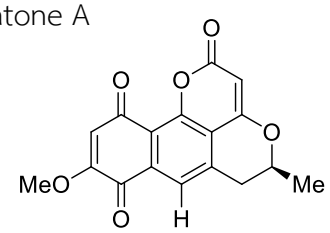	Benzisochromanquinone	[9]
Ventilatone B 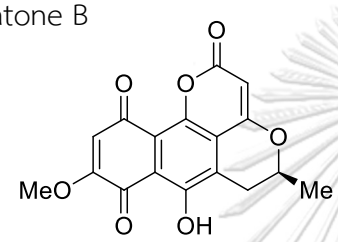	Benzisochromanquinone	[9]
Islandicin 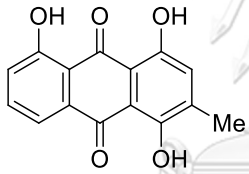	Anthraquinone	[10]
Chrysophanol 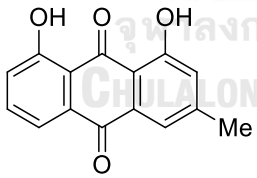	Anthraquinone	[10]
Chrysophanol 8- methyl ether 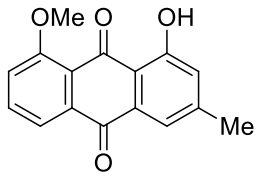	Anthraquinone	[10]

Table2.1 Compounds isolated from the root bark of *V. calyculata Tul*. (*V. dentilago* Willd.) (continued)

Compound and structure	Type	Reference
Emodin 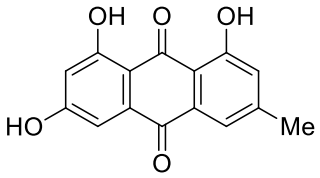	Anthraquinone	[10]
Emodin-6,8- dimethyl ether 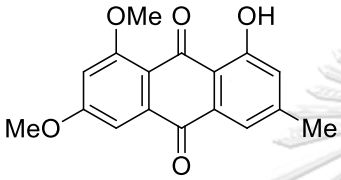	Anthraquinone	[10]
Physcion 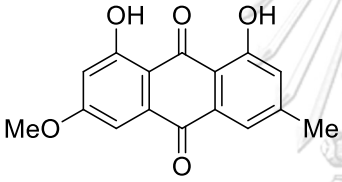	Anthraquinone	[10]
Xanthorin 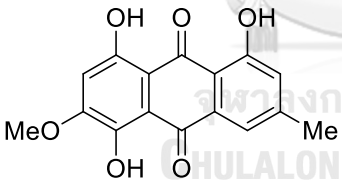	Anthraquinone	[10]
Xanthorin- 5-methyl ether 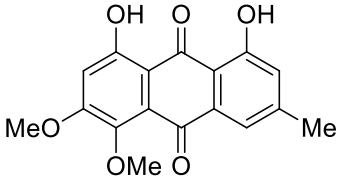	Anthraquinone	[10]

Table2.1 Compounds isolated from the root bark of *V. calyculata* Tul. (*V. dentilago* Willd.) (continued)

Compound and structure	Type	Reference
4,5-Dihydroxynordigitolutein 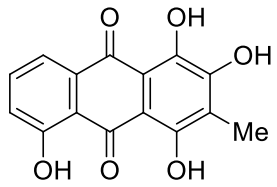	Anthraquinone	[10]
Calyculatone 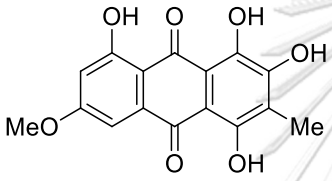	Anthraquinone	[10]
2,4,8-Trihydroxy-1-methoxy-3-methylanthraquinone 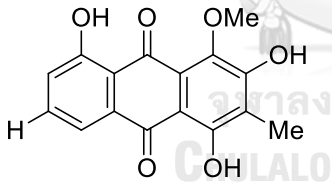	Anthraquinone	[11]
2,4,8-Trihydroxy-1,6-dimethoxy-3-methylanthraquinone 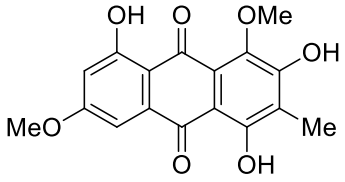	Anthraquinone	[11]

2.3 Traditional medicine of *Ventilago denticulata* Willd.

V. denticulata has been used in herbal medicine in India and neighboring regions for longtime.

The stem barks have been used to treat various kinds of diseases, for example, skin diseases, yellow urination [12], earache [13], cool, rheumatism, sprain [14], eye diseases, stomach ulcers, used medicinally in blood and heart related diseases [15], menorrhagia [16, 17]. Stem bark of the plant paste ground with ginger is applied for curing of cracking bone [18]. The stem bark decoction is given with ground black pepper for treatment of stomach ulcer. The paste of the stem bark is also applied to relieve body pain [15]. Powdered stem bark mixed with sesame oil is externally applied to skin diseases and sprains. Root bark is used for treatment of atonic dyspepsia, mild fever, debility [19], and eye diseases [15]. Sap of the plant is used for the treatment of deafness [19]. The stems are used in the treatment of heart diseases, wounds, eye diseases, stomach ulcer, body pain [15], and herpes simplex virus type 1 [20]. Juice from roots is used for ear against pus formation [18]. The leaves are used for various types of skin diseases [21].

2.4 Pharmacological activities of *V. denticulata (V. calyculata)*

Extensive traditional medicines of *V. denticulata* Willd. led to many pharmacological studies of this plant.

In 2003, V. Lipipun and coworkers reported that *V. denticulata* was effective against thymidine kinase-deficient HSV-1 and phosphonoacetate-resistant HSV-1 strains. These therapeutic efficacies were characterized using a cutaneous HSV-1 infection in mice and the extract of *V. denticulata* was also significantly effective in limiting the development of skin lesions ($P < 0.05$). There were no significant differences between acyclovir and plant extract in the delay of the development of skin lesions. Toxicity of plant extract was not observed in treated mice. Thus, *V. denticulata* extract may be a possible candidate of anti-HSV-1 agent [22].

In 2008, T. Prapapun and coworkers showed the concentrations that could inhibit 50% PDE activity (IC_{50}) of *V. denticulata* extract. The extract was determined in comparison to the standard inhibitor, 3-isobutyl- 1-methylxanthine (IBMX) that showed moderate effect on PDE activity (IC_{50} more than 10 µg/ml) [23].

In 2009, Akram and coworkers showed the anti-inflammatory effect of an ethanolic extract obtained from aerial parts of *V. denticulata*. The effects of extract on the acute and sub acute phases of inflammation were studied in carrageenan induced rat paw edema and cotton pellet-induced granuloma methods in doses of 100 mg/kg and 200 mg/kg body weight. The results of the study indicated that the ethanolic extract of aerial parts of *V. denticulata* possessed significant anti-inflammatory activity at dose 200 mg/kg [24].

In 2011, Das and coworkers reported that the methanolic extract of *V. denticulata* possessed moderate antimicrobial activities showing the inhibition zones with diameters of 9 to 12 mm. The highest activity was observed against *E. coli* [15].

In 2012, P. Venkata and coworkers showed that the methanolic extract of bark *V. denticulata* showed inhibitory activity against several bacteria including *S. aureus, E. coli, B. cereus, P. aeruginasa, P. vulgaris, B. subtilis,* and *Salmonella* sp. with inhibition zones of 6-7 mm. In addition, the MIC results of the *V. denticulata* extracts were 50 and 100 mg/ml against *S. aureus, E. coli, B. cereus, P. aeruginasa, P. vulgaris, B. subtilis,* and *Salmonella* sp [25].

In 2012, Preeti and coworkers studied the aqueous and ethanolic extracts of whole plant of *V. denticulata* and evaluated for *in vitro* anthelmintic activity on the Indian adult earthworm *Pheretima posthuma*. Three concentrations (10, 25, 50 mg/ml) of each extracts were tested, and results were expressed in terms of time for paralysis and time for death of the earthworms. The extracts of *V. denticulata* exhibited inhibition of spontaneous motility (Paralysis) of earthworms in a dose

dependent manner; albendazole (10 mg/ml) was used as a reference compound. Both the extracts showed better anthelmintic activity than that of albendazole. Considerating to the aqueous extract, the alcoholic extract required shorter period of time to cause paralysis and death of the earthworms [26].

In 2015, Pranaya and coworkers evaluated analgesic and anti-inflammatory activities of methanolic extract of bark of *V. calyculata*. For evaluating analgesic activity, hot plate method, tail-flick method, formalin test, and writhing methods were used. Administration of the extract (100 and 200 mg/kg) to adulf Swiss albino mice significantly reduced the total number of writhings in acetic acid induced writhing method. In hot plate and tail-flick methods, there was a significant increase in baseline. A significant reduction in ear edema was observed in xylene induced ear edema method. The results suggested that the methanolic extract of bark of *V. calyculata* might have analgesic and anti-inflammatory activities [29].

In 2016, Pongjanta and coworkers reported that the ethanolic extract from *V. denticulata* exhibited a strong antioxidant activity and prevention of hemolysis. The high amount of phenolics (91.03±12.43 mg of gallic acid equivalents/g extract) and flavonoids (69.76±10.84 mg of catechin equivalents/g) were found in the extract. Interestingly, the extract exhibited higher cytotoxicity toward HepG2 celline than that of peripheral blood mononuclear cells (PBMC) [27].

In 2017, Rani reported phytochemical analysis on the leaves of *V. denticulata*. GC-MS analysis of the leaves extract revealed a presence of 14 compounds by a comparing of their retention time and interpretation of their mass spectra. The analysis of MS/MS fragmentation pattern showed that the major compound was L-(+) ascorbic acid at retention time of 4.4 min with peak area percentage of 16.27. The second highest compound is methyl hexadecanoate or palmitic acid methyl ester at the retention time of 11.1 min with 14.7% of peak area. These compounds exhibited good biological activities, e.g., antioxidant, immunomodulator, antiandrogenic, flavor, hemolytic, antioxidant, anti-bacterial,

hypocholestrolemic nematicide, pesticide, and 5 α reductase inhibitory activities. Squalene was observed at 25.4 min (4.6% of peak area) and it helped the improvement of human immunity. The antibacterial activities of leave extracts were investigated against *Escherichia coli* and *Staphylococcus aureus* and it showed excellent antibacterial activity with the values of 50 µL/well and 100 µL/well, respectively. The zones of inhibition against *Escherichia coli* were 9.24±0.22 and 14.25±0.71 mm and *Staphylococcus aureus* were 7.08±0.54 and 13.20±0.22 mm [28].

CHAPTER III

EXPERIMENTS

3.1 Plant material

Ventilago denticulata Willd. was collected from Prachinburi Province, Thailand, in October 2014. It was identified by comparison with an authentic herbarium specimen No. BKF 194025 which was deposited at the Forest Herbarium, Royal Forest Department, Ministry of Agriculture and Cooperatives, Bangkok, Thailand. A voucher specimen (No. CRI712) was deposited at Chulabhorn Research Institute, Bangkok, Thailand.

3.2 Instruments and equipments

3.2.1 Nuclear magnetic resonance spectrometer (NMR)

NMR spectra were recorded on a Bruker AVANCE (300 MHz) spectrometer operated at 300 MHz for 1H and 75 MHz for 13C, a Bruker AVANCE (400 MHz) spectrometer operated at 400 MHz for 1H and 100 MHz for 13C, and a Bruker AVANCE (600 MHz) spectrometer operated at 600 MHz for 1H and 150 MHz for 13C.

3.2.2 Mass spectrometer (MS)

EI-MS spectra were obtained from Finnigan Mat GCQ mass spectrometer. Accurate mass was obtained from the time of flight (TOF) technique, using a Micro TOF, Bruker daltoincs by APCI ionization mode or ESI mode.

3.2.3 Fourier transform infrared spectrophotometer (FT-IR).

FT-IR spectra were recorded on a Perkin Elmer Spectrum One spectrophotometer.

3.2.4 Ultraviolet-visible spectrometer (UV-vis)

UV-vis spectra were recorded on a Shimadzu UV-vis 2001s spectrophotometer.

3.2.5 Optical rotation

Optical rotations were recorded with a sodium D line, using a JASCO DPI-370 digital polarimeter.

3.2.6 High-performance liquid chromatography (HPLC)

HPLC was performed with a Water 1525 Binary HPLC Pump, connected to a Water 2998 Photodiode Array Detector. Sorbent for the HPLC column was C18 reversed-phase, with a column size of 250 × 20.5 mm.

3.2.7 Circular dichroism (CD) spectra

CD spectra were recorded by a JASCO J-810 spectropolarimeter.

3.3 Chemicals

3.3.1 Solvents

All solvents used in this research such as methanol, dichloromethane, acetronitrile, dimethyl sulfoxide, hexane and ethyl acetate were commercial grade and purified prior to use by distillation.

3.3.2 Other chemicals

3.3.2.1 Sephadex LH-20 (No. 17-009-01)

3.3.2.2 Merck's silica gel 60 Art.

3.4 Extraction and Separation

3.4.1 Extraction

Dried stem of *V. denticulata* (5.48 kg) was extracted sequentially with hexane (2×5 L) and dichloromethane (2×5 L) at room temperature for 2 days. The solution was filtered and evaporated under reduced pressure to obtain hexane crude extract (8.5 g) and dichloromethane crude extracts (9.5 g), respectively. The extraction procresses are shown in **Scheme 3.1**.

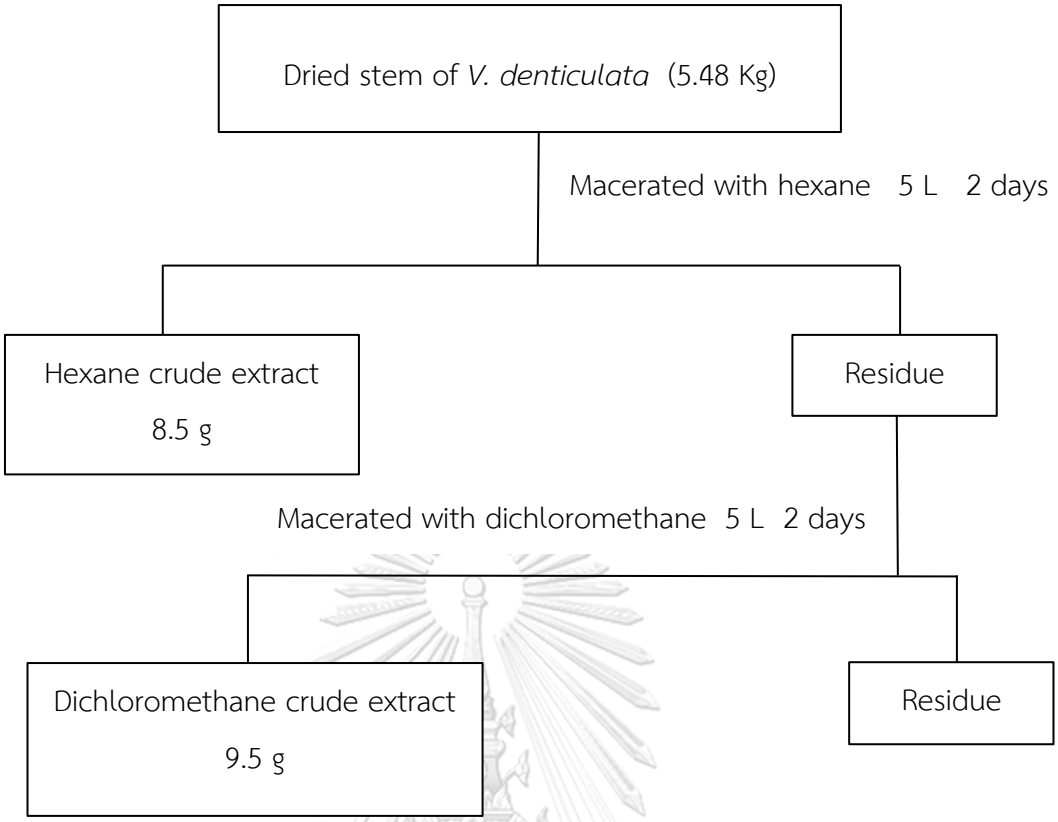

Scheme 3.1: The extraction procedure of the stem of *V. denticulata*

3.4.2 Separation of crude extracts of *V. denticulata*

The hexane crude extract (8.5 g) was divided into two parts, solids (2.53 g) and liquid (5.96 g). The liquid was fractionated on a Sephadex LH-20 column (4×65 cm) and eluted with MeOH to obtain twelve fractions (SH1 to SH12). Fraction SH5 (108.8 mg) was separated on TLC (20×20 cm), eluted with a mixture of hexane:EtOAc (8:2) to obtain 6 fractions (SH5-1A to SH5-5). Fraction SH5-1A (26.5 g) was further purified by C18 reversed phase HPLC eluted with a mixture of MeOH:H_2O (60:40) to give compound **3** (6.7 mg). Fraction SH6 was separated by TLC, eluted by a mixture of hexane:EtOAc (8:2), giving compound **2** (9.89 mg) and compound **3** (35.1 mg). Fraction SH7 was separated by TLC and eluted by a mixture of hexane:EtOAc (8:2) to give compound **1** (5.1 mg) as shown in **Scheme 3.2.**

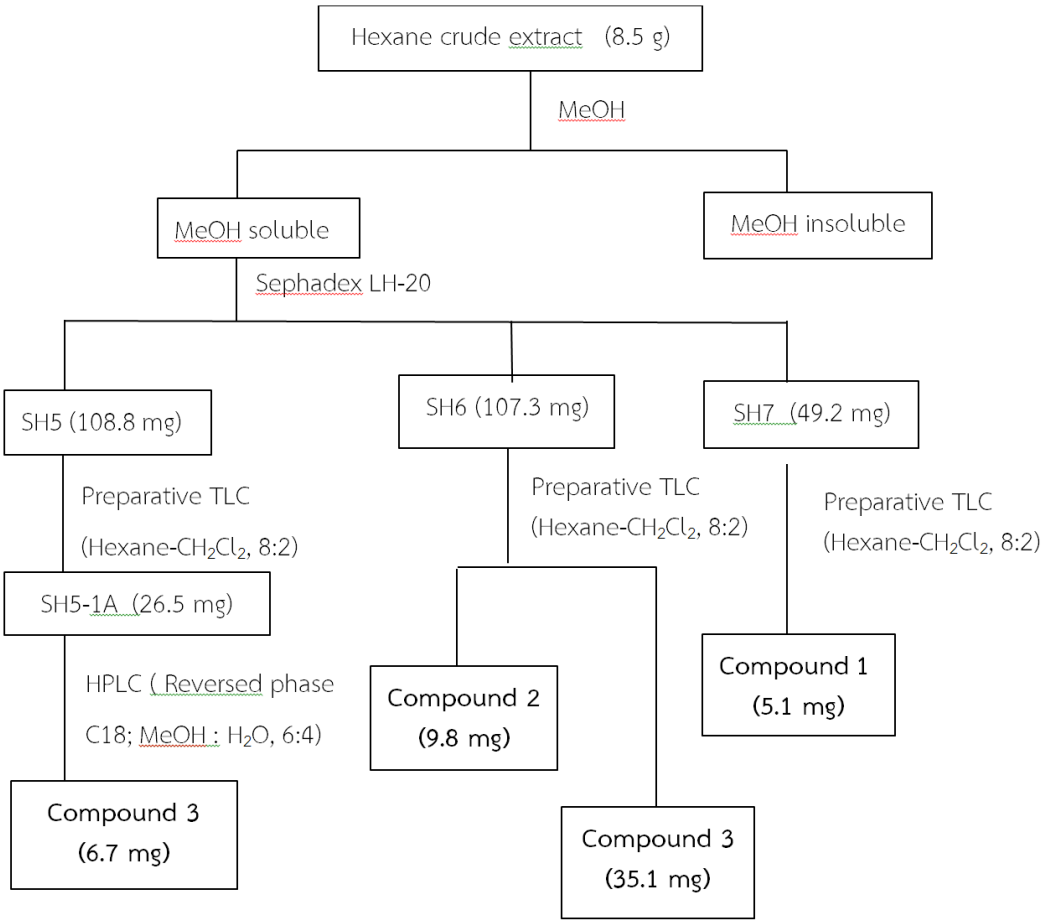

Scheme 3.2 : The isolation procedure of a hexane crude extract.

The CH_2Cl_2 crude extract was fractionated by Sephadex LH-20 column chromatography (eluted with MeOH), giving twelve fractions (SC1-SC12). Fraction 5 (230.1 mg) was refractionated with Sephadex LH-20 column chromatography, eluted with MeOH, to give five fractions (SC5.1-SC5.5). Fraction SC5.3 contained compound **1** (2.7 mg), while fraction SC5.2 was compound **2** (1.5 mg). Fraction SC5.1 (88.2 mg) was further separated by C18 reversed phase HPLC, eluted with a mixture of MeOH:H_2O (8:2), yielding compound **3** (47.2 mg). Fraction SC6 (86.1 mg) was separated by preparative TLC (developed with a mixture of EtOAc:CH_2Cl_2, 3:7) to give a mixture of compound **4** (1.5 mg) and compound **5** (4.9 mg). Fraction SC8 (35.5 mg) was purified by preparative TLC, developed with a mixture of CH_2Cl_2:EtOAc, 8:2, to yield 10.2 mg of compound **6** as shown in **Scheme 3.3.**

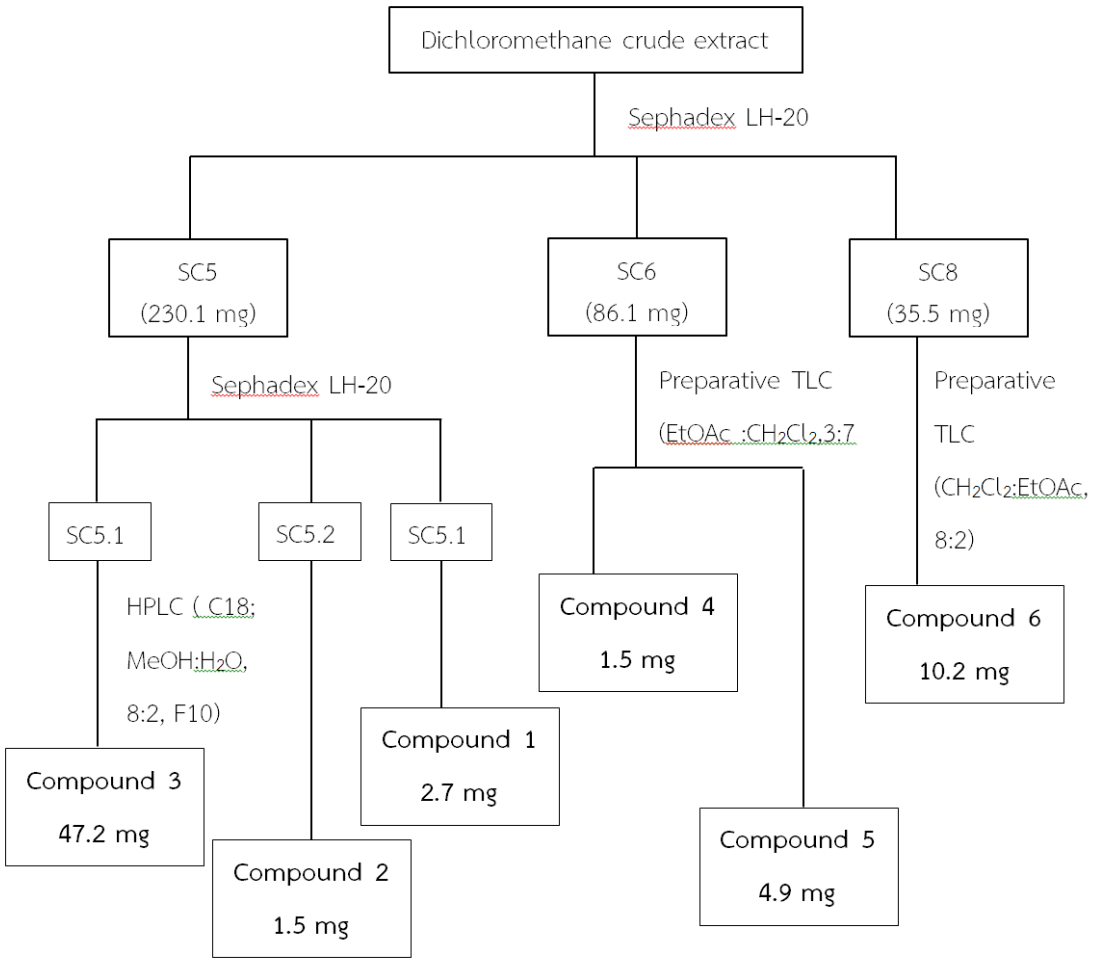

Scheme 3.3 : The isolation procedure of a dichloromethane crude extract.

3.5 Physio-chemical properties of the isolated compounds from *V. denticulata*

3.5.1 Physio-chemical properties of compound 1

Compound **1** was obtained as a red amorphous solid; $[\alpha]_D^{25}$ +8.02 (*c* 0.4, $CHCl_3$); UV (EtOH) λ_{max} (log ε) 336 (3.28), 304.5 (3.62), 244.5 (4.66) nm; positive HRESI-MS *m/z* 277.1063 $[M + H]^+$ (calcd for $C_{15}H_{17}O_5$, 277.1076).

FT-IR (ATR) V_{max} 3325, 2973, 2940, 2857, 1655, 1630, 1590, 1502, 1473, 1435, 1418, 1347, 1330, 1286, 1262, 1199, 1172, 1149, 1056, 1010, 933, 880, 849, 791, 777, 753, 737, 710, 679 cm^{-1}.

^{1}H-NMR spectrum ($CDCl_3$, 300 MHz) (Figure 3.1, Table) δ ppm : 9.36 (1H, s, 4-OH), 7.02 (1H, s, H-8), 6.96 (1H, s, H-9), 5.92 (1H, s, 7-OH), 5.50 (1H, q , *J* = 6.3 Hz, H-3), 5.19 (1H, dt, *J* = 1.4, 12.6 Hz, H-1), 5.05 (2H, d, *J* = 12.6 Hz, H-1), 4.11 (1H, s, 5-OMe), 4.00 (1H, s, 6-OMe), 1.60 (3H, d, *J* = 6.3 Hz, H-10)

^{13}C NMR spectrum, see ($CDCl_3$, 75 MHz) (Figure 3.2, Table) δ ppm : 147.9 (C, C-7), 147.4 (C, C-4), 147.3 (C, C-5), 140.4 (C, C-9a), 137.5 (C, C-6), 133.5 (C, C-8a), 123.1 (C, C-4a), 112 (C, C-5a), 108.8 (CH, C-9), 106.3 (CH, C-8), 79.1 (CH, C-3), 71.8 (CH_2, C-1), 61.7 (C, 5-OMe), 61.1 (C, 6-OMe), 20.4 (CH_3, C-10)

3.5.2 Physio-chemical properties of compound 2.

Compound **2** : Red amorphous solid; UV (EtOH) λ_{max} (log ε) 309 (3.95), 270 (4.53), 239 (4.61) nm; ESIMS *m/z*; 277.1065 $[M + H]^+$ (calcd for $C_{15}H_{17}O_5$ 277.1076)

FT-IR (UATR) V_{max} 3321, 2941, 1680, 1632, 1580, 1497, 1472, 1406, 1380, 1351, 1259, 1204, 1159, 1079, 1048, 1011, 961, 930, 868, 792, 764, 703, 666 cm^{-1}.

^{1}H NMR spectrum ($CDCl_3$, 300 MHz), (Figure 3.11, Table) δ ppm : 10.49 (1H, s, 1-OH), 6.93 (1H, s, H-5), 6.92 (1H, d, *J* = 0.5 Hz, H-4), 6.09 (1H, brs, 4-OH), 4.09 (3H, s, 8-OMe), 4.01 (3H, s, 7-OMe), 2.63 (3H, s, H-10), 2.37 (3H, d, *J* = 0.5 Hz, H-11)

^{13}C NMR ($CDCl_3$, 75 MHz) (Figure 3.12, Table) δ ppm : 205.2 (C, C-9), 153.6 (C, C-1), 149.7 (C, C-6) 147.9 (C, C-8), 138.0 (C, C-7), 133.6 (C, C-3), 133.4 (C, C-5a), 121.6 (C, C-2), 118.9 (CH, C-4), 111.0 (C, C-10), 105.8 (CH, C-11), 61.8 (CH_3, 8-OMe), 61.2 (CH_3, 7-OMe), 32.4 (CH_3, C-10), 20.7 (CH_3, C-11)

^{1}H NMR spectrum (acetone-d6, 300 MHz), (Figure 3.18 , Table) δ ppm : 10.49 (1H, s, 1-OH), 6.93 (1H, s, H-5), 6.92 (1H, d, *J* = 0.5 Hz, H-4), 6.09 (1H, brs, 6-OH), 4.09 (3H, s, 8-OMe), 4.01 (3H, s, 7-OMe), 2.63 (3H, s, H-10), 2.37 (3H, d, *J* = 0.5 Hz, H-11)

^{13}C NMR spectrum (acetone-d6 75 MHz), (Figure 3.19, Table) δ ppm : 205.2 (C, C-9), 153.6 (C, C-1), 149.7 (C, C-6), 147.9 (C, C-8), 138.0 (C, C-7), 133.6 (C, C-3), 133.4 (C, C-5a), 121.7 (C, C-2), 118.9 (CH, C-4), 111.0 (C, C-8a), 105.8 (CH, C-5), 61.8 (CH_3, 8-OMe), 61.2 (CH_3, 7-OMe), 32.4 (CH_3, C-10), 20.7 (CH_3, C-11)

3.5.3 Physio-chemical properties of compound 3.

Compound **3**: Red amorphous solid; $[\alpha]_{D}^{25}$; 1428.62 (*c* 0.02, MeOH); UV (EtOH) λ_{max} (log ε) 375 (3.98), 289 (4.38), 237 (4.44), 212 (4.37) nm; ESIMS m/z; 333.0965 [M + H]$^{+}$ (calcd for $C_{17}H_{17}O_7$, 333.0968)

FT-IR (UATAR) V_{max} 3368, 2929, 2855, 1739, 1633, 1598, 1447, 1415, 1381, 1303, 1259, 1198, 1165, 1082, 1039, 1008, 953, 925, 821, 774, 735 cm^{-1}

^{1}H NMR ($CDCl_3$, 300 MHz) (Figure 3.28, Table) δ ppm : 12.06 (1H, s, 10-OH), 5.91 (1H, s, H-4), 5.71 (1H, q, *J* = 6.5 Hz, H-1), 4.15 (3H, s, 7-OMe), 3.80 (3H, s, 5-OMe), 2.00 (3H, s, 3-Me), 1.44 (3H, d, *J* = 6.6 Hz, 1-Me)

^{13}C NMR ($CDCl_3$, 75 MHz) (Figure 3.29, Table) δ ppm : 184.0 (C, C-6), 179.4 (C, C-9), 159.1 (C, C-3), 154.0 (C, C-10), 148.7 (C, C-5), 141.3 (C, C-8), 140.6 (C, C-7), 136.9 (C, C-5a), 123.7 (C, C-10a), 120.3 (C, C-6a), 109.2 (C, C-9a), 93.9 (CH, C-4), 69.3 (CH, C-1), 61.4 (CH_3, 5-OMe), 60.6 (CH_3, 7-OMe), 20.9 (CH_3, 3-Me), 18.7 (CH_3, 1-Me)

3.5.4 Physio-chemical properties of compound 4.

Compound **4**: yellow needle; ESIMS m/z; 253.0506 [M + H]$^{+}$ (calcd for $C_{15}H_9O_4$, 253.0506)

FT-IR (UATAR) V_{max} 2923, 1675, 1626, 1473, 1456, 1370, 1270, 1209, 1162, 1086, 1025, 902, 868, 839, 752 cm^{-1}

^{1}H NMR ($CDCl_3$, 400 MHz) (Figure 3.36, Table) δ ppm : 12.13 (1H, s, 8-OH), 12.03 (1H, s, 1-OH), 7.83 (1H, dd, *J* = 7.5, 1.1 Hz, H-5), 7.67 (1H, t, *J* = 7.6 Hz, H-6), 7.66 (1H,

d, *J* = 1.1 Hz, H-4), 7.29 (1H, dd, *J* = 8.4, 1.1 Hz, H-7), 7.11 (1H, brq, *J* = 0.8 Hz, H-2), 2.47 (3H, s, 3-Me)

^{13}C NMR ($CDCl_3$, 100 MHz) (Figure 3.37, Table) δ ppm : 192.5 (C, C-9), 182.0 (C, C-10), 162.7 (C, C-1), 162.4 (C, C-8), 149.3 (C, C-3), 136.9 (CH, C-6), 133.6 (C, C-11), 133.3 (C, C-14), 124.5 (CH, C-7), 124.4 (CH, C-2), 121.3 (CH, C-4), 119.9 (CH, C-5), 115.9 (C, C-12), 113.7 (C, C-13), 22.2 (C, 3-Me)

3.5.5 Physio-chemical properties of compound 5

Compound **5**: Orange amorphous solid ; UV (ETOH) λ_{max} (log ε) ; 434 (3.66) 287 (3.78) 262 (3.83) 255 (3.83) 224 (4.08) nm; ESIMS m/z; 285.0757 $[M + H]^+$ (calcd for $C_{16}H_{13}O_5$, 285.0756)

FT-IR (UATAR) V_{max} 2922, 2847, 2108, 1676, 1619, 1564, 1480, 1367, 1317, 1297, 1271, 1221, 1158, 1105, 1036, 901, 852, 761, 667 cm^{-1}

^{1}H NMR ($CDCl_3$, 400 MHz) (Figure 3.46, Table) δ ppm : 12.31 (1H, s, 1-OH), 12.11 (1H, s, 8-OH), 7.62 (1H, d, *J* = 1.0 Hz, H-5), 7.36 (1H, d, *J* = 2.5 Hz, H-4), 7.08 (1H, brq, *J* = 0.7, H-7), 6.68 (1H, d, *J* = 2.5, H-2), 3.93 (3H, s, 3-OMe), 2.45 (3H, s, 6-Me)

^{13}C NMR ($CDCl_3$, 75 MHz) (Figure 3.47, Table) δ ppm : 190.7 (C, C-9), 182.0 (C, C-10), 166.5 (C,C-3), 165.1 (C, C-1), 162.4 (C, C-8), 148.4 (C, C-6), 135.2 (C, C-14), 133.2 (C, C-11), 124.5 (CH, C-7), 121.2 (CH, C-5), 113.6 (C, C-12), 110.2 (C, C-13), 108.2 (CH, C-4), 106.7 (CH, C-2), 56.0 (CH_3, 3-OMe), 22.1 (CH_3, 6-Me)

3.5.6 Physio-chemical properties of compound 6

Compound **6** : Orange amorphous solid; UV (EtOH) λ_{max} (log ε) 437 (4.01), 289 (4.25), 266 (4.17), 252 (4.17), 222.5 (4.44), 202.5 (4.18) nm; ESIMS m/z; 269.0445 $[M + H]^-$ (calcd for $C_{15}H_{19}O_5$, 269.0455)

FT-IR (UATAR) V_{max} 3383, 2924, 2853, 1618, 1590, 1478, 1370, 1331, 1296, 1265, 1221, 1161, 1103, 1033, 907, 874, 757 cm^{-1}

^{1}H NMR (Acetone, 400 MHz) (Figure 3.56, Table) δ ppm : 12.14 (1H, s, 1-OH), 12.02 (1H ,s, 8-OH), 7.50 (1H, s, H-5), 7.20 (1H, d, *J* = 2.1 Hz, H-4), 7.09 (1H, s, H-7), 6.62 (1H, d, *J* = 2.1 Hz, H-2), 2.44 (3H, s, 6-Me)

^{13}C NMR ($CDCl_3$, 100 MHz) (Figure 3.57, Table) δ ppm : 191.4 (C, C-9), 181.9 (C, C-10), 166.2 (C, C-3), 166.0 (C, C-1), 163.0 (C, C-8), 149.3 (C, C-6), 136.3 (C, C-14), 134.0 (C, C-11), 124.7 (CH, C-7), 121.2 (CH, C-5), 114.2 (C, C-12), 110.2 (C, C-13), 109.4 (CH, C-4), 108.6 (CH, C-2), 21.8 (CH_3, 6-Me)

3.6 Evaluation of biological activities

3.6.1 Antibacterial activity

3.6.1.1 Bacterial strains, culture media and chemicals

Both Gram-positive and Gram-negative bacteria obtained from the American Type Culture Collection (ATCC) and used in this study were *Bacillus cereus* (ATCC 11778), *Staphylococcus aureus* (ATCC 6538), *Escherichia coli* (ATCC 8739), and *Pseudomonas aeruginosa* (ATCC 9027).

Mueller-Hinton broth, MHB (Sisco Research Laboratories, SRL) was used as media for minimum inhibitory concentrations (MICs) and Mueller-Hinton agar (MHA) was used for a preparation of bacterial agar plates. Both tetracycline HCl and chloramphenicol (Sigma) were used as standard antibiotics.

3.6.1.2 Bioassay for antibacterial activity

All antibacterial experiments based on MICs assay were determined by broth micro dilution method under the guidelines of the European Society of Clinical Microbiology and Infectious Diseases (ESCMID) [30]. The isolated compounds were tested on aforementioned bacterial strains, compared to two selected antibiotics as positive controls. Each tested compound/antibiotic was dissolved in DMSO, and also prepared for a stock solution (conc. 12.8 mg/mL for antibiotics and conc. 40.0 mg/mL for compounds). A preparation of concentration of either compounds or antibiotic was made by a two-fold serial dilution. A 96-well plate containing 50 µL of prepared solutions of each compound was added 50 µL of each bacterial suspension (final concentrations obtained between 400.0 - 0.39 µg/mL for compounds, and 128.0 - 0.125 µg/mL for antibiotics), and subsequently incubated at 36 ºC for 18-20 h. Absorbance was measured by Synergy H1 microplate reader (according to BioTek's suggestion) at wavelength 625 nm to determine the MICs value of the tested compound.

3.6.2 Anticancer activity

The compounds were tested for their cytotoxic activity against adhesive cell line, i.e., HuCCA-1, HepG2, and A549 cancer cell lines using the MTT assay [31], while that toward the non-adhesive MOLT-3 cell line using the XTT assay. Etoposide and doxorubicin were used as the reference drugs.

3.6.2.1 Cytotoxic activity by MTT assay

The cancer cell lines (HuCCA-1, HepG2, and A549) were seeded into 96 well plates at density of $5x10^3$ cells (180 µl/well), incubated 72 h; 10 µl of MTT solution (5 mg/ml) was added to each well and the plates were incubated at 37 ºC for 4 h. Then, the media containing MTT was dissolved by 150 µl of DMSO to each well. The absorbance was measured at 540 nm by a 96-well plate reader. Data were collected for three replicated and calculated as:

$$\% \text{ Cell viability} = \frac{\textbf{(Absorbance of treated cells)}}{\textbf{(Absorbance of untreated cells)}} \times 100$$

% Cytotoxicity = 100 – percentage of cell viability

3.6.2.2 XTT assay

The assay was performed in a 96-well microtiter plate. In the standard procedure, each well contained 60 µL of 0.5 mM XTT solution prepared with 0.2 M potassium phosphate buffer (pH 7.0) containing menadione at the saturated level. Then 40 µl of sample was added into the well. After it was mixed in a microplate shaker for 15 s at a speed of 500 rpm, the difference in the absorbance at 492 nm was read on a microplate reader [32].

3.6.3 DPPH Radical Scavenging Assay

Radical scavenging potential was determined photometrically by reaction with 1,1-diphenyl-2-picrylhyd- razyl (DPPH) free radicals in a microplate format at 515 nm. Dilutions of tested compounds (in 100% DMSO) were treated with a solution of 100 µM DPPH in ethanol for 30 min at 37 °C. Scavenging potential was compared with a solvent control (0% radical scavenging) and Vitamin C (250 µM final concentration, 100% radical scavenging, used as a blank). The samples which contain scavenging activity higher than 50% were further analyzed the value of 50% inhibitory concentration (IC_{50}) [33].

$$\% \text{ Scavenging} = 100 - \frac{(\text{OD sample})}{OD\ control)} \times 100$$

3.6.4 Aromatase Inhibition Assay

This method was followed the Gentlest kit utilizing a recombinant human aromatase (CYP19) and a fluorometric substrate *O*-benzyl fluorescein benzyl ester (DBF). DBF is dealkylated by aromatase and then was hydrolyzed providing the fluorescein product.

For the aromatase Inhibition assay, 100 µl of C/SD which contains 78.4 µl of 50 mM PB, pH 7.4, 20 µl of 20x NADPH-generating system and 1.6 µl of 100 U/ml G-6-PDH were pipetted in 96-well black plate and then preincubated in 37 ºC water bath for 10 min. The reaction was initiated by addition of 100 µl of enzyme/substrate (E/S) mix containing 77.3 µl of 50 mM PB, pH 7.4, 12.5 µl of 16 pmol/ml CYP19, 0.2 µl of 0.2 mM DBF, and 10% DMSO as negative control or 0.76 mM ketoconazole as positive control. To exclude background fluorescence of sample, E/S was added after the reaction was terminated. After incubation at 37 ºC for 30 min, the reaction was

stopped by addition of 50 µl of 2.2 N NaOH. To develop adequate signal to background radio, the plate was then incubate for 2 hrs in 37 ºC air incubator. Fluorescence signal was measured using an excitation wavelength of 490 nm and emission wavelength of 530 nm with cutoff 515 nm. Percentage of inhibition (%inhibition) was calculated as shown below.

3.6.5 Nitric Oxide Radical Scavenging

100mM of SNP was prepared by dissolving the powder in phosphate buffered saline (PBS) pH 7.4. The reaction mixture (2 ml) containing 100 mM SNP (0.2 ml, final concentration 10 mM) and PBS (1.8 ml) was incubated at 25 °C for 180 min. At 30 min intervals, samples (1ml) of the incubation were removed and diluted with 1 ml of Griess reagent (1% sulphanilamide and 0.1% naphthyletylenediamine dihydrochloride in 2% H_3PO_4). The absorbance of the chromophore formed during the diazotization of nitrite with sulphanilamide and subsequent coupling with naphthylethylene-diamine was read at 540 nm, and referred to the absorbance of standard solutions of sodium nitrite treated in the same way with Griess reagent. The plot between the concentration of nitrite and incubation time exhibited the best incubation time for nitrite production from SNP. Various concentrations of the tested compounds and SNP (10 mM, final concentration) in PBS in a final volume of 2 ml were incubated at 25 °C for 150 min. A control experiment without tested compounds but with the equivalent amount of vehicles was conducted in an identical manner of control. After incubation, 1.0 ml samples of reaction mixtures containing nitrite were removed and diluted with 1.0 ml of Griess reagent. Astaxanthin was used as a reference standard. The absorbance of these solutions was measured at 540 nm against the corresponding blank solutions. The IC_{50} value is the concentration of sample required to inhibit 50% of the NO radicals [34].

3.6.6 Phosphodiesterase 5 inhibitory activity

The reaction mixture comprised 20 µL of Reagent A (100 mM Tris-HCl (pH 7.5), 100 mM imidazole, 15 mM $MgCl_2$, 1.0 mg/mL BSA and 2.5 mg/mL snake venom), 20 µL of 10 mM EGTA, 20 µL of PDE5 solution, and 20 µL of test sample, or only solvent (5% DMSO) as a control. The reaction was started by adding 20 µL of 5 µM [3H]cGMP (~50,000 cpm) and performed at 30qC for 40 min. Then, 100 PL of 50% DEAE resin was added to the reaction. After shaking for 10 min, the resin was allowed to settle (20 min). The supernatant was transferred to a fresh 100 PL of 50% DEAE resin, shaken for 10 min and the resin allowed to settle again. The supernatant (100 PL) was shaken with 200 PL of Microscint® 20 and tritium counted on a TopCount NXT for 2 h. Each experiment was duplicated in a 96-well plate. In preliminary screening, 50 µg/mL of plant extracts was tested and pure compounds tested at 10 PM final conc. All samples were dissolved in DMSO and diluted with water. DMSO was limited to 1% in the final assay medium Sildenafil was the positive control [35] [36].

CHAPTER IV

RESULTS AND DISCUSSION

In the present study, the hexane and dichloromethane crude extracts of the stems of *V. denticulata* were separated by chromatographic techniques to obtain new naphthalene derivatives (1 and 2) and a new quinone isomer (3), together with three know anthraquinones, chrysophanol (4), physcion (5), and emodin (6). Structures of the isolated compounds were elucidated by analysis of NMR, IR and MS spectral data.

4.1 Structure elucidation of the compounds isolated from the stems of *V. denticulata*

4.1.1 Structure elucidation of compound **1**

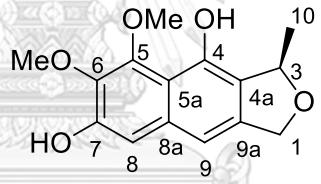

1

Compound **1** was obtained as red amorphous solid. The molecular formula of $C_{15}H_{16}O_5$ was determined by HRESI-MS (*m/z*: 277.1063 $[M+H]^+$, calcd 277.1076). Its IR spectrum exhibited adsorption bands at 3325 cm^{-1}. The UV spectrum absorption at 336, 304, and 244 nm. The ^1H NMR data for compound **1** (Table 4.1) showed signals of two methine singlets at δ_H 7.02 (1H, s) and 6.96 (1H, s), an oxygenated sp^3 methine at δ_H 5.50 (1H, q, *J*=6.3 Hz), non-equivalent methylene protons at δ_H 5.05 and 5.19 (1H, d, *J*=12.6 Hz), a methyl doublet at δ_H 1.60 (3H, d, *J*=6.3 Hz), two methoxy groups at δ_H 4.11 (1H, s) and 4.00 (1H, s), and two exchangeable protons at 5.92 (1H, s) and 9,36 (1H, s).

The ^{1}H-^{1}H COSY spectrum showed the correlation of H-10 and H-3. The HMBC correlations from H-8 (δ_H 7.02) to C-6, C-7, C-5a, and C-9; from H-9 (δ_H 6.96) to C-1, C-4a, C-5a, C-8 and C-8a; from 4-OH proton (δ_H 9.36) to C-4, C-4a, and C-5a; and from 7-OH proton (δ_H 5.92) to C-6, C-7, and C-8. On the basis of these spectroscopic data, the structure of compound **1** was established. Naphthalene derivatives having similar structure to that of **1** were previously isolated from the root bark of *Ventilago maderaspatana*; the derivative with the 3*S* configuration has negative optical rotation, while that with 3*R* has positive optical rotation[3]. Compound **1** exhibited positive optical rotation, $[\alpha]_D^{25}$+8.02 (*c* 0.4, $CHCl_3$), therefore the absolute configuration at C-3 was assigned to be *R*. Compound **1** was therefore identified to be (*R*)-5,6-dimethoxy-3-methyl-1,3-dihydronaphtho[2,3-c]furan-4,7-diol.

Table 4.1 ^{1}H and ^{13}C NMR spectral data ($CDCl_3$) of compound **1**

position	δ_C type	δ_H (J in Hz)	HMBC
1	71.8, CH_2	5.05, d (12.6) 5.19, d (12.6)	3, 4a, 9, 9a 3, 4a, 9, 9a
2	-	-	-
3	79.1, CH	5.50, q (6.3)	-
4	147.4, C	-	-
4a	123.1, C	-	
5	147.3, C	-	-
5a	112.0, C	-	-
6	137.5, C	-	
7	147.9, C	-	-
8	106.3, CH	7.02, s	5a, 6, 7, 9
8a	133.5, C	-	-
9	108.8, CH	6.96, s	1, 4a, 5a, 8, 8a
9a	140.4, C	-	-
10	20.4, CH_3	1.60, d (6.3)	3, 4a
5-OMe	61.7, CH_3	4.11, s	5
6-OMe	61.1, CH_3	4.00, s	6
4-OH	-	9.36, s	4, 4a, 5a
7-OH	-	5.92, s	6, 7, 8

4.1.2 Structure elucidation of compound **2**

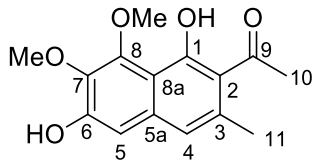

2

Compound **2** was obtained as red amorphous solid. The molecular formula of $C_{15}H_{16}O_5$ was determined by HRESI-MS (*m/z*: 277.1065 $[M+H]^+$ (calcd. for 277.1070). Its IR spectrum exhibited adsorption bands at 3321 and 1680 cm^{-1} indicated the presence of –OH and carbonyl functional groups, respectively. The UV spectrum absorptions at 309, 270, and 239 nm. The ^{1}H NMR spectrum of compound **2** showed two aromatic methines at 6.92 (d, *J* = 0.5 Hz) and 6.93 (d, *J* = 0.5 Hz), four methyl groups at δ_H 2.37 (d, *J* = 0.5 Hz), 2.63, 4.01, and 4.09, and two exchangeable protons at δ_H 6.09 and 10.49 (Table 4.2). The ^{13}C NMR spectrum of compound **2** displayed 15 lines attributable to two methine, four methyl, and nine non hydrogen-bearing carbons (by DEPT techniques). The ^{1}H and ^{13}C NMR signals of C-9 (δ_H 205.2) and C-10 (δ_H 2.63, s; δ_C 32.4) are characteristic signals for an acetyl group. The HMBC spectrum of **2** revealed the correlations from H-11 to C-2, C-3, and C-4; H-4 to C-2, C-3, C-5a, C-8a, and C-11; H-5 to C-6, C-7, C-5a, and C-8a; 7-OMe proton to C-7 and 8-OMe proton to C-8; and 1-OH to C-1, C-2, and C-8a. However, δ_H 6.09 exhibited as broad singlet, therefore it did not show the HMBC correlations to any carbon. But, ^{1}H NMR spectrum of compound **2** acquired in acetone-d_6 (Table 4.3) exhibited a sharp singlet (δ_H 8.74) of 6-OH proton that showed the HMBC correlation to C-5, C-6, and C-7. On the basis of these data, the structure of compound **2** was identified as 1-(1,6-dihydroxy-7,8-dimethoxy-3-methylnaphthalen-2-yl)ethanone. It should be noted that the substituents on the two aromatic rings of compound **2** were the same as those of compound **1**, therefore **1** may be biosynthetically derived from compound **2**.

Table 4.2 ^{1}H and ^{13}C NMR spectral data ($CDCl_3$) of compound **2**

position	$\delta_{C,}$ type	δ_H (J in Hz)	HMBC
1	153.6, C	-	-
2	121.7, C	-	-
3	133.6, C	-	-
4	118.9, CH	6.92, d (0.5 Hz)	C-2, C-3, C-5a, C-8, C-11
5	105.8, CH	6.93, s	C-5a, C-6, C-7, C-8a
5a	133.4, C	-	-
6	149.7, C	-	-
7	138.0, C	-	-
8	147.9, C	-	-
8a	111.0, C	-	-
9	205.2, C	-	-
10	32.4, CH_3	2.63, s	C-2, C-10
11	20.7, CH_3	2.37, d (0.5 Hz)	C-2, C-3, C-4
7-OMe	61.2, CH_3	4.01, s	C-7
8-OMe	61.8, CH_3	4.09, s	C-8
1-OH	-	10.49, s	C-1,C-2, C-8a
6-OH	-	6.09, br, s	-

Table 4.3 ^{1}H and ^{13}C NMR spectral data (acetone-d6) of compound **2**

Position	δ_C type	δ_H (*J* in Hz)	HMBC
1	153.3, C	-	-
2	122.8, C	-	-
3	134.0, C	-	-
4	119.0, CH	6.94, s	C-2, C-3, C-5, C-5a, C-8, C-8a, C-11
5	107.0, CH	6.93, s	C-1, C-3, C-4, C-5a, C-6, C-7, C-8a
5a	133.9, C	-	-
6	152.4, C	-	-
7	140.0, C	-	-
8	149.4, C	-	-
8a	111.1, C	-	-
9	204.2, C	-	-
10	32.3, CH_3	2.54, s	C-2, C-9
11	20.3, CH_3	2.27, d (0.9)	C-2, C-3, C-4
7-OMe	61.2, CH_3	3.94, s	C-7
8-OMe	62.5, CH_3	4.17, s	C-8
1-OH	-	10.17, s	C-1, C-2, C-8a
6-OH	-	8.74, s	C-5, C-6, C-7

4.1.3 Structure elucidation of compound **3**

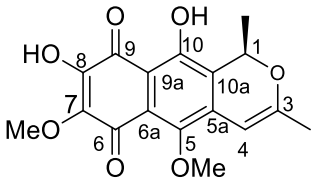

3

Compound **3** was obtained as red amorphous solid; $[\alpha]_D^{25}$; 1428.62 (*c* 0.02, MeOH). The HRESI-MS data revealed the molecular formula of $C_{17}H_{16}O_7$, showing the *m/z* 333.0965 $[M+H]^+$ (calcd. for $C_{17}H_{17}O_7$, 333.0968). Its IR spectrum exhibited adsorption bands at 3368 and 1633 cm^{-1}, indicating the presence of hydroxy and carbonyl functional groups, respectively. The UV spectrum absorptions at 375, 289, 237, and 212 nm. The ^{1}H NMR data for compound **3** (Table 4.4) showed two methoxy groups at δ_H 3.80 (3H, s) and δ_H 4.15 (3H, s), an exchangeable proton at δ_H 12.06 (1H, s), a methyl at δ_H 5.71 (1H, q, *J*=6.5 Hz). The ^{13}C spectrum of **3** showed 17 lines, and the DEPT technique revealed the presence of 2 methyl, 1 methylene, 2 methoxy, 2 hydroxyl, and 10 quaternary carbons. The HMBC spectrum showed the correlations of H-1 to C-3, C-5a, C-10, C-10a, and 1-Me; and from H-4 to C-3, C-5, C-10a, 3-Me. Compound **3** had the same planar structure as that of ventilagolin, which was previously isolated from the plant, *Ventilago leiocarpa* [37]. In the present study, compound **3** had a large positive specific rotation, $[\alpha]_D^{25}$ +1428 (*c* 0.02, MeOH), whose value was far from zero, indicating that **3** was optically active. The structure of compound **3** is related to those of prealnumycin and alnumycin A1; these natural products had 1*R* configuration with large positive specific rotations ranging from +855° to +1100° [38, 39]. Compound **3** had CD spectrum pattern similar to prealnumycin and alnumycin A1, and thus it should have 1*R* configuration. Previously, ventiloquinones H and I and other structurally related quinones were isolated from *V. maderaspatana* and *V. calyculata*, these quinones have 1*R* configuration [2]. Compound **3** was obtained from the same plant, and it should have the same biosynthetic pathway as that of ventiloquinones H and I, supporting

that **3** should have 1*R* configuration. Finally, compound **3** was identified as (*R*)-8,10-dihydroxy-5,7-dimethoxy-1,3-dimethyl-1*H*-benzo[g]isochromene-6,9-dione, which is an optically active isomer of ventilagolin.

Table 4.4 ^{1}H and ^{13}C NMR spectral data ($CDCl_3$) of compound **3**

Position	δ_C type	δ_H (J in Hz)	HMBC
1	69.3, CH	5.71, q (6.5)	C-1, C-3, C-5a, C-10, C-10a
2	-	-	-
3	159.1, C	-	-
4	93.9, CH	5.91, s	C-3, C-5, C-10a, 3-Me
5	148.7, C	-	-
5a	136.9, C	-	-
6	184.0, C	-	-
6a	120.3, C	-	-
7	140.6, C	-	-
8	141.3, C	-	-
9	179.4, C	-	-
9a	109.2, C	-	-
10	154.0, C	-	-
10a	123.7, C	-	-
1-Me	18.7, CH_3	1.44, d (6.6)	C-1, C-10a
3-Me	20.9, CH_3	2.00, s	C-3, C-4
5-OMe	61.4, CH_3	3.80, s	C-5
7-OMe	60.6, CH_3	4.15, s	C-7
10-OH	-	12.06, s	C-9a, C-10, C-10a

4.1.4 Structure elucidation of compound **4**

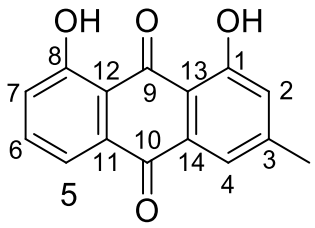

4

Compound **4** was obtained a yellow needle. HRESI-MS established the molecular formula $C_{15}H_{10}O_4$, showing the *m/z* 253.0506 $[M + H]^+$ (calcd for $C_{15}H_9O_4$ 253.0506). IR spectrum of compound **4** showed absorptions at 2923 and 1626 cm^{-1} which indicated the presence of –OH and carbonyl functional groups, respectively. The UV absorptions at 336.0, 304.5, and 244.5 nm. The ^1H NMR data (Table 4.5) showed signals of one methyl group at δ_H 2.48 (3H, s, 3-Me), five aromatic protons at δ_H 7.11 (1H, brq, *J* = 0.8 Hz, H-2), 7.29 (1H, dd, *J* = 8.4, 1.1 Hz, H-7), 7.66 (1H, d, *J*=1.1 Hz, H-4), 7.67 (1H, t, *J*=8.2 Hz, H-6), and 7.83 (1H, dd, *J* = 7.5, 11 Hz), and two hydroxyl groups at 12.03 (1H, s, 1-OH) and 12.13 (1H, s, 8-OH). The ^{13}C NMR and DEPT data for compound **4** showed 15 signals, including one methyl, five methine, and nine quaternary carbons (Table 4.5). ^1H-^1H COSY spectrum showed correlation of H-2 and H-4. The HMBC correlations of H-2 to 3-Me, C-1, C-4, and C-13; H-4 to C-1, C-2, C-10, C-13, C-14, and C3-Me; H-5 to C-7, C-8, C-10, and C-12, and ; H-6 to C-7, C-8, C-11, and C-12; H-7 to C-5, C-8, and C-12. The HMBC correlations from 1-OH to C-1, C-2, and C-13 and from 8-OH to C-7, C-8, and C-12. These spectroscopic data established a structure of compound **4**. The spectral data were identical to those of chrysophanol. Chrysophanol was previously isolated from *Ventilago madaraspatana* [40] and Rhubarb [41]. Therefore, compound **4** was identified as chrysophanol.

Table 4.5 ^{1}H and ^{13}C NMR spectral data ($CDCl_3$) of compound **4**

Position	δ_C type	δ_H (mult., *J* in Hz)	HMBC
1	162.7, C	-	-
2	124.4, CH	7.11 (1H, brq, *J* = 0.8 Hz)	C-1, C-4, 3-Me, C-13
3	149.3, C	-	-
4	121.3, CH	7.66 (1H, d, *J* = 1.1 Hz)	C-1, C-2, C-10, C-13, C-14, 3-Me
5	119.9, CH	7.83 (1H, dd, *J* = 7.5, 1.1 Hz)	C-7, C-8, C-10, C-12
6	136.9, CH	7.67 (1H, t, *J* = 7.6 Hz)	C-7, C-8, C-11, C-12
7	124.5, CH	7.29 (1H, dd, *J* = 8.4, 1.1 Hz)	C-5, C-8, C-12
8	162.4, C	-	-
9	192.5, C	-	-
10	182.0, C	-	-
11	133.6, C	-	-
12	115.9, C	-	-
13	113.7, C	-	-
14	133.3, C	-	-
3-Me	22.2, CH_3	2.48 (3H, s)	-
1-OH	-	12.03 (1H, s)	C-1, C-2, C-13
8-OH	-	12.13 (1H, s)	C-7, C-8, C-12

4.1.5 Structure elucidation of compound **5**

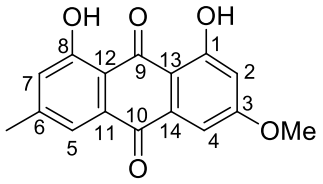

5

Compound **5** was obtained an orange-red needle. The molecular formula, $C_{16}H_{12}O_{5,}$ was established by HRESI-MS, showing the *m/z* 285.0757 $[M + H]^+$ (calcd for $C_{16}H_{13}O_{5,}$ 285.0756). IR spectrum of compound **5** revealed the presence of hydroxyl at 2922 cm^{-1}, and carbonyl at 1676 cm^{-1}. The UV spectrum of compound **5** showed absorptions at 434, 262, and 224 nm. The ^{1}H NMR data (Table 4.6) showed characteristic signals of one aromatic methyl group at δ_H 2.45 (3H, s, 6-Me), one methoxy group δ_H 3.93 (3H, s, 3-OMe), four aromatic protons at δ_H 6.68 (1H, d, *J* = 2.5 Hz, H-2), 7.36 (1H, d, *J* = 2.5 Hz, H-4), 7.62 (1H, d, *J* = 1.0 Hz, H-5), and 7.08 (1H, brq, *J* = 0.7 Hz, H-7), and two hydroxyl groups at 12.31 (1H, s, 1-OH) and 12.11 (1H, s, 8-OH). The ^{13}C NMR and DEPT data for compound **5** displayed 16 lines signals comprising one methyl, one methoxy, four methine, ten quaternary carbons (Table 4.6). ^{1}H-^{1}H COSY spectrum showed correlation of H-5 and H-7. HMBC correlations of H-2 to C-4 and C-1; H-4 to C-2, C-3, C-1 and C-13; H-5 to C-7, C-10, and C-12, 6-Me; and H-7 to C-5, C-8, C-12, and 6-Me. The HMBC correlations from 1-OH to C-1, C-2, and C-13; 8-OH to C-7, C-8, and C-12; 3-OMe to C-3; and 6-Me to C-5, C-6, and C-7. On the basis of these spectroscopic data, as well as data comparison with structure of physcion, the structure of compound **5** was established as shown. Physcion was a known compound, previously isolated from *Ventilago bombaiensis* [42] and Rhubarb [41].

Table 4.6 ^{1}H and ^{13}C NMR spectral data ($CDCl_3$) of compound **5**

Position	δ_C type	δ_H (mult., J in Hz)	HMBC
1	165.1, C	-	-
2	106.7, CH	6.68 (1H, d, *J* = 2.5)	C-4, 1-OH
3	166.5, C	-	-
4	108.2, CH	7.36 (1H, d, *J* = 2.5 Hz)	C-2, C-3, C-10, C-13
5	121.2, CH	7.62 (1H, d, *J* = 1.0 Hz)	C-7, C-10, C-12, 6-Me
6	148.4, C	-	-
7	124.5, CH	7.08 (1H, brq, *J* = 0.7 Hz)	C-5, C-8, C-12, 6-Me
8	162.4, C	-	-
9	190.7, C	-	-
10	182.0, C	-	-
11	133.2, C	-	-
12	113.6, C	-	-
13	110.2, C	-	-
14	135.2, C	-	-
3-OMe	56.0, CH_3	3.93 (3H, s)	C-3
6-Me	22.1, CH_3	2.45 (3H, s)	C-5, C-6, C-7,
1-OH	-	12.31 (1H, s)	C-1, C-2, C-13
8-OH	-	12.11 (1H, s)	C-7, C-8, C-12

4.1.6 Structure elucidation of compound **6**

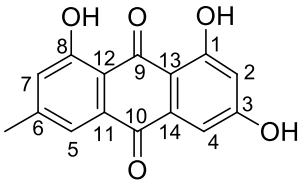

6

Compound **6** was obtained an orange needle. The molecular formula, $C_{15}H_{10}O_{5,}$ was obtained from HRESI-MS showing the *m/z* 269.0445 $[M + H]^+$ (calcd for $C_{15}H_9O_{5,}$ 269.0455). IR spectrum of compound **6** showed absorptions at 3383 and 1618 cm^{-1}. The UV spectrum of compound **6** showed absorptions at 437, 266, 222, and 202 nm. The ^{1}H NMR data (Table 4.7) showed characteristic signals of one aromatic methyl group at δ_H 2.44 (3H, s, 6-Me), four aromatic protons at δ_H 6.62 (1H, d, *J* = 2.1 Hz, H-2), 7.20 (1H, d, *J* = 2.1 Hz, H-4), 7.50 (1H, s, H-5), and 7.09 (1H, s, H-7), and hydroxyl groups at δ_H 12.14 (1H, s, 1-OH) and 12.02 (1H, s, 8-OH). The ^{13}C NMR and DEPT data for compound **6** displayed 15 lines signals attributable to one methyl, four methine, and ten quaternary carbons (Table 4.7). The HMBC correlations of H-2 to C-2, C-3, and C-13; H-4 to C-3, C-4, C-9, C-13 and C-14; H-5 to C-6, C-7, C-10, C-12, and 3-Me; H-7 to C-5, C-8, and C-12; 1-OH to C-1 and C-2; and 8-OH to C-7, C-8, and C-12. On the basis of these spectroscopic data, as well as data comparison with structure of emodin, compound **6** was identified as emodin. Emodin was a known natural product, previously isolated from Rhubarb [41] and *Ventilago bombaiensis* [6].

Table 4.7 ^{1}H and ^{13}C NMR spectral data ($CDCl_3$) of compound **6**

Positive	δ_C type	δ_H (J in Hz)	HMBC
1	166.0, C	-	-
2	108.6, CH	6.62 (1H, d, *J* = 2.1 Hz)	C-3, C-13
3	166.2, C	-	-
4	109.4, CH	7.20 (1H, d, *J* = 2.1 Hz)	C-3, C-10, C-13, C-14
5	121.2, CH	7.50 (1H, s)	C-6, C-7, C-10, C-12, 6-Me
6	149.3, C	-	-
7	124.7, CH	7.09 (1H, s)	C-5, C-8, C-12, 6-Me
8	163.0, C	-	-
9	191.4, C	-	-
10	181.9, C	-	-
11	134.0, C	-	-
12	114.2, C	-	-
13	110.2, C	-	-
14	136.3, C	-	-
1-OH	-	12.14 (1H, s)	C-1, C-2
8-OH	-	12.02 (1H, s)	C-7, C-8, C-12
6-Me	21.8, CH_3	2.44 (1H, s)	C-5, C-6, C-7

4.2 Biological activities of bioactive compounds from the *V. denticulata*

4.2.1 Nitric oxide scavenging activities

Nitric oxide (NO), a short-lived free radical generated endogenously, exerts influence on a number of functions including vasodilation, neurotransmission, synaptic plasticity and memory in the central nervous system. Besides mediating normal function, NO has been implicated in pathophysiologic states. Overproduction of NO can mediate toxic effects, *e.g.,* DNA fragmentation, cell damage and neuronal cell death. NO also shows neurotoxicity and acts as a pathological mediator in pathophysiological processes such as cerebral ischemia, epilepsy, Alzheimer's disease, Parkinson's disease and certain neurodegenerative disease [34].

In the present study, the anti-inflammatory activity of the isolated compounds from *V. denticulata* was tested by nitric oxide scavenging assay[34]. The results are presented as the half maximal inhibitory concentration (IC_{50}). New naphthalene derivatives (**1** and **2**) and a new quinone isomer (**3**), physcion (**5**), and emodin (**6**) exhibited relatively strong nitric oxide scavenging activity (Table 4.8). When compared with curcumin which was used as a positive control (IC_{50} = 164.3±4.9 μM), compound **1** displayed stronger inhibitory activity (IC_{50} = 232.0±2.6 μM) but its activity was lower than of the positive control curcumin. Compounds **2**, **3**, and **6** exhibited nitric oxide scavenging activity with IC_{50} values of 325.6, 298.6, and 604.3 μM, respectively.

Table 4.8 Nitric oxide scavenging activities of compounds isolated from *V. denticulata*

Compounds	NO radical scavenging activity (IC_{50}, μM)
Compound **1**	232.0±2.6
Compound **2**	325.6±13.7
Compound **3**	298.6±2.2
Compound **4**	ND
Compound **5**	>1000
Compound **6**	604.3±5.2
Curcumin	164.3±4.9

ND = not determined

4.2.2 DPPH radical scavenging activities, Inhibition of xanthine oxidase and aromatase

Free radicals are atoms or molecules with unpaired electrons. Many diseases are caused by free radicals, for instance, cancer, Alzheimer's disease, arthritis, allergies, high blood pressure, and nervous system abnormality. Normally free radical formation is controlled naturally by various beneficial compounds known as antioxidants [43, 44]. Inhibition of xanthine oxidase is the drug target for the treatment of gout, a disease occurred from an abnormal metabolism of uric acid in human[45]. Inhibition of aromatase is one of the drug targets for the treatment of breast cancer [46].

4.2.2.1 DPPH radical scavenging activity of the isolated compounds from the extract of *V. denticulata* was performed. Ascorbic acid was employed as a positive control (21.2±2.7 μM). DPPH can be quantitatively determined by reading the absorbance at 515 nm. Compounds **1** and **2** could scavenge 2,2-diphenyl-1-picrylhydrazyl (DPPH) free radicals with respective IC_{50} values of 44.1 and 85.7 μM,

respectively. Compounds **3**, **5**, and **6** did not have DPPH radical scavenging activity, and the results are shown in Table 4.9.

4.2.2.2 Inhibition of xanthine oxidase is shown in Table 4.9. Compounds **1**, **2**, **3**, and **6** inhibited xanthine oxidase with the IC_{50} values of 401.6, 413.0, 284.9, and 374.6 μM, respectively.

4.2.2.3 Inhibition of aromatase is shown in Table 4.9. Among the compounds tested, only compound **6** was found to be an aromatase inhibitor, exhibiting the IC_{50} value of 10.1 μM.

Table 4.9 DPPH radical scavenging activities, inhibition of xanthine oxidase, and inhibition of aromatase of compounds isolated from *V. denticulata*

Compounds	DPPH Radical scavenging activity (IC_{50}, μM)	Inhibition of xanthine oxidase (IC_{50}, μM)	Inhibition of aromatase (IC_{50}, μM)
Compound **1**	44.1±3.0	401.6±6.2	Inactive[c]
Compound **2**	85.7±1.7	413.0±14.8	Inactive[c]
Compound **3**	Inactive[a]	284.9±4.0	Inactive[c]
Compound **4**	ND	ND	ND
Compound **5**	Inactive[a]	Inactive[b]	Inactive[c]
Compound **6**	Inactive[a]	374.6±28.4	10.1±0.3
Ascorbic acid	21.2±2.7	-	-
Allopurinol	-	3.0±0.4	-
Letrozole	-	-	0.0011±0.0002

ND = not determined

[a] Inactive at 250 μM; [b] Inactive at 500 μM; [c] Inactive at 12.5 μM

4.2.3 Anticancer activity

The isolated compounds were tested for cytotoxic activity against HuCCA-1 (human cholangiocarcinoma), HepG2 (human hepatoblastoma carcinoma), A549 (human lung adenocarcinoma, and MOLT-3 (T-cell leukemia). Etoposide and doxorubicin were used as positive controls. The results are shown in Table 4.10.

Table 4.10 Cytotoxic activities of compounds isolated from *V. denticulata*

Compounds	Cytotoxicity activity (IC_{50} μg/mL)			
	HuCCA-1	A549	HepG-2	MOLT-3
Compound **1**	Inactive	Inactive	Inactive	11.99±2.00
Compound **2**	11.05 ± 0.07	12.55 ± 0.63	9.06 ± 1.58	1.15±0.32
Compound **3**	Inactive	Inactive	Inactive	19.57 ± 1.06
Compound **4**	ND	ND	ND	ND
Compound **5**	Inactive	Inactive	14.28 ± 1.47	Inactive
Compound **6**	19.92±1.16	38.81±1.15	40.54±1.50	4.99±0.24
Etoposide	-	-	24.29 ± 1.7	0.02±0.001
Dexorubicin	0.67±0.05	0.14±0.01	0.26 ± 0.03	-

ND = not determined

Inactive at 50 μg/ml

Compounds **1** and **3** selectively exhibited cytotoxic activity toward MOLT-3 cell line (respective IC_{50} values of 11.99 and 19.57 μg/mL), but it was inactive (at 50 μg/mL) against HuCCA-1, A549, and HepG2 cell lines. Compounds **2** and **6** exhibited cytotoxic activity against the cell lines tested with IC_{50} values ranging from 1.15 to 40.54 μg/mL, while compound **5** selectively inhibited the growth of HepG2 cell line (IC_{50} value of 14.28 μg/mL), but was inactive toward other cell lines.

4.2.4 Phosphodiesterase 5 inhibitory activity

Phosphodiesterase 5 (PDE5) inhibitors can be used for the treatment of erectile dysfunction, pulmonary hypertension, and cardiovascular disease. The

isolated compounds were tested for PDE5 inhibitory activity using the [^{3}H]cGMP radio assay method. In the case of > 50% PDE inhibition, the IC_{50} values were measured by the determinations of serial concentrations of the samples. Sildenafil was the positive control. The results expressed as IC_{50} are shown in the Table 4.11. Among the tested compounds, the most potent activity was demonstrated by compounds **2** and **1** with IC_{50} values of 6.48±0.80 μM and 8.28±0.90 μM, respectively.

Table 4.11 Phosphodiesterase 5 inhibitory activity of the isolated compounds

Compounds	**IC_{50} (μM)**
Compound **1**	8.28±0.90 μM
Compound **2**	6.48±0.80 μM
Compound **3**	ND
Compound **4**	ND
Compound **5**	ND
Compound **6**	ND
Sildenafil (Positive control)	0.002 ± 0.0008 μM

ND = not determined

4.2.5 Antibacterial activity

Evaluation of antibacterial activity against either Gram-positive or Gram-negative bacteria was carried out using a method of broth microdilution. As shown in Table 4.12, compounds **1**, **2** and **3** exhibited a low level of the inhibition of Gram-positive bacteria (*Bacillus cereus* and *Staphylococcus aureus*) with MIC values between 200.0 and 400.0 μg/mL. Compound **6** could inhibit both strains of Gram-positive bacteria with the MIC value of 25.0 μg/mL.

Table 4.12 Antibacterial activity of compounds from *V. denticulata*

Compounds	*B. cereus* MIC (μg/mL)	*S. aureus* MIC (μg/mL)	*E. coli* MIC (μg/mL)	*P. aeruginosa* MIC (μg/mL)
Compound **1**	400.0	200.0	Inactive	Inactive
Compound **2**	200.0	200.0	Inactive	Inactive
Compound **3**	400.0	400.0	Inactive	Inactive
Compound **4**	ND	ND	ND	ND
Compound **5**	Inactive	Inactive	Inactive	Inactive
Compound **6**	25.0	25.0	Inactive	Inactive

ND = not determined

Inactive at conc. 400.0 μg/mL

CHAPTER V

CONCLUSION

In this study, new naphthalene derivatives **1** and **2**, and a new quinone isomer **3** of ventilagolin were isolated from a hexane crude extract of *V.denticulata*. Known anthraquinones, chrysophanol (**4**), physcion (**5**), and emodin (**6**) were isolated from the CH_2Cl_2 crude extract of *V.denticulata*. The isolated compounds from the stem of *V. denticulata* were evaluated for their anti-inflammatory, antioxidant, anticancer, phosphodiesterase 5 inhibitory, and antibacterial activities.

Compounds **1**-**3** and **6** exhibited nitric oxide radical scavenging activity with IC_{50} values of 232.0, 325.6, 298.6, and 604.3, respectively. Compounds **1** and **2** could scavenge 2,2-diphenyl-1-picrylhydraxyl (DPPH) free radical with respective IC_{50} values of 44.1 and 85.7 μM. Compounds **1**-**3** and **6** inhibited xanthine oxidase with the IC_{50} values ranging from 284.9 to 413.0 μM. Compound **6** was found to be an aromatase inhibitor exhibiting the IC_{50} value of 10.1 μM. Compounds **1** and **3** selectively exhibited cytotoxic activity toward MOLT-3 cell line at IC_{50} values of 11.99 and 19.57 μg/mL, respectively. Compounds **2** and **6** exhibited cytotoxic activity against the cell line tested with IC_{50} values ranging from 1.15 to 40.54 μg/mL, while compound **5** selectively inhibited the growth of Hep-G2 cell line (IC_{50} value of 14.28 μg/mL). Compounds **1** and **2** exhibited PED5 inhibitory activity with IC_{50} values of 8.28 and 6.48 μM, respectively. Compounds **1**-**3** selectively exhibited antibacterial activity toward Gram-positive bacteria (*Bacillus cereus* and *Staphylococcus aureus*) with MICs values ranging from 200.0 and 400.0 μg/mL. Compound **6** was the most active antibacterial agent, showing the MIC value of 25.0 μg/mL selectivety active toward Gram-positive bacteria. Compound **5** did not exhibit antibacterial activity.

REFERENCES

[1] Hanumaiah, T., et al. Isofuranonaphthoquinones from *ventilago maderaspatana.* Tetrahedron 41(3) (1985): 635-642.

[2] Hanumaiah, T., et al. Benzisochromanquinones in *ventilago* species. Phytochemistry 24(10) (1985): 2373-2378.

[3] Hanumaiah, T., et al. Naphthalenes and naphthoquinones from *Ventilago* species. Phytochemistry 24(8) (1985): 1811-1815.

[4] Periyasamy, K. and K, S. Ethnobotanical, phytochemical and pharmceutical studies of medicinal plant, *ventilago maderaspatana* gaertn (red creeper): A review International Journal of Current Pharmaceutical Research 8 (2016).

[5] Jammula, S.R., Pepalla, S.B., Telikepalli, H., Rao, K.V.J., and Thomson, R.H. An acetonaphthone and an isofuranonaphthoquinone from *Ventilago goughii.* Phytochemistry 30(7) (1991): 2427-2429.

[6] Pepalla, S.B., Jammula, S.R., Rao, K.V.J., and Thomson, R.H. Quinones and tetracosanolide in *Ventilago bombaiensis.* Phytochemistry 31(6) (1992): 2103-2104.

[7] Lin, C.C., Chang, C.H., Yang, J.J., Namba, T., and Hattori, M. Hepatoprotective effects of emodin from *Ventilago leiocarpa.* J Ethnopharmacol 52(2) (1996): 107-11.

[8] Lin, C.-C., Lin, W.-C., Chang, C.-H., and Namba, T. Antiinflammatory and hepatoprotective effects of *Ventilago leiocarpa.* Phytotherapy Research 9(1) (1995): 11-15.

[9] Hanumaiah, T., Marshall, D.S., Rao, B.K., Rao, J.U.M., Rao, K.V.J., and Thomson, R.H. Naphthoquinone-lactones and extended quinones from *Ventilago calyculata.* Phytochemistry 24(11) (1985): 2669-2672.

[10] Rao, B.K., Hanumaiah, T., Rao, C.P., Rao, G.S.R., Rao, K.V.J., and Thomson, R.H. Anthraquinones in *Ventilago* species. Phytochemistry 22(11) (1983): 2583-2585.

[11] Rao, B.K., Hanumaiah, T., Rao, J.U.M., Rao, K.V.J., and Thomson, R.H. Two anthraquinones from *Ventilago calyculata.* Phytochemistry 23(9) (1984): 2104-2105.

[12] Patil, V. and A Patil, D. Ethnomedicinal practices of Nasik District, Maharashtra. Indian journal of traditional knowledge 4(3) (2004): 287-290.

[13] Kumar, K. and Abbas, S.G. Ethnomedicinal composition depends upon floristic composition: A case studied in Sal forests of Jharkand. INTERNATIONAL JOURNAL OF PHARMACY & LIFE SCIENCES 3(5) (2012): 1710-1719.

[14] Irshad, S. Bark Drugs as indian ethnomedicine - modern therapeutics and future prospects. Indian Ethnobotany: Emerging Trends, 2015.

[15] Das, P.K., Mondal, F.L.S.F.A., and Parui, S.M. Antibacterial activity of some selected dye yielding plants in Eastern India. African Journal of Plant Science 5 (2011): 510-520.

[16] Jain, S.P., Singh, S., Srivastava, S., Singh, J., Mishra, N.P., and Prakash, A. Hitherto unreported ethnomedicinal uses of plants of Betul district of Madhya Pradesh. Indian journal of traditional knowledge 9 (2010): 522-525.

[17] Saheb, S., Boyina, R., Parveen, N., and Obaidullah. Medicanal plants used against gastrointestinal disorders by the tribal people of nallamallais andhrapraesh. Vol. 1, 2012.

[18] Chakraborty, M.K. and Bhattacharjee, A. Some common ethnomedicinal uses of various diseases in Purulia district, West Bengal. Indian journal of traditional knowledge 5 (2006): 554-558.

[19] Chopra, R.N., et al. Glossary of Indian medicinal plants ; [with] Supplement. New Delhi: Council of Scientific & Industrial Research, 1956.

[20] Abdulamir, A. Asia is the Mine of Natural Antiviral Products for Public Health. The Open Complementary Medicine Journal 1 (2009): 58-68.

[21] Korpenwar, A.N. Ethnomedicinal Plants Used To Cure Skin Diseases In Ambabarwa Wild Life Sanctuary Area Of Buldhana District (M.S.), India. International Journal of Recent Trends in Science And Technology 2 (2012): 36-39.

[22] Lipipun, V., et al. Efficacy of Thai medicinal plant extracts against herpes simplex virus type 1 infection in vitro and in vivo. Antiviral Research 60(3) (2003): 175-180.

[23] Temkitthawon, P., et al. Screening for phosphodiesterase inhibitory activity of Thai medicinal plants. Journal of Ethnopharmacology 119(2) (2008): 214-217.

[24] Akram, M.T., Dhenge, R.M., and Itankar, P.R. Anti-inflammatory activity of ethanolic extract of Ventilago denticulata. Indian Journal of Natural Products 25(2) (2009): 22-24.

[25] P. Venkata, S., Challa, M.M., Teixeira da Silva, J., Butchi Raju, A., and Sravani, R. Screening the Antimicrobial and Antioxidant Potential of Ventilago denticulata, Scolopia crenata and Rivea hypocrateriformis from Maredumilli Forest, India. Medicinal and Aromatic Plant Science and Biotechnology 6 (2012): 58-62.

[26] Preeti, M., Shweta, P., and Shreyas, S. In vitro anthelmintic activity of whole plant of Ventilago Denticulata Willd. against Pheretima posthuma. Asian Journal of Pharmaceutical and Clinical Research 5 (2012): 200-201.

[27] Pongjanta, A., Pangjit, K., and Srichairatanakool, S. Antioxidant Activity and Cytotoxic Effect of Ventilago denticulata Willd Leaves Extracts. J Med Assoc Thai 99 Suppl 1 (2016): S51-7.

[28] RANI, K.S. Phytochemical screening and GC-MS analysis of n-hexane/ethylacetate leaf extract of *Ventilago denticulata* Willd. Journal of Advanced Studies in Agricultural, Biological and Environmental Science 4(2) (2017): 14-23.

[29] Pranaya, G., Venkata Smitha, P., Srinivasa Reddy, N., Vinay, R., Challa, M.M., and Butchi Raju, A. Evaluation of Analgesic and Anti-Inflamatory Activity of Ventilago calyculata. International Journal of Life science 9(1) (2015): 43-46.

[30] Determination of minimum inhibitory concentrations (MICs) of antibacterial agents by broth dilution. Clinical Microbiology and Infection 9(8): ix-xv.

[31] Carmichael, J., DeGraff, W.G., Gazdar, A.F., Minna, J.D., and Mitchell, J.B. Evaluation of a Tetrazolium-based Semiautomated Colorimetric Assay: Assessment of Radiosensitivity. Cancer Research 47(4) (1987): 943.

[32] Ukeda, H., Goto, Y., Sawamura, M., Kusunose, H., Kamikado, H., and Kamei, T. A Spectrophotometric Microtiter-Based Assay of the Ability of UHT-Treated Milk to Reduce XTT. Food Science and Technology International, Tokyo 2(1) (1996): 48-50.

[33] Gerhäuser, C., et al. Mechanism-based in vitro screening of potential cancer chemopreventive agents. Mutation Research/Fundamental and Molecular Mechanisms of Mutagenesis 523–524 (2003): 163-172.

[34] Sumanont, Y., Murakami Y Fau - Tohda, M., Tohda M Fau - Vajragupta, O., Vajragupta O Fau - Matsumoto, K., Matsumoto K Fau - Watanabe, H., and Watanabe, H. Evaluation of the nitric oxide radical scavenging activity of manganese complexes of curcumin and its derivative. Biological and Pharmaceutical Bulletin 27(2) (2004): 170-173.

[35] Sonnenburg, W.K., Rybalkin, S.D., Bornfeldt, K.E., Kwak, K.S., Rybalkina, I.G., and Beavo, J.A. Identification, Quantitation, and Cellular Localization of PDE1 Calmodulin-Stimulated Cyclic Nucleotide Phosphodiesterases. Methods 14(1) (1998): 3-19.

[36] Temkitthawon, P., Changwichit, K., Khorana, N., Viyoch, J., Suwanborirux, K., and Ingkaninan, K. Phenanthrenes from Eulophia macrobulbon as novel phosphodiesterase-5 inhibitors. Natural Product Communications 11 (2016): 1-4.

[37] Wang, X.F., et al. [Studies on the chemical constituents of Ventilago leiocarpa Benth]. Yao Xue Xue Bao 28(2) (1993): 122-5.

[38] Tatsuta, K., Tokishita, S., Fukuda, T., Kano, T., Komiya, T., and Hosokawa, S. The first total synthesis and structural determination of antibiotics K1115 B1s (alnumycins). Tetrahedron Letters 52(9) (2011): 983-986.

[39] Tähtinen, P., et al. Epimers vs. inverse epimers: The C-1 configuration in alnumycin A1. RSC Advances 2(12) (2012): 5098-5100.

[40] Krishnakumari, G.N., Bhuvaneswari, B., and Raja Swapna, I. Antifeedant activity of quinones from Ventilago madaraspatana. Fitoterapia 72(6) (2001): 671-675.

[41] Danielsen, K., W. Aksnes, D., and Francis, G. NMR study of some anthraquinones from rhubarb. Magnetic Resonance in Chemistry 30(4) (1992): 359-360.

[42] Sridahrababu pepalla, S.W.J., K. V. Jagannadharao and Ronaldh. Thomso. Quinones and tetracosanolide in ventilago bombazenszs. Phytochemistry 31 (1992): 2103-2104.

[43] Rahman, K. Studies on free radicals, antioxidants, and co-factors. Clinical Interventions in Aging 2(2) (2007): 219-236.

[44] Wei, S.-D., Zhou, H.-C., and Lin, Y.-M. Antioxidant Activities of Extract and Fractions from the Hypocotyls of the Mangrove Plant Kandelia candel. International Journal of Molecular Sciences 11(10) (2010): 4080-4093.

[45] Pacher, P., Nivorozhkin A Fau - Szabo, C., and Szabo, C. Therapeutic effects of xanthine oxidase inhibitors: renaissance half a century after the discovery of allopurinol. Pharmacological Reviews 1(0031-6997 (Print)) (2006): 87-114.

[46] Brueggemeier, R.W., Hackett Jc Fau - Diaz-Cruz, E.S., and Diaz-Cruz, E.S. Aromatase inhibitors in the treatment of breast cancer. Endocrine Reviews 26(3): 331-345.

APPENDIX

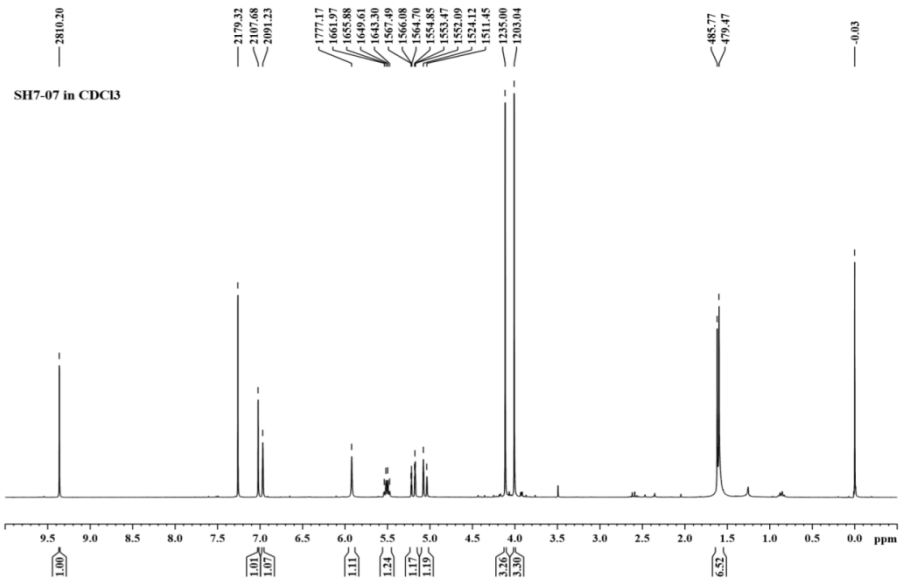

Figure 3.1 300 MHz ^{1}H NMR ($CDCl_3$) spectrum of compound 1

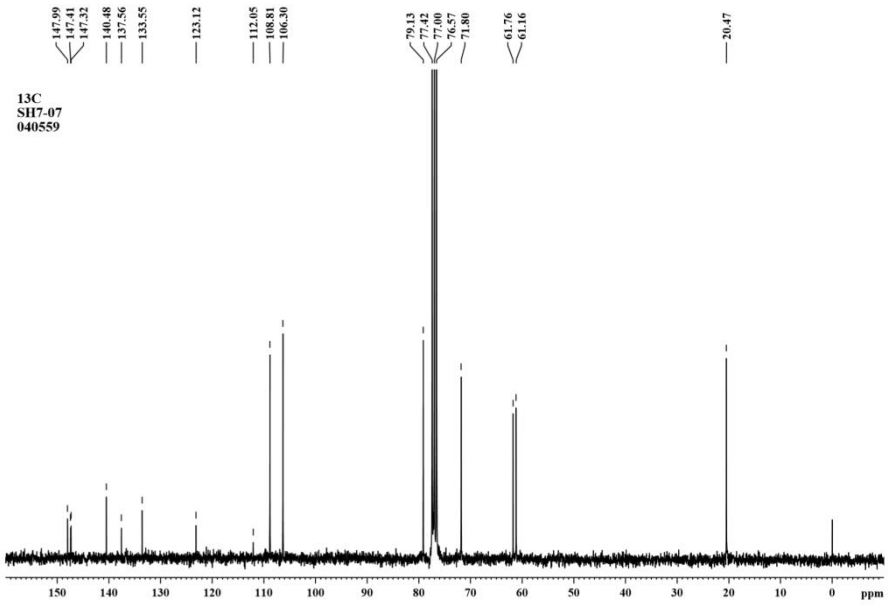

Figure 3.2 75 MHz ^{13}C NMR ($CDCl_3$) spectrum of compound 1

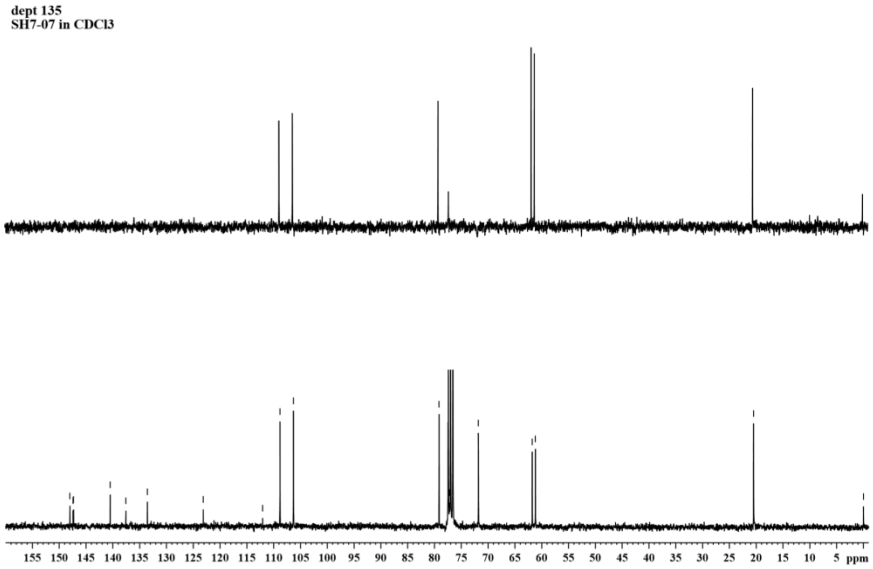

Figure 3.3 Dept135 ($CDCl_3$) spectrum of compound 1

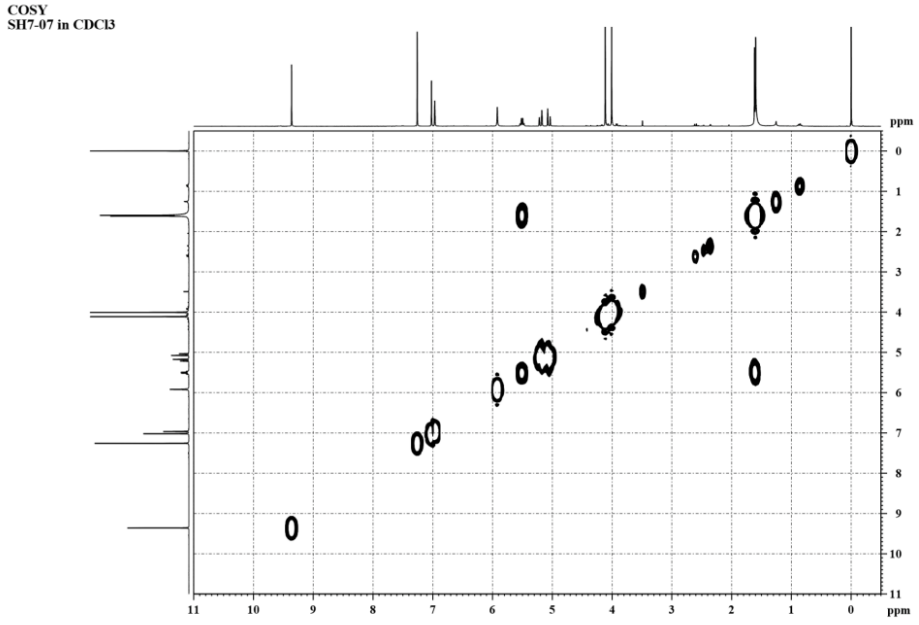

Figure 3.4 COSY ($CDCl_3$) spectrum of compound 1

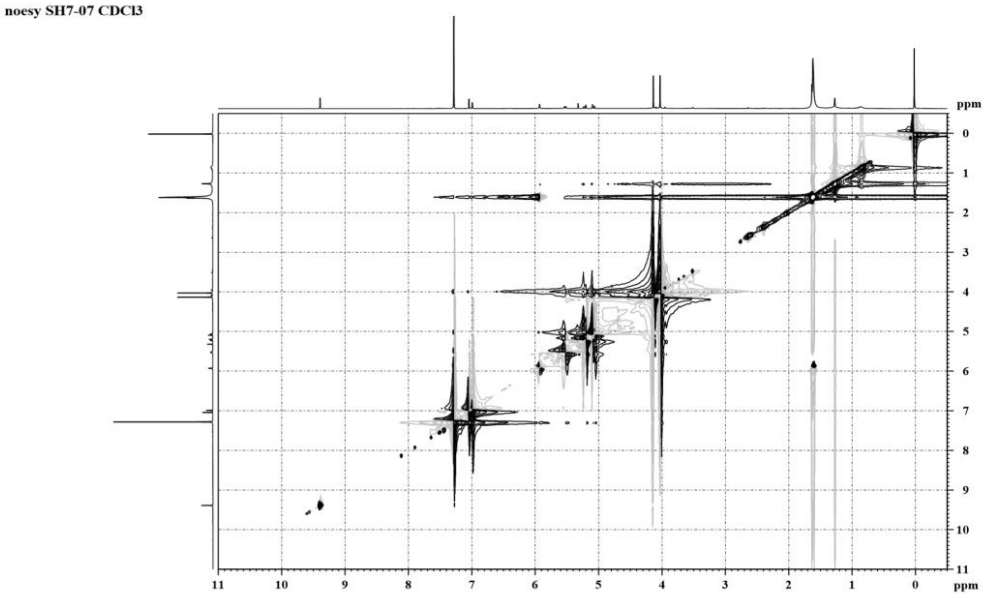

Figure 3.5 NOESY ($CDCl_3$) spectrum of compound 1

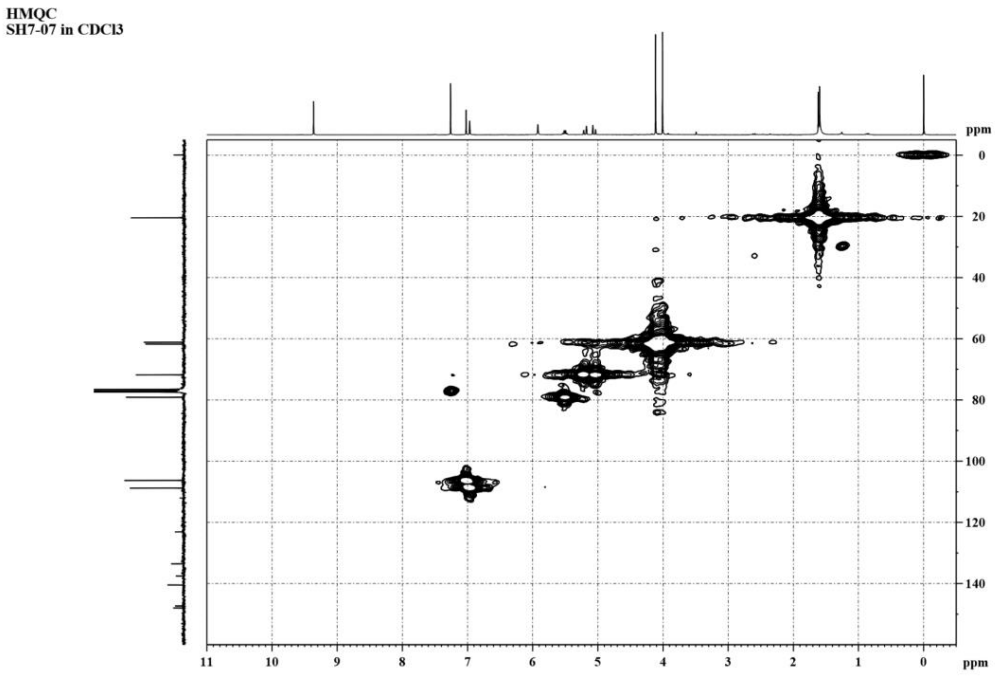

Figure 3.6 HMQC ($CDCl_3$) spectrum of compound 1

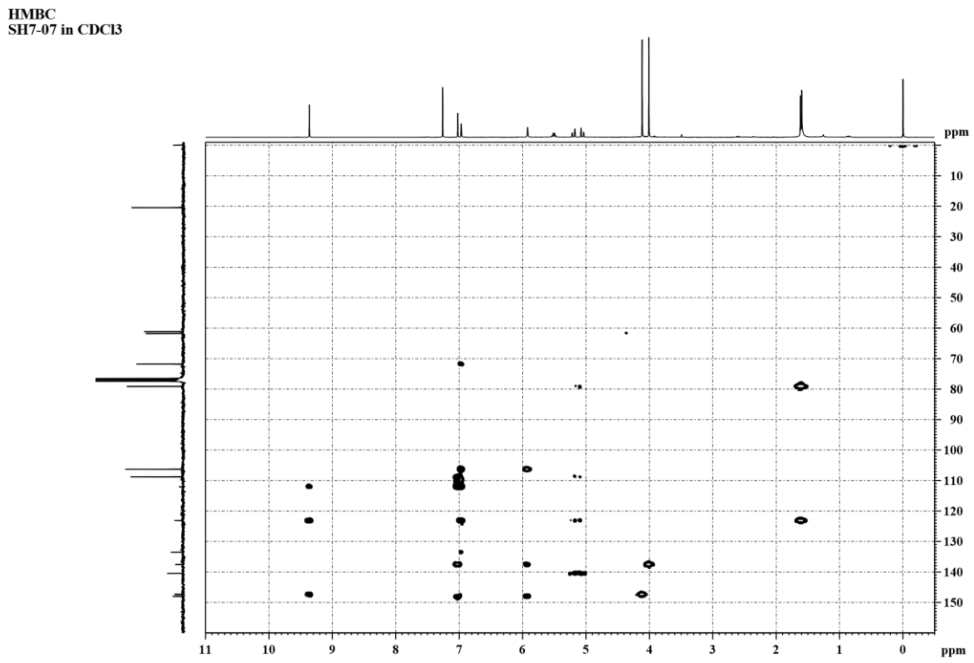

Figure 3.7 HMQC ($CDCl_3$) spectrum of compound 1

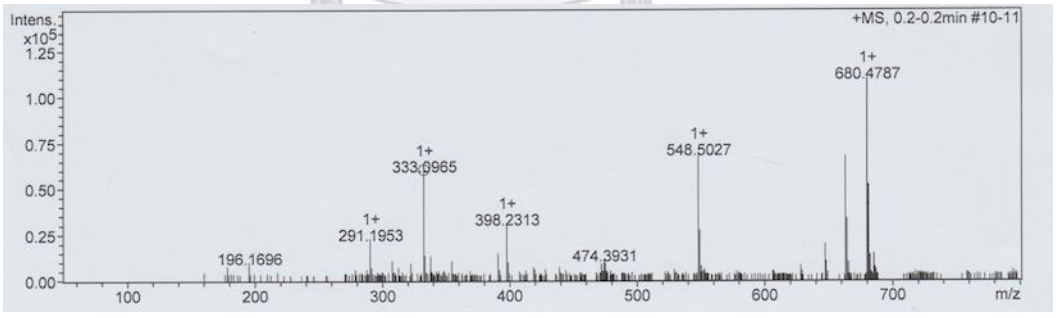

Figure 3.8 Mass spectrum of compound 1

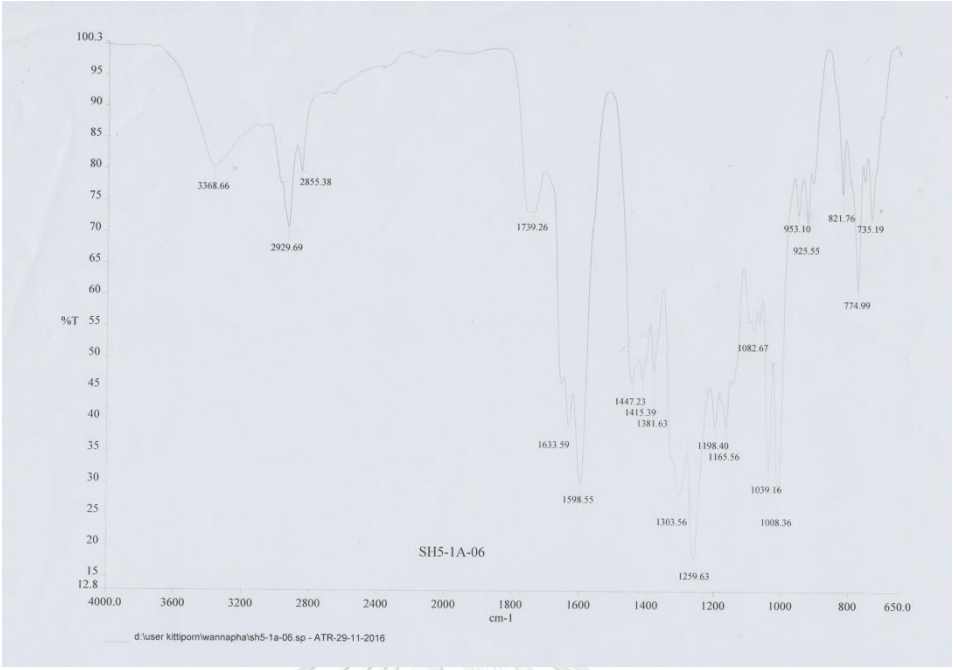

Figure 3.9 IR spectrum of compound 1

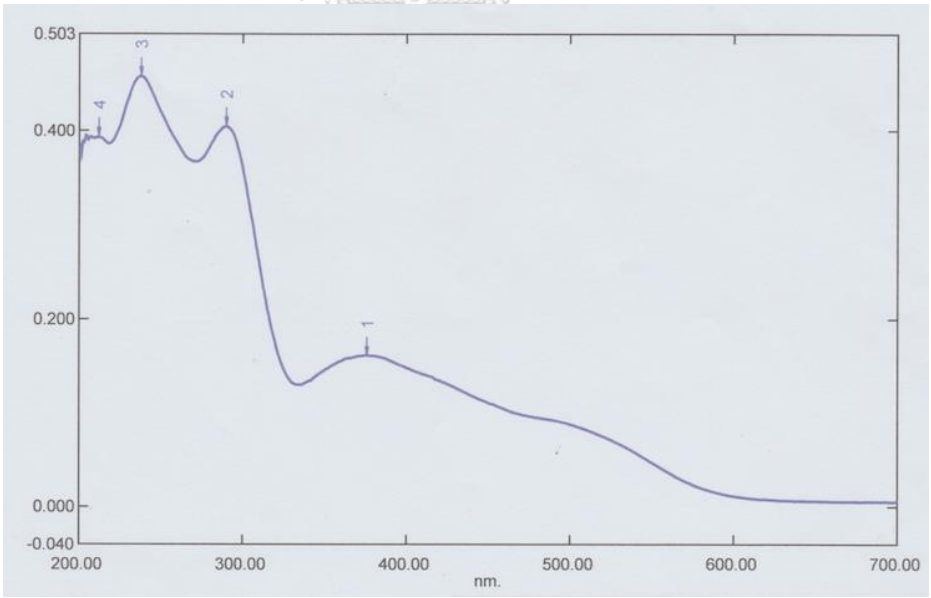

Figure 3.10 UV spectrum of compound 1

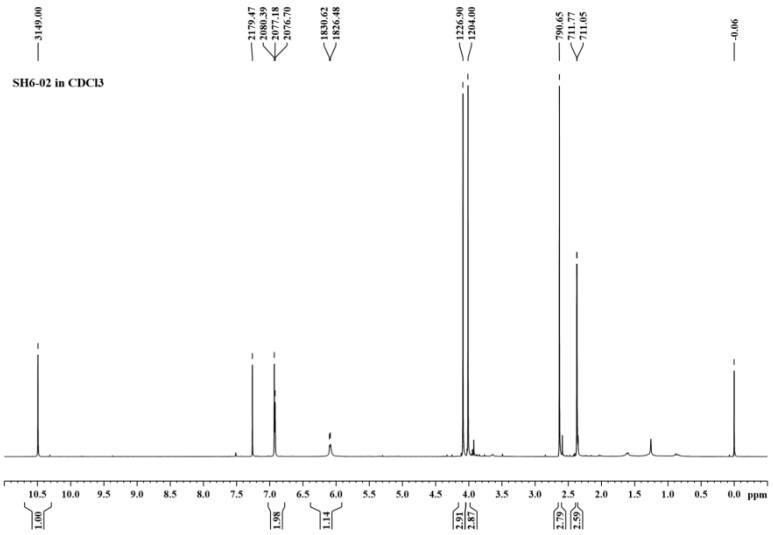

Figure 3.11 300 MHz ^{1}H ($CDCl_3$) spectrum of compound 2

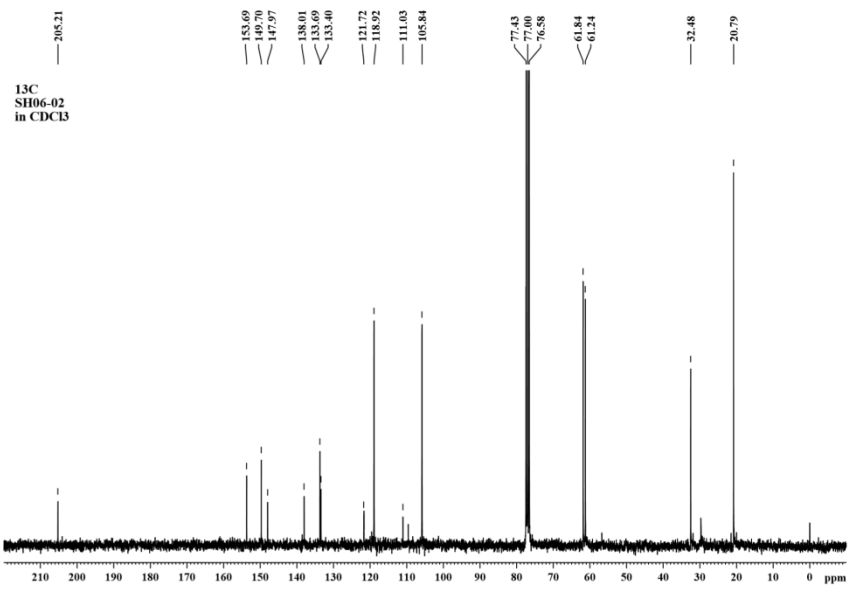

Figure 3.12 75 MHz ^{13}C ($CDCl_3$) spectrum of compound 2

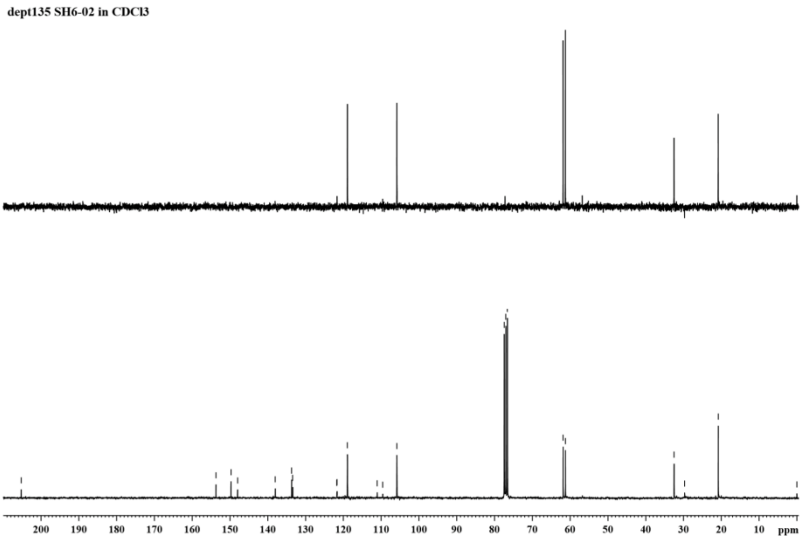

Figure 3.13 Dept135 ($CDCl_3$) spectrum of compound 2

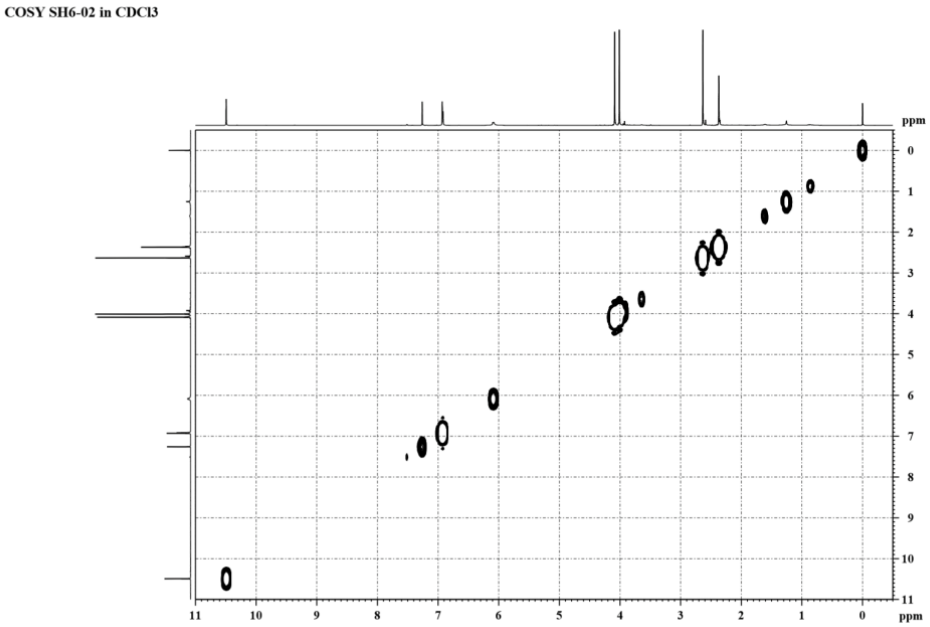

Figure 3.14 COSY ($CDCl_3$) spectrum of compound 2

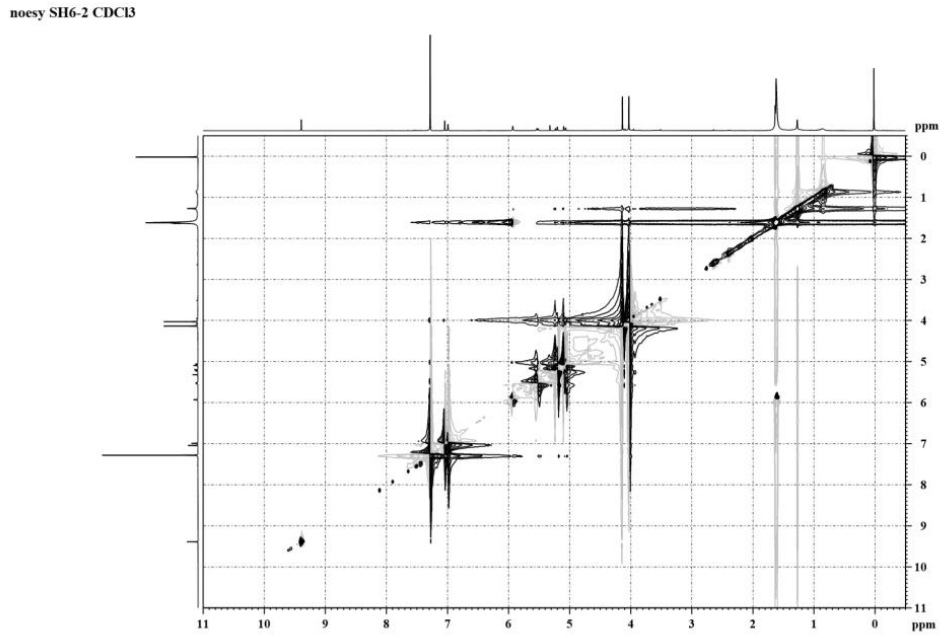

Figure 3.15 NOESY ($CDCl_3$) spectrum of compound 2

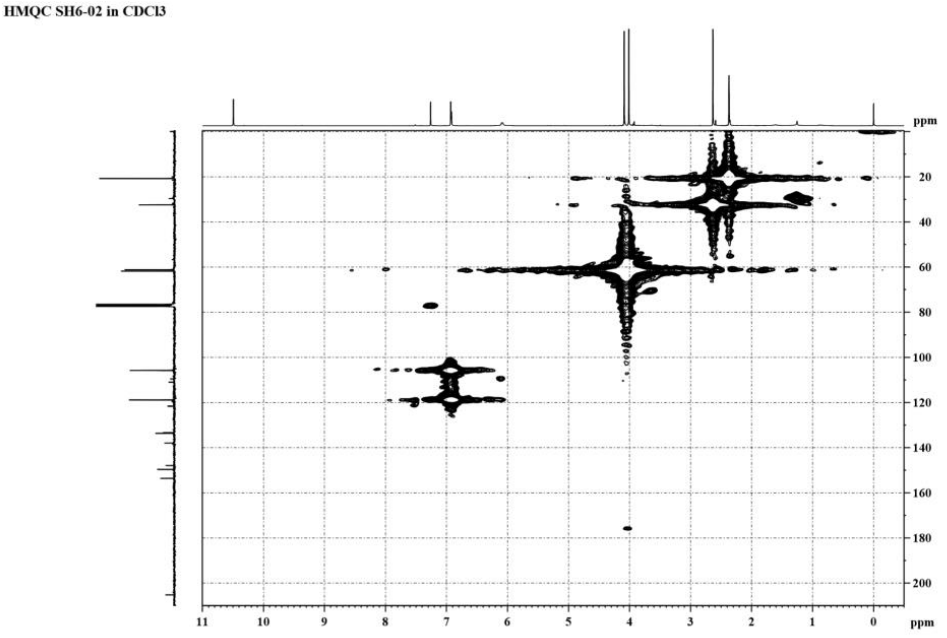

Figure 3.16 HMQC ($CDCl_3$) spectrum of compound 2

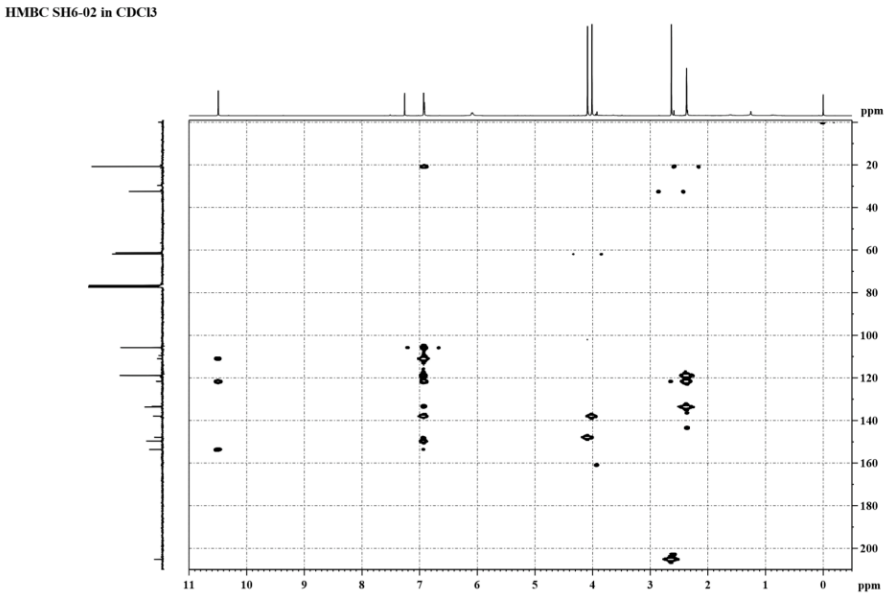

Figure 3.17 HMBC ($CDCl_3$) spectrum of compound 2

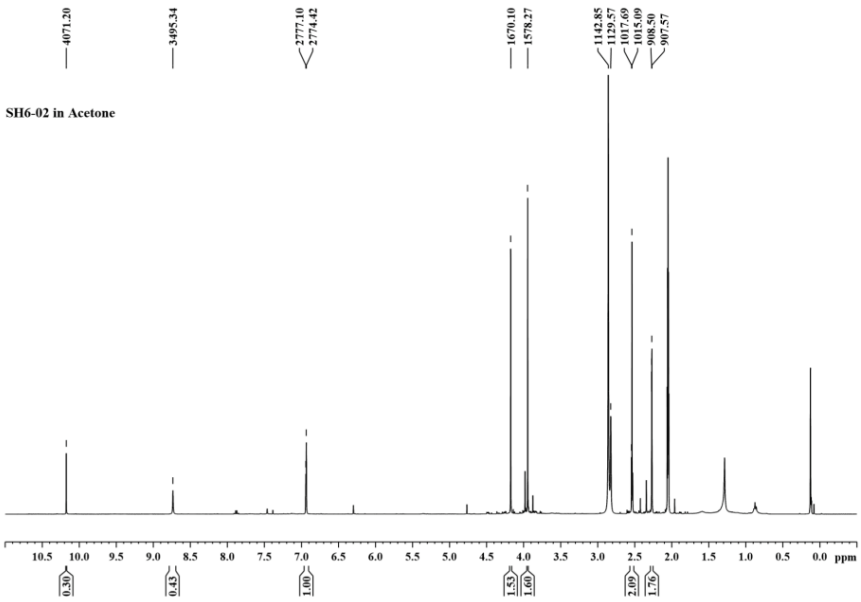

Figure 3.18 400 MHz ^{1}H (Acetone-d6) spectrum of compound 2

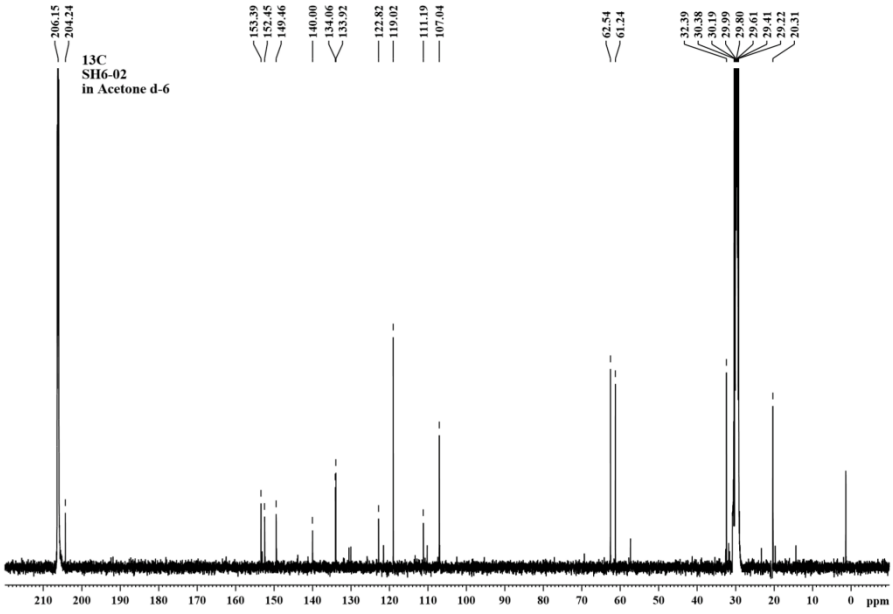

Figure 3.19 100 MHz ^{13}C (Acetone-d6) spectrum of compound 2

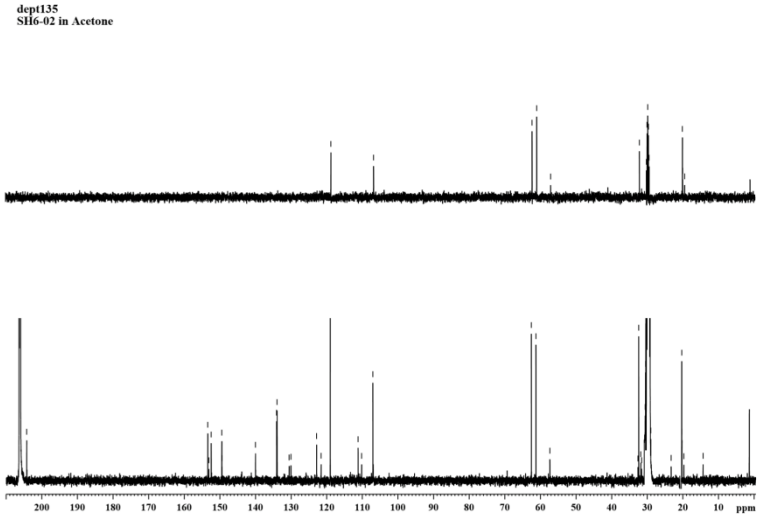

Figure 3.20 Dept135 (Acetone-d6) spectrum of compound 2

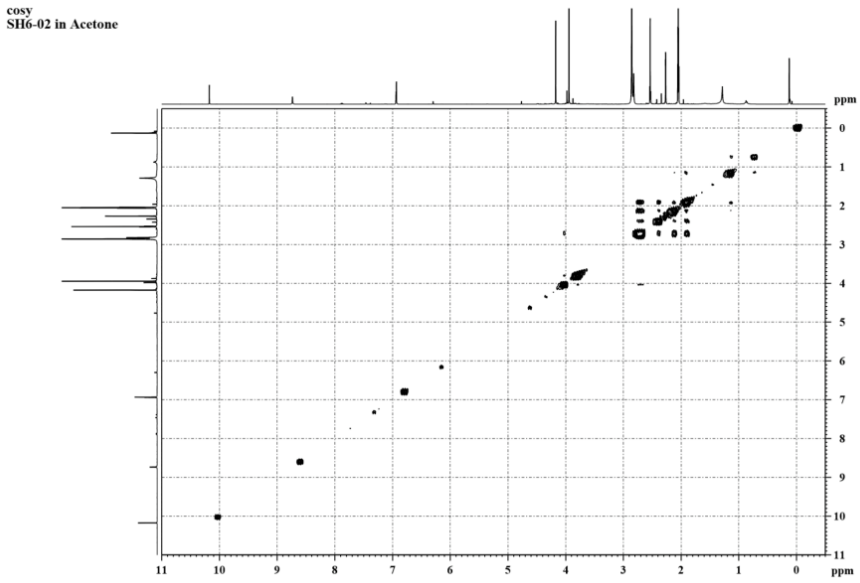

Figure 3.21 COSY (Acetone-d6) spectrum of compound 2

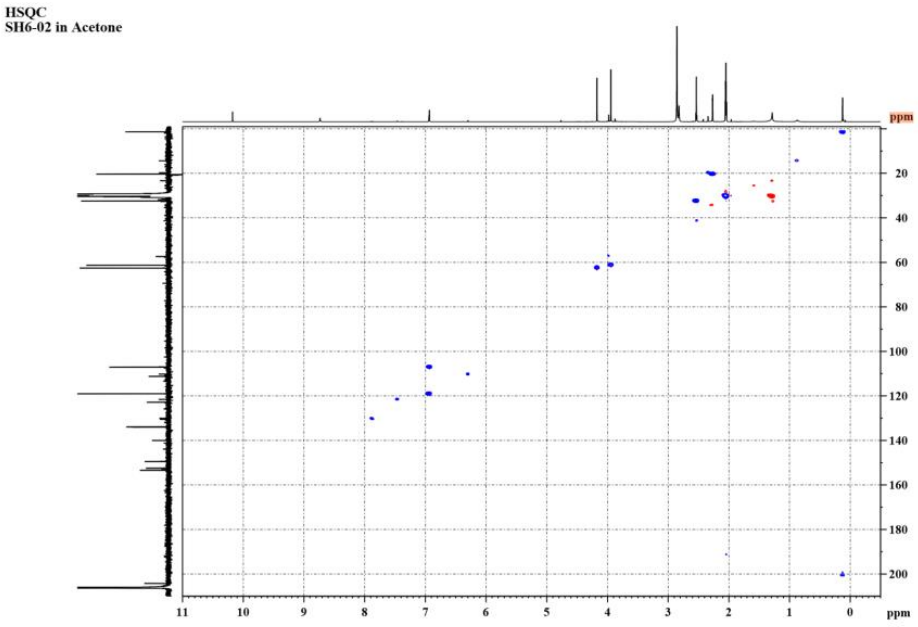

Figure 3.22 HSQC (Acetone-d6) spectrum of compound 2

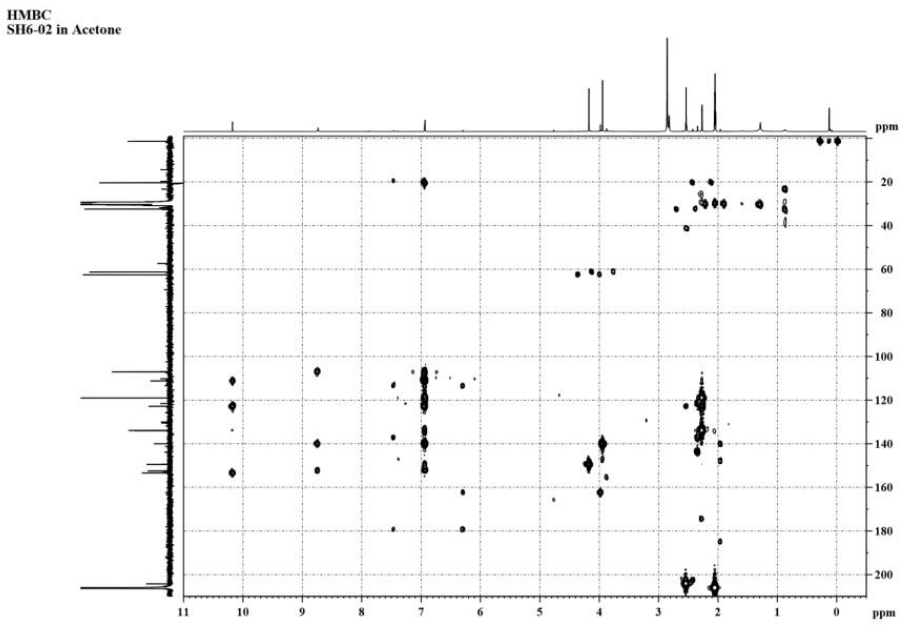

Figure 3.23 HMBC (Acetone-d6) spectrum of compound 2

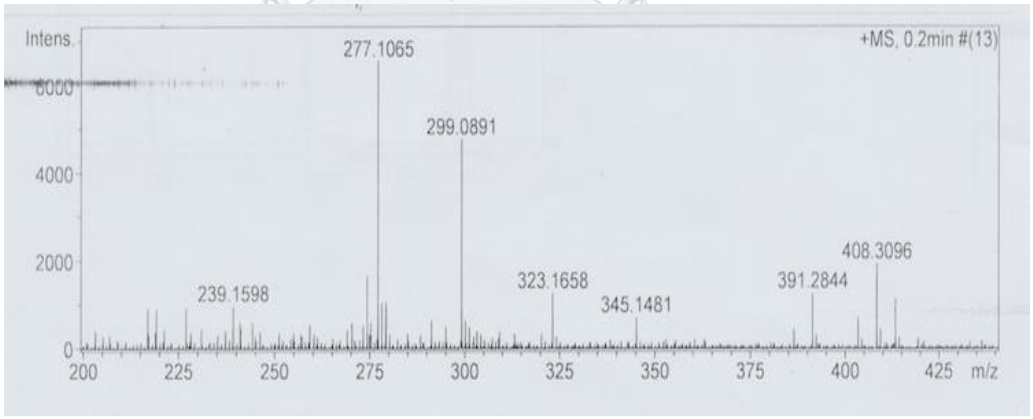

Figure 3.24 Mass spectrum of compound 2

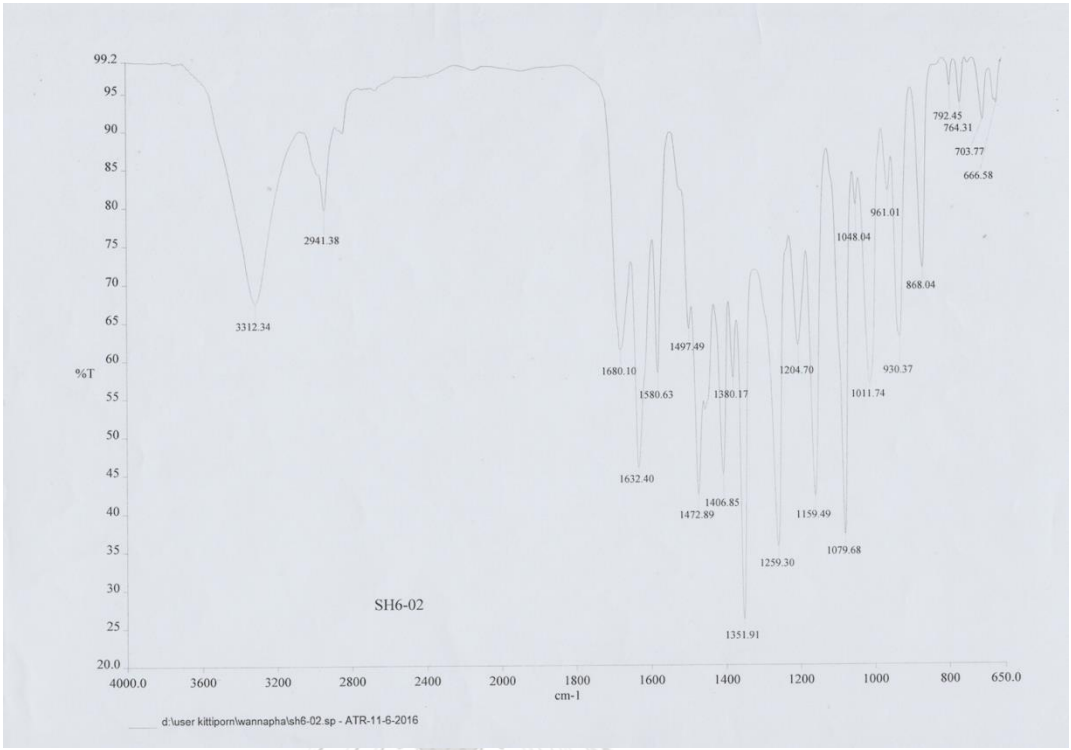

Figure 3.25 IR spectrum of compound 2

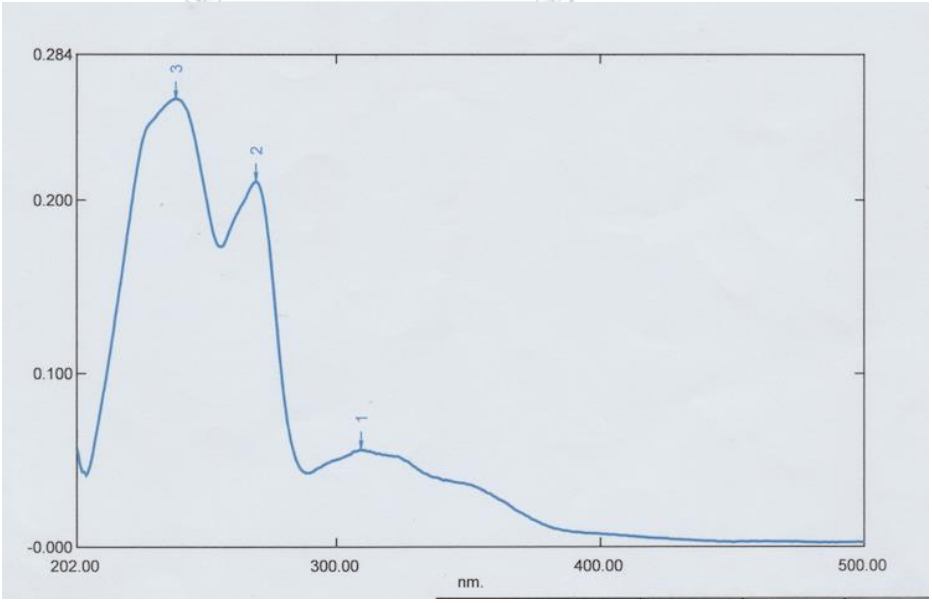

Figure 3.26 UV spectrum of compound 2

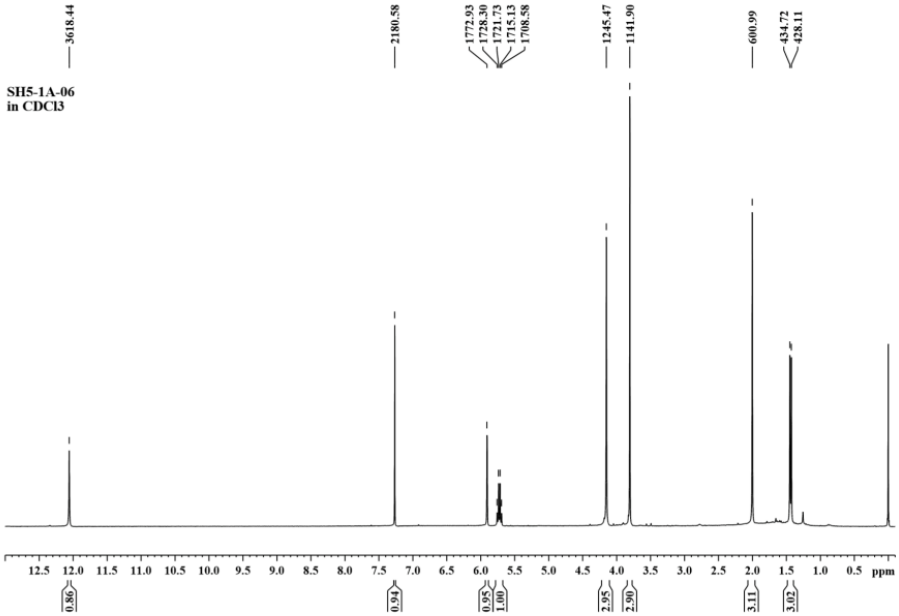

Figure 3.27 300 MHz ^{1}H ($CDCl_3$) spectrum of compound 3

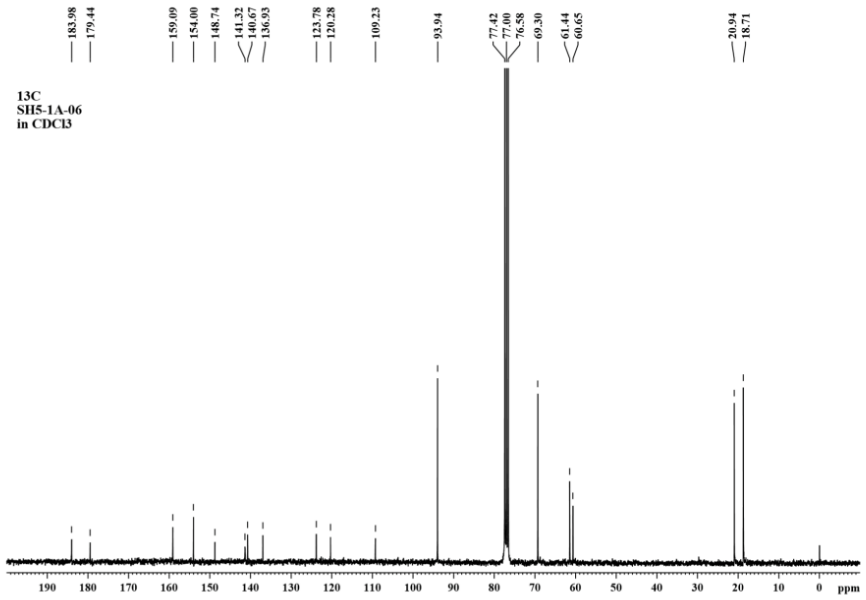

Figure 3.28 75 MHz ^{13}C ($CDCl_3$) spectrum of compound 3

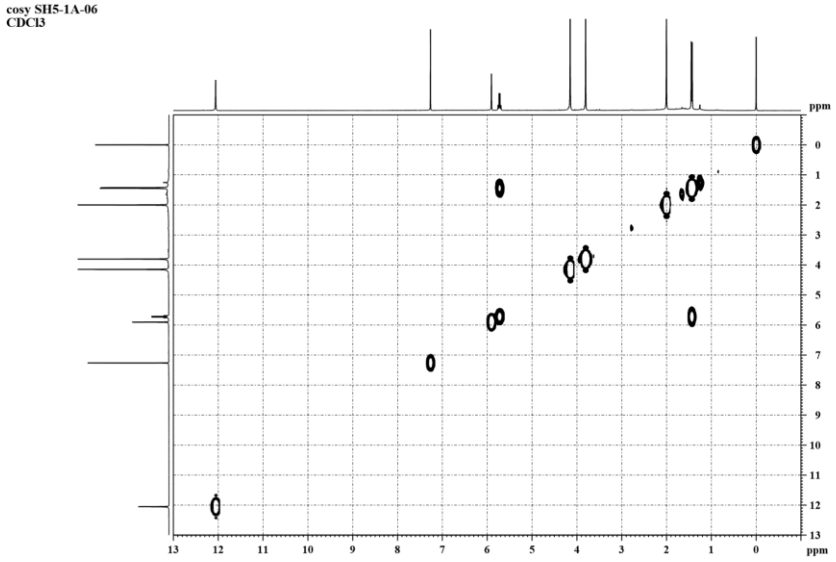

Figure 3.29 COSY ($CDCl_3$) spectrum of compound 3

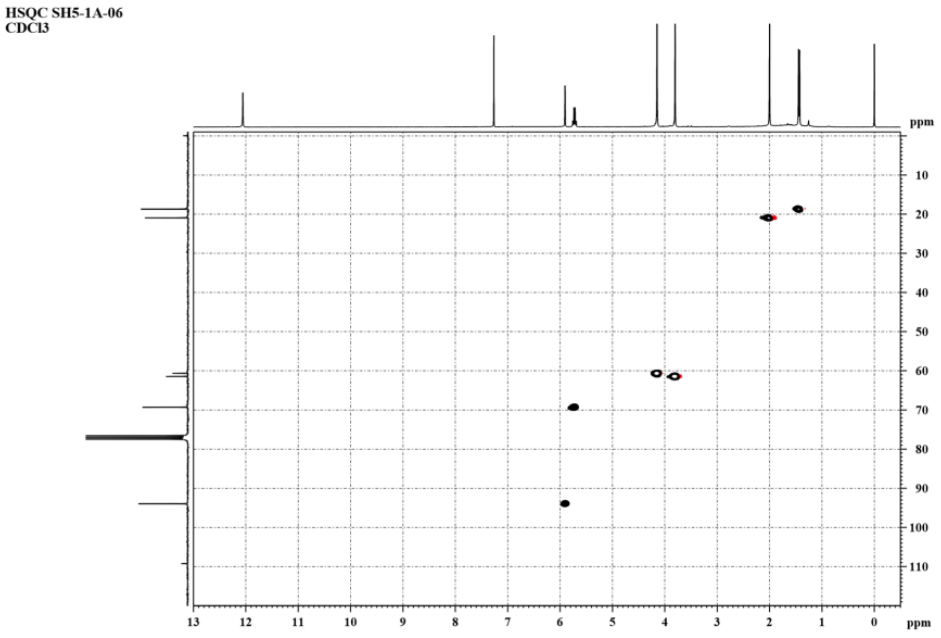

Figure 3.30 HSQC ($CDCl_3$) spectrum of compound 3

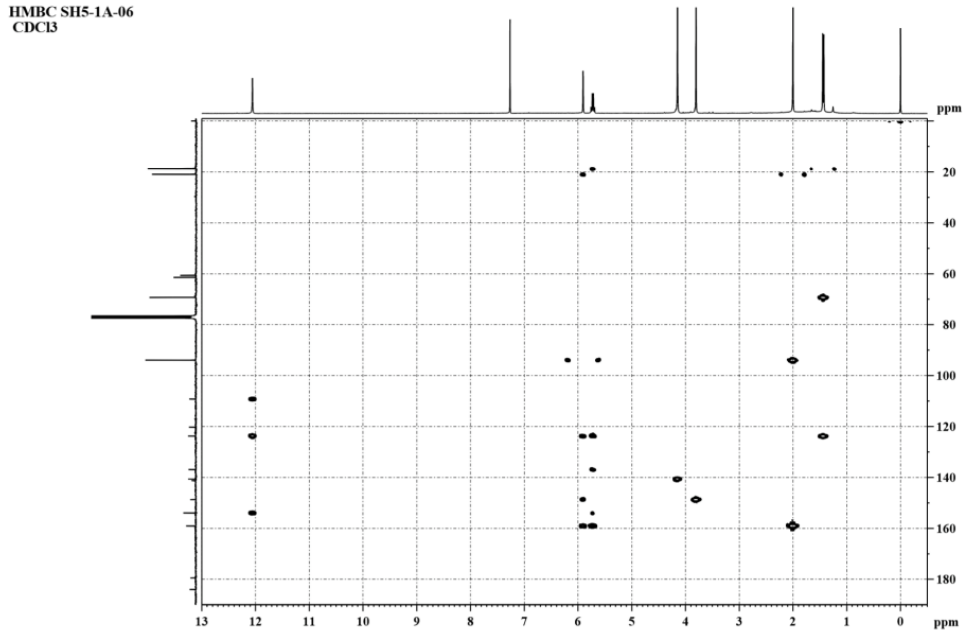

Figure 3.31 HMBC ($CDCl_3$) spectrum of compound 3

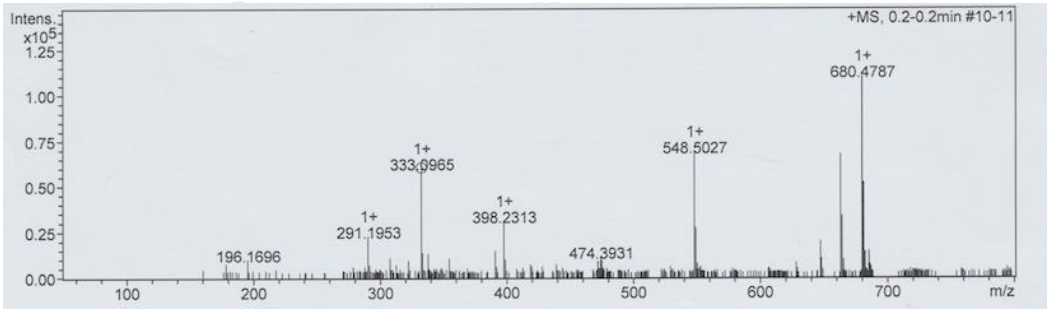

Figure 3.32 Mass spectrum of compound 3

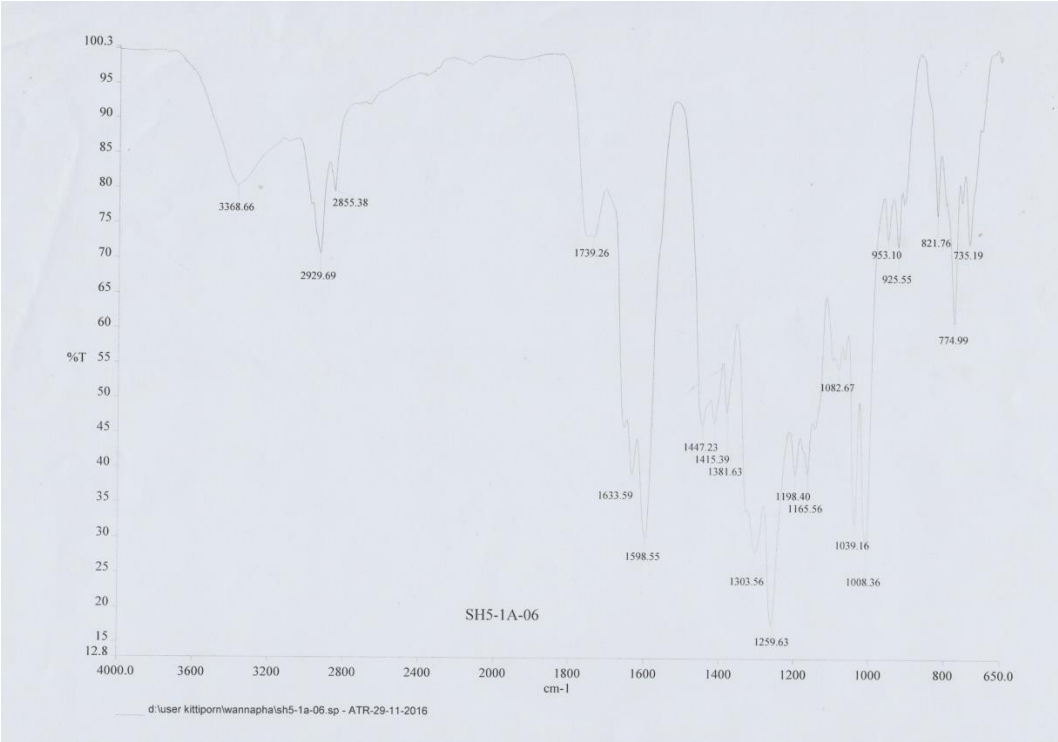

Figure 3.33 IR spectrum of compound 3

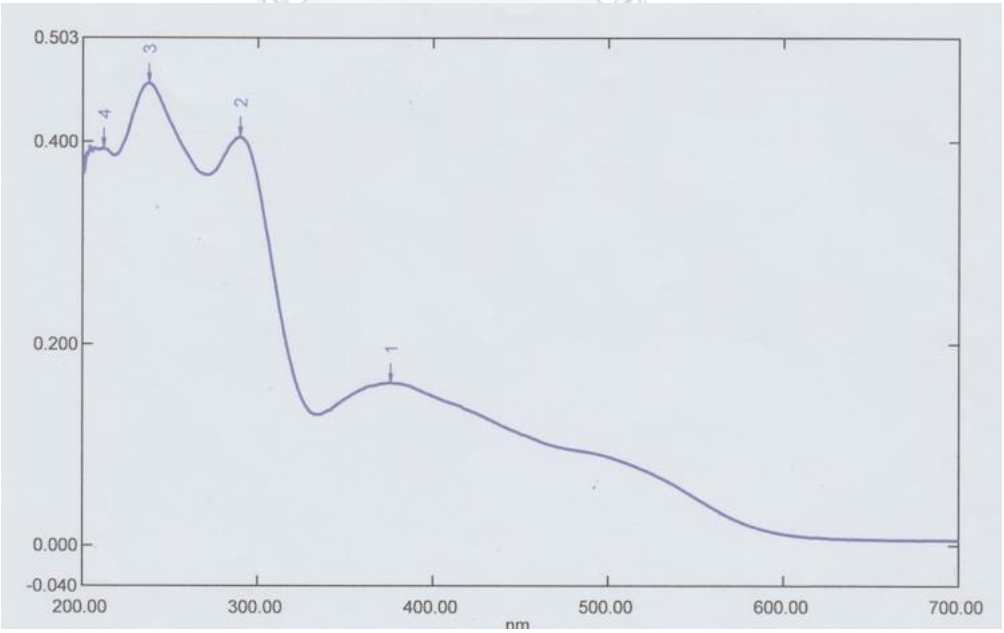

Figure 3.34 UV spectrum of compound 3

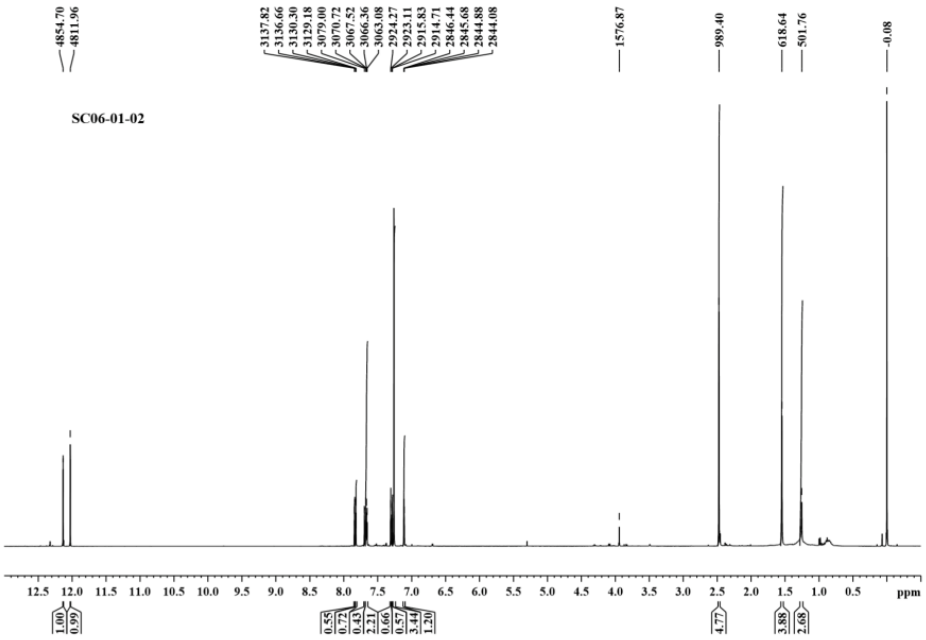

Figure 3.35 400 MHz ^{1}H ($CDCl_3$) spectrum of compound 4

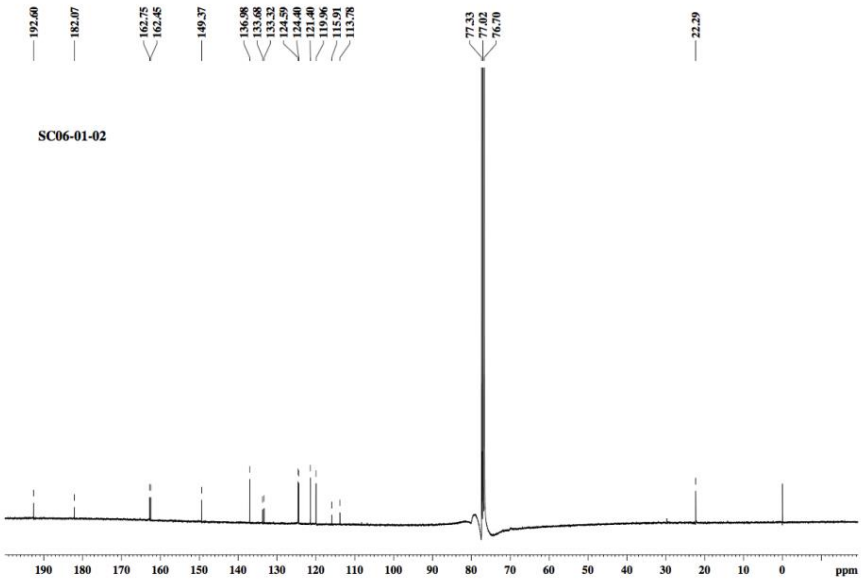

Figure 3.36 100 MHz ^{13}C ($CDCl_3$) spectrum of compound 4

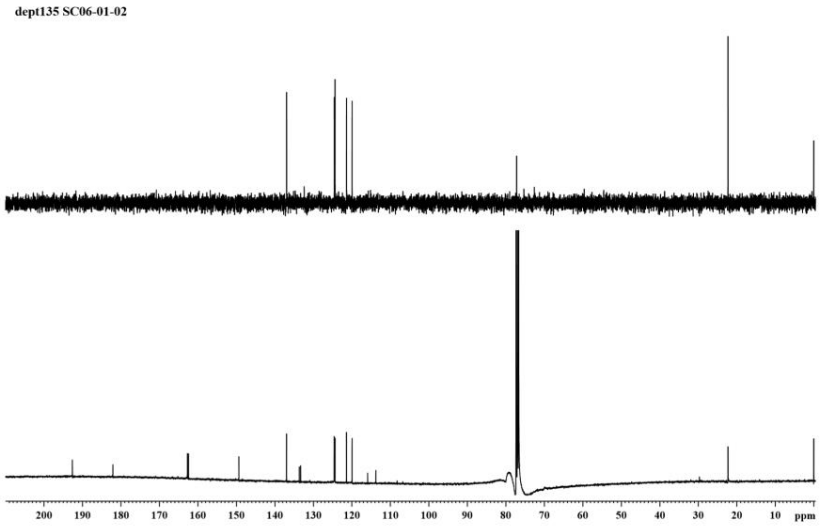

Figure 3.37 Dept135 ($CDCl_3$) spectrum of compound 4

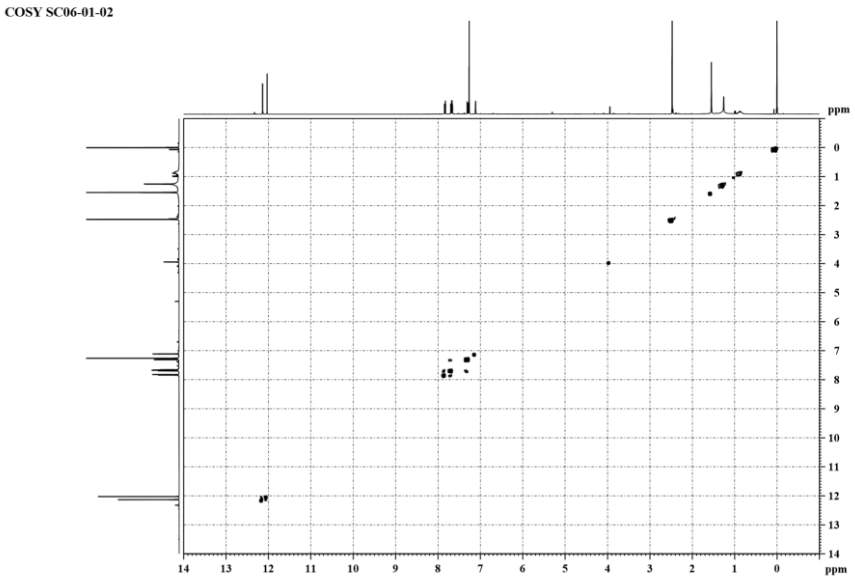

Figure 3.38 COSY ($CDCl_3$) spectrum of compound 4

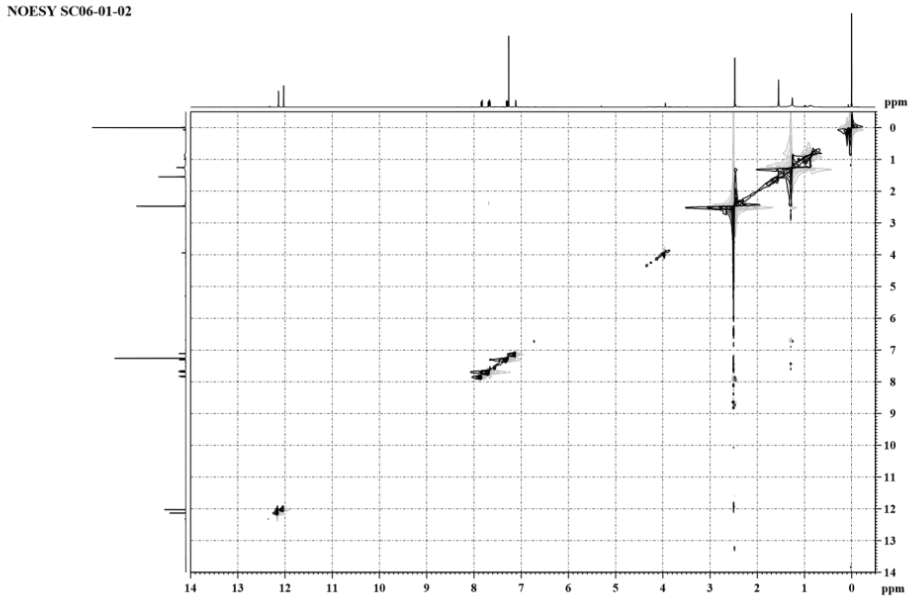

Figure 3.39 NOESY ($CDCl_3$) spectrum of compound 4

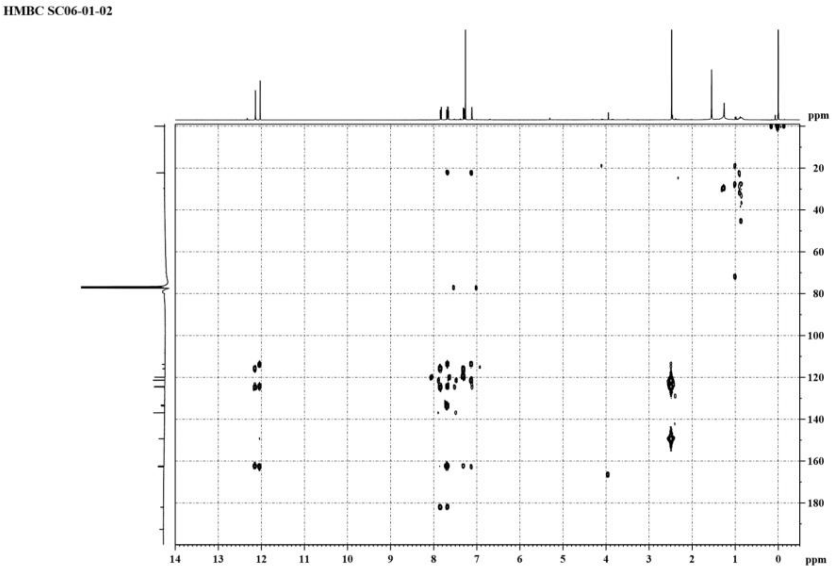

Figure 3.40 HMBC ($CDCl_3$) spectrum of compound 4

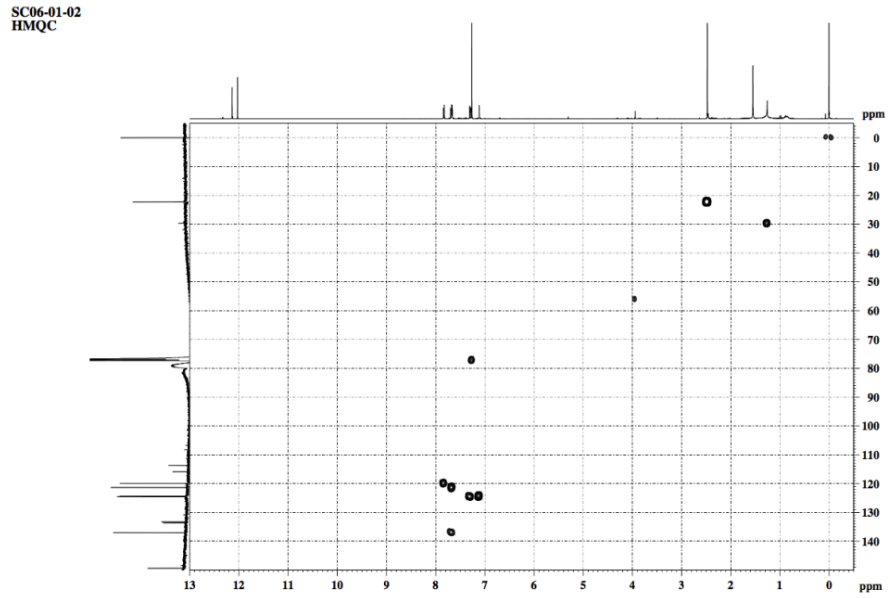

Figure 3.41 HMQC ($CDCl_3$) spectrum of compound 4

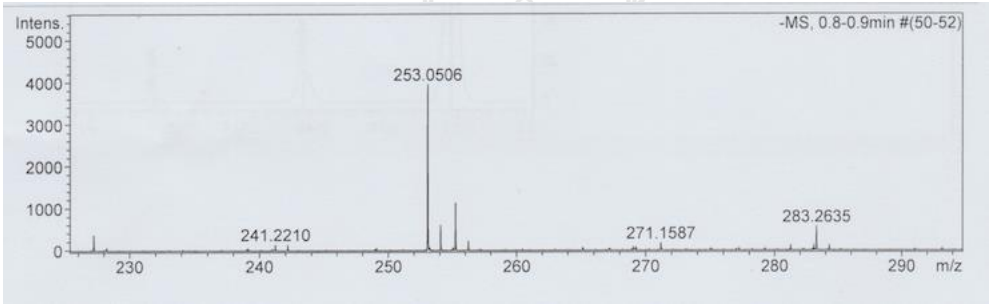

Figure 3.42 Mass spectrum of compound 4

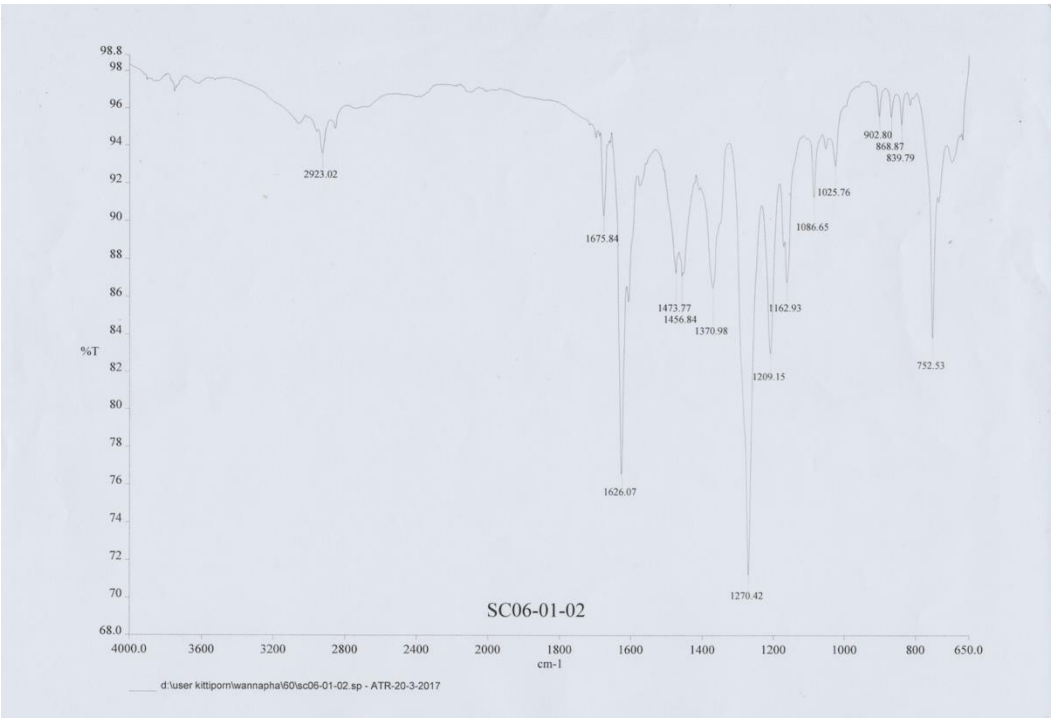

Figure 3.43 IR spectrum of compound 4

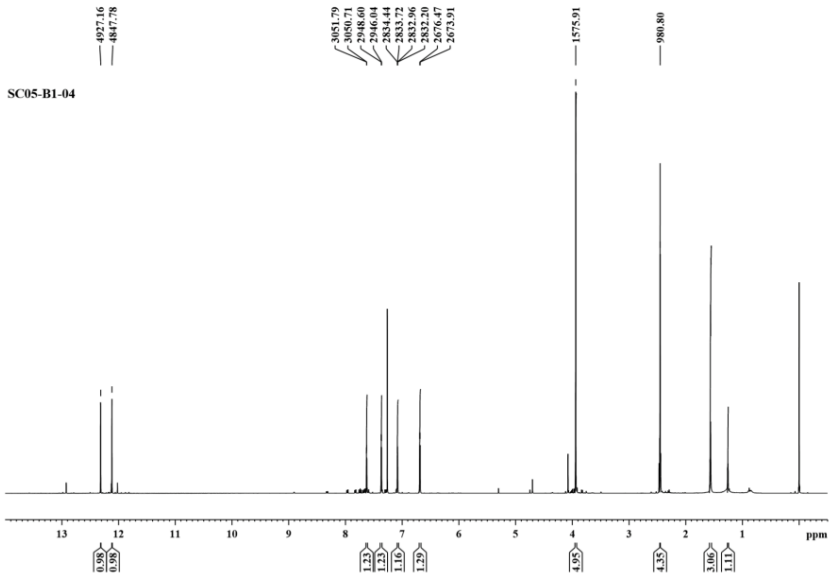

Figure 3.44 400 MHz ^{1}H ($CDCl_3$) spectrum of compound 5

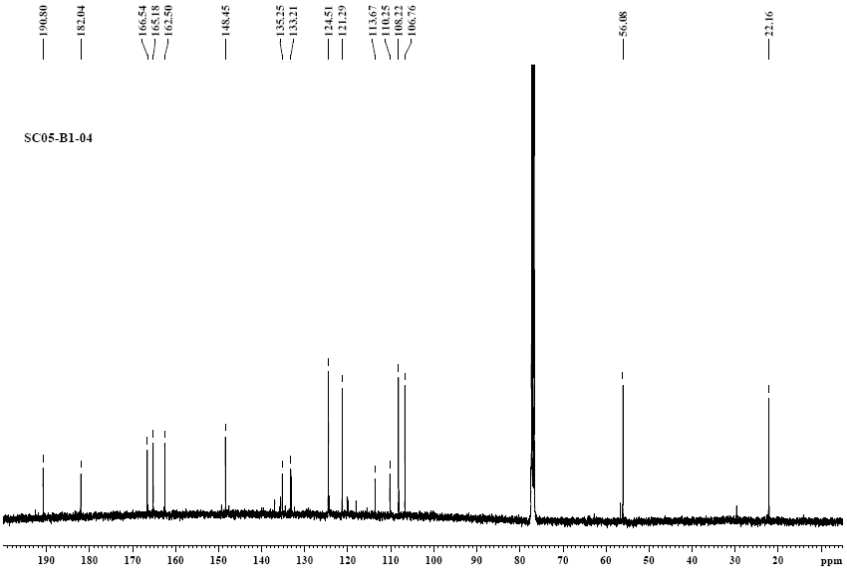

Figure 3.45 100 MHz ^{13}C ($CDCl_3$) spectrum of compound 5

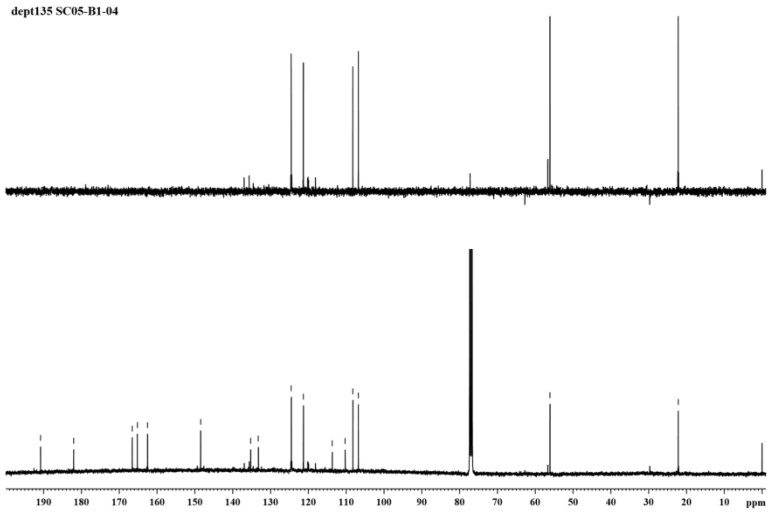

Figure 3.46 Dept135 ($CDCl_3$) spectrum of compound 5

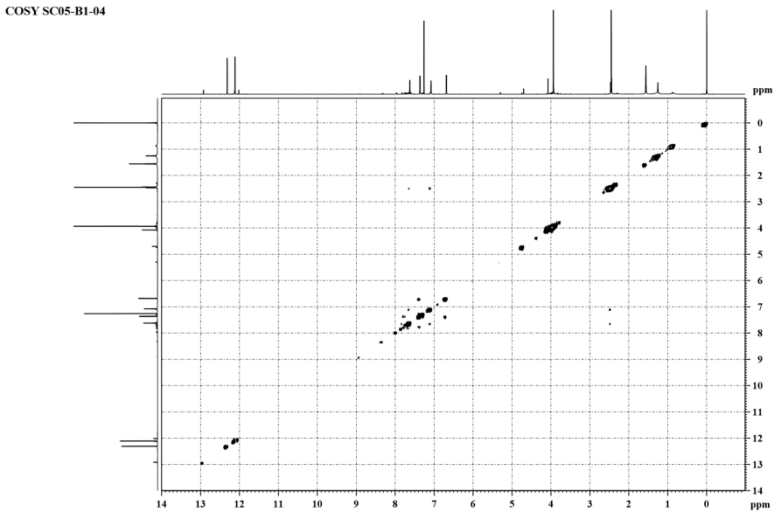

Figure 3.47 COSY ($CDCl_3$) spectrum of compound 5

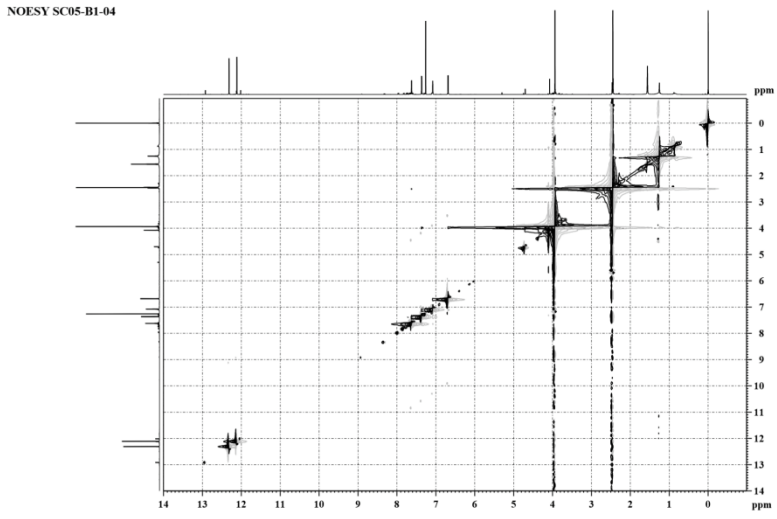

Figure 3.48 NOESY ($CDCl_3$) spectrum of compound 5

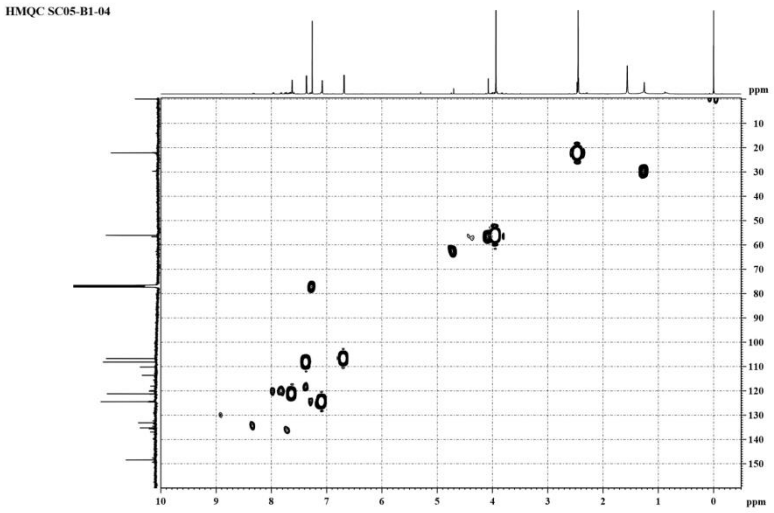

Figure 3.49 HMQC ($CDCl_3$) spectrum of compound 5

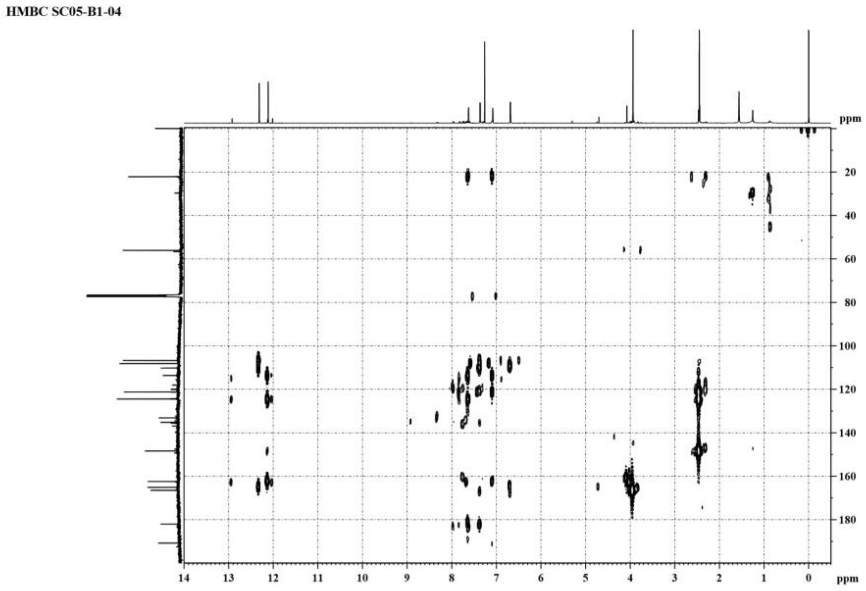

Figure 3.50 HMBC ($CDCl_3$) spectrum of compound 5

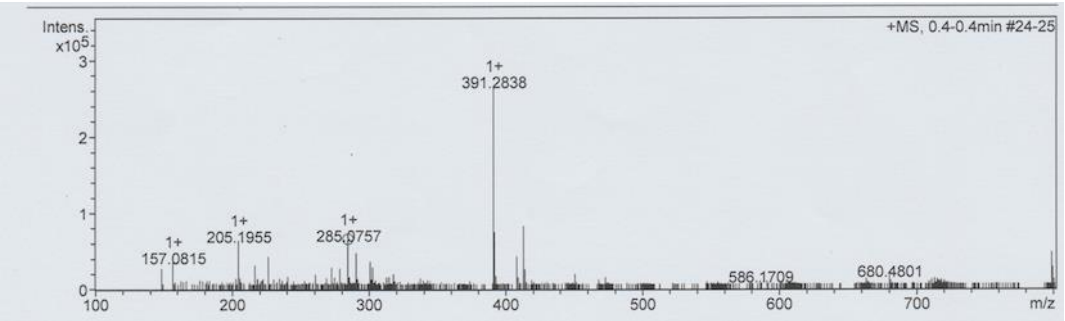

Figure 3.51 Mass spectrum of compound 5

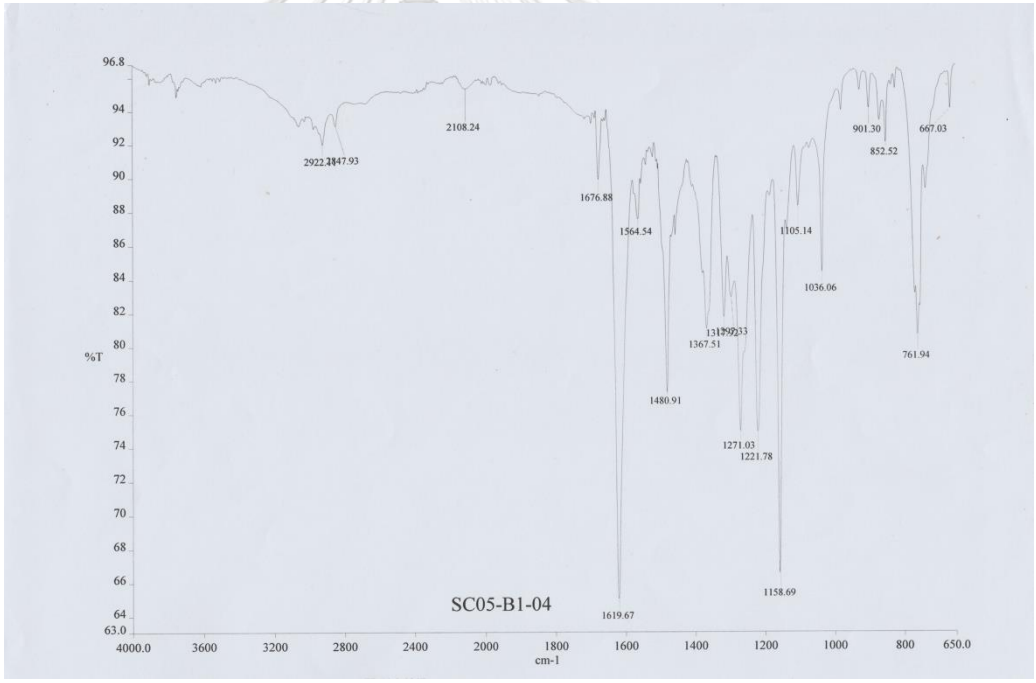

Figure 3.52 IR spectrum of compound 5

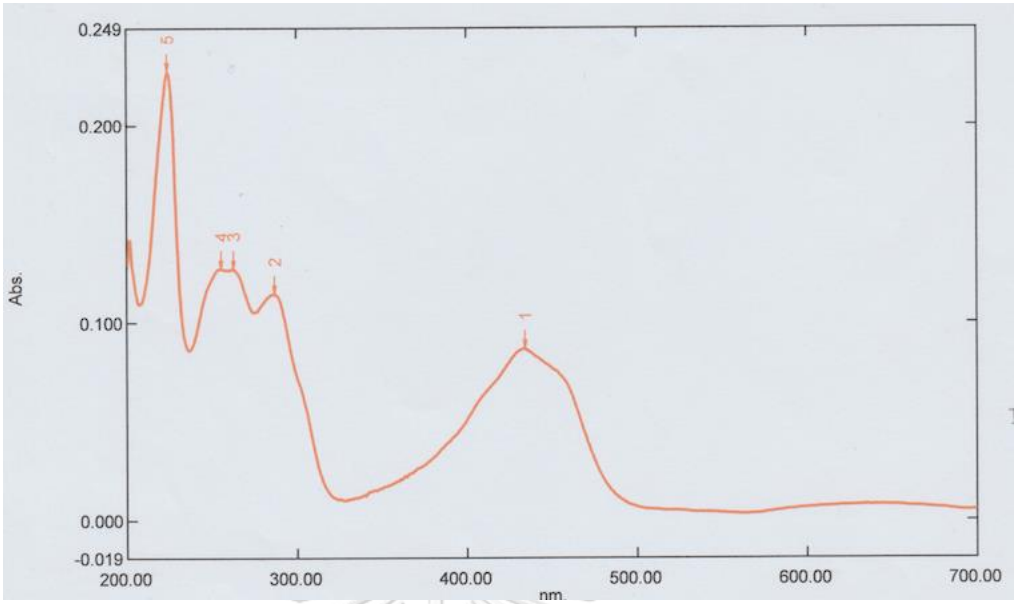

Figure 3.53 UV spectrum of compound 5

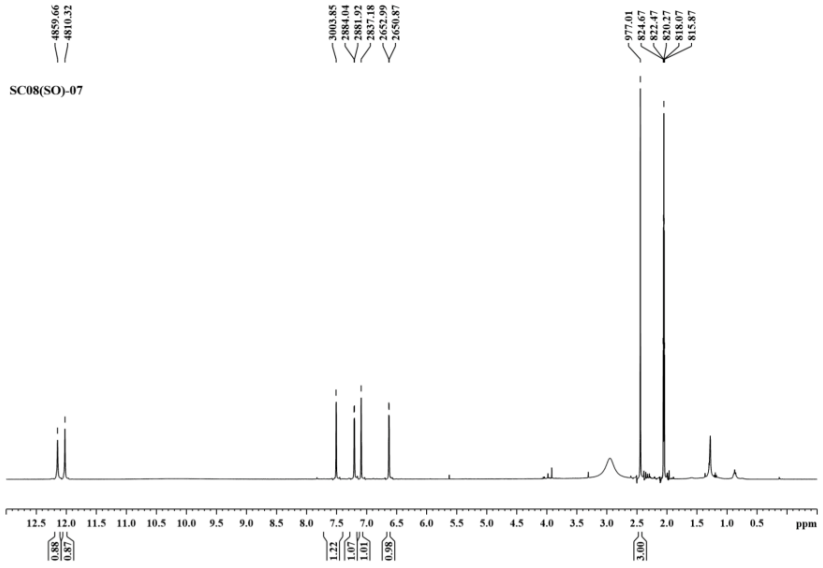

Figure 3.54 400 MHz ^{1}H (Acetone-d6) spectrum of compound 6

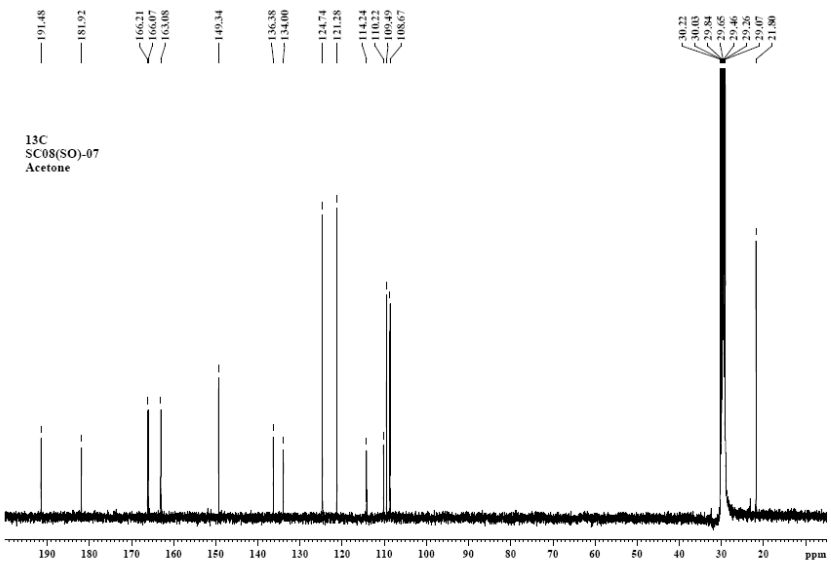

Figure 3.55 100 MHz ^{13}C (Acetone-d6) spectrum of compound 6

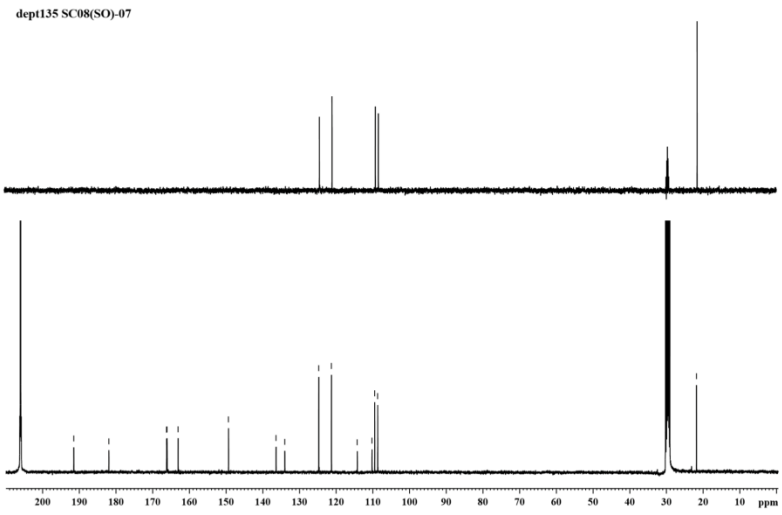

Figure 3.56 Dept135 (Acetone-d6) spectrum of compound 6

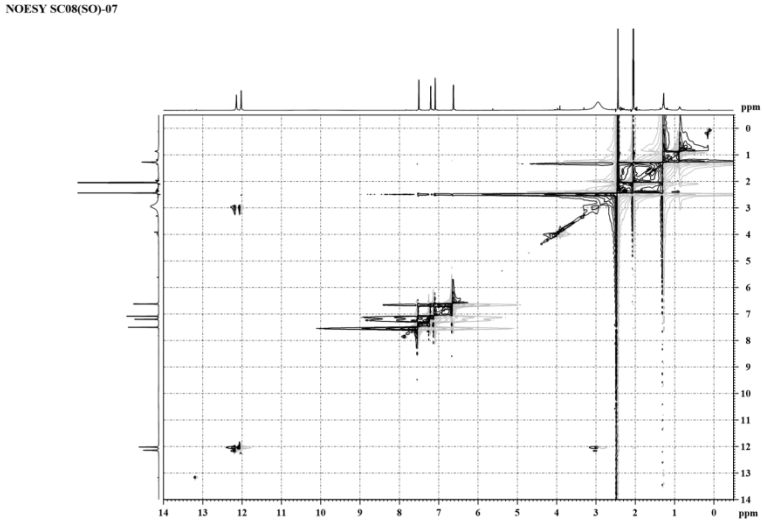

Figure 3.57 NOESY (Acetone-d6) spectrum of compound 6

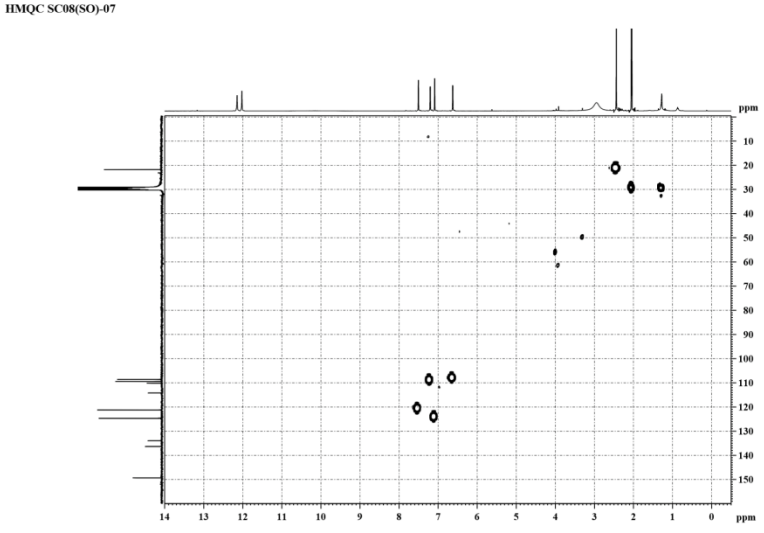

Figure 3.58 HMQC (Acetone-d6) spectrum of compound 6

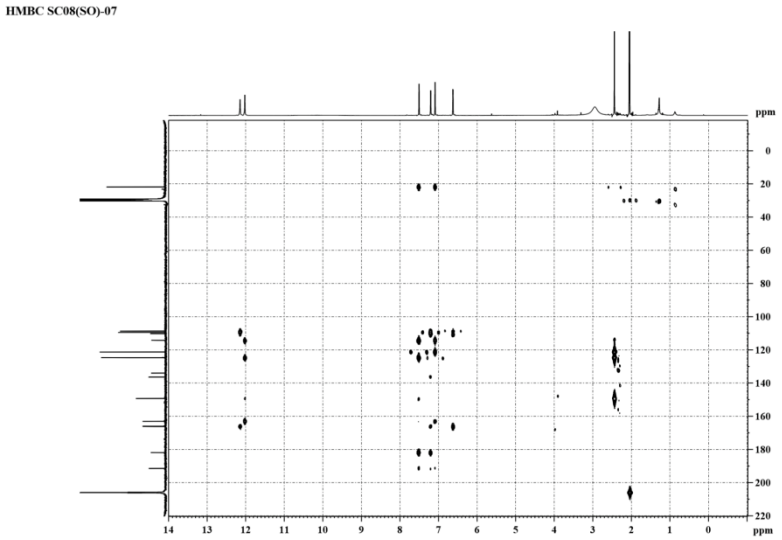

Figure 3.59 HMBC (Acetone-d6) spectrum of compound 6

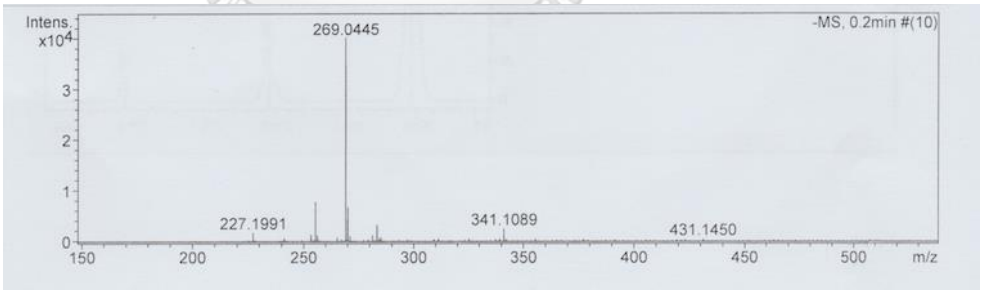

Figure 3.60 Mass spectrum of compound 6

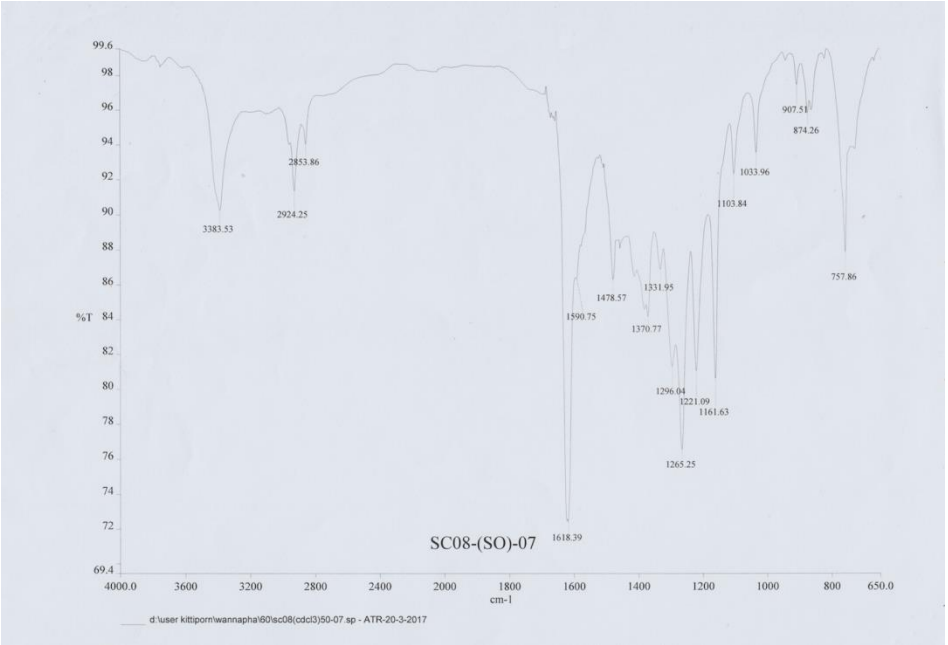

Figure 3.61 IR spectrum of compound 6

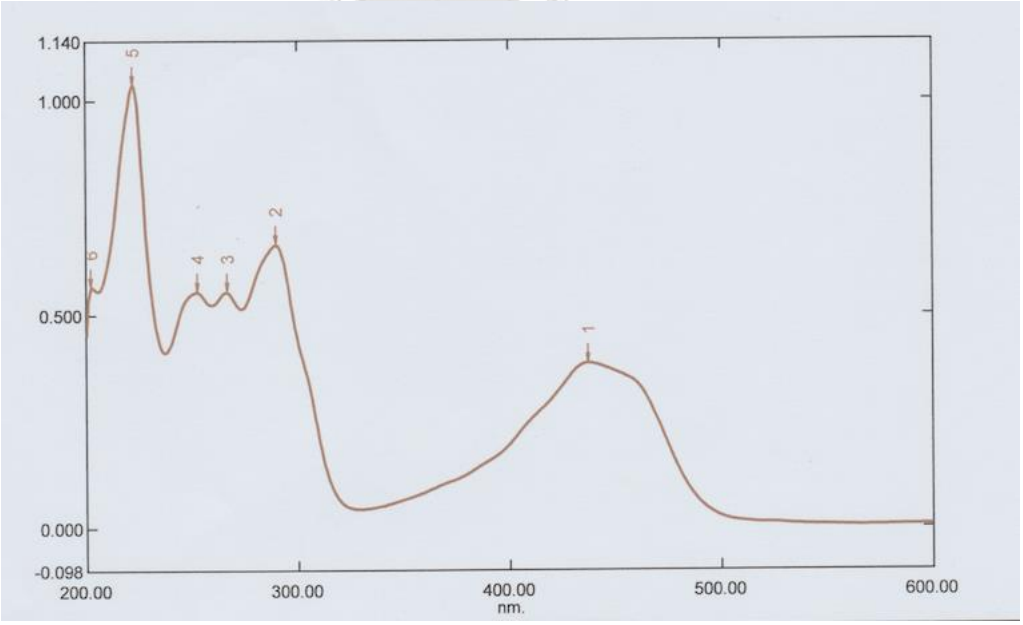

Figure 3.62 UV spectrum of compound 6

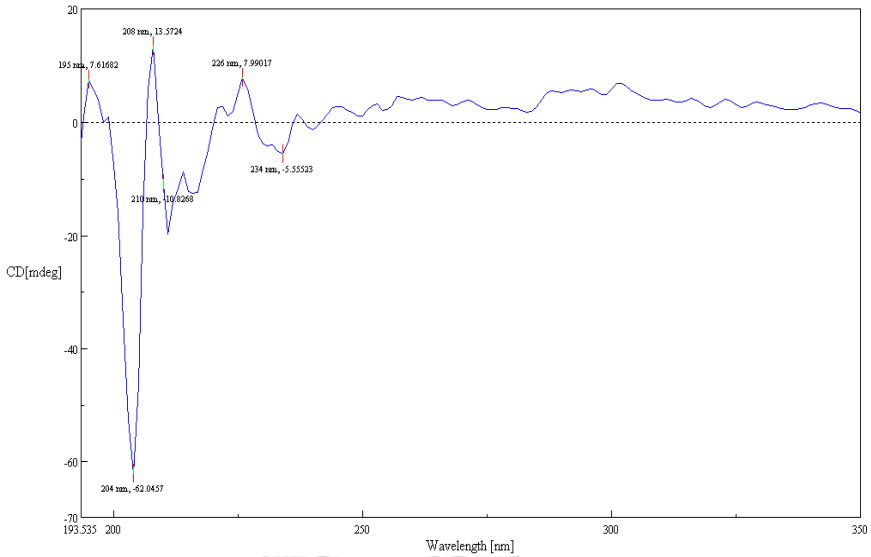

Figure 3.63 CD spectrum of compound 3

VITA

Miss Wannapha Molee was born on March 3, 1985 in Prachinburi, Thailand. She received Bachelor degree of Science from Agro-Industry Technology and Management, King Mongkut's University of Technology North Bangkok in 2008. She graduated with Master' s degree Biotechnology of academic year 2017 from Chulalongkorn University.

Academic presentation :

Molee W., Phanumartwiwath A., Kesornpun C., Sureram S., Ngamrojanavanich N., Ingkaninan K., Mahidol C., Ruchirawat S., and Kittakoop P. Naphthalene Derivatives and Quinones from Ventilago denticulata and their Nitric Oxide Radical Scavenging, Antioxidant, Cytotoxic, Antibacterial, and Phosphodiesterase Inhibitory Activities. Chemistry & Biodiversity, 2018, 15